Beach-dune morphodynamics and climate variability impacts on Wickaninnish Beach, Pacific Rim National Park Reserve, British Columbia, Canada

by

Hawley Elizabeth Ruth Beaugrand
B.Sc., University of Victoria, 2007

A Thesis Submitted in Partial Fulfillment
of the Requirements for the Degree of

MASTERS OF SCIENCE

in the Department of Geography

Supervisory Committee

Beach-dune morphodynamics and climate variability impacts on Wickaninnish Beach, Pacific Rim National Park Reserve, British Columbia, Canada

by

Hawley Elizabeth Ruth Beaugrand
B.Sc., University of Victoria, 2007

Supervisory Committee

Dr. Ian J. Walker, Supervisor
(Department of Geography)

Dr. Stephen Wolfe, Departmental Member
(Department of Geography Adjunct, Geological Survey of Canada)

Abstract

Supervisory Committee
Dr. Ian J. Walker, Supervisor
(Department of Geography)

Dr. Stephen Wolfe, Departmental Member
(Department of Geography Adjunct, Geological Survey of Canada)

To date, there has been little research on the morphodynamics of Canada's Pacific mesotidal beach-dune systems and their potential response to climate variability and change. Accordingly, this study examines and characterizes the morphodynamics of a mesotidal beach-dune system on western Vancouver Island (Wickaninnish Beach) and investigates its potential response to extreme seasonal storms, climate variability events, and climate change trends. This research also informs protected areas management approaches, whose effectiveness is important to the conservation of early successional and proportionately rare specialized dune species. Research methods include repeat cross-sectional surveys, repeat vantage photographs, and analysis of the wind, wave, and water level regime.

Both the regional wind regime and aeolian sediment transport regime are bimodal, with a WNW (summer) component and a SE (winter) component. The nearshore littoral sediment transport regime is characterized by both longshore and rip cell circulation cells. To date, survey results are informative only of seasonal changes. Longer-term monitoring will better reveal contemporary trends of the beach-dune system. A high dune rebuilding potential (aeolian sand transport potential = 9980 $m^3 m^{-1} a^{-1}$, resultant aeolian sand transport = 3270 $m^3 m^{-1} a^{-1}$ at 356 degrees) was found based on the incident wind regime and sand grain diameter.

A threshold elevation for dune erosion was defined at 5.5 m aCD. Erosive water levels were analyzed using three approaches yielding the following results. Erosive water levels are reached on average, ~3.5 times per year; with a probability of 65% in any given year; and, annual return levels are 5.59 m aCD, suggesting erosive water levels are reached annually. Statistical relations show that the positive phase of El Niño Southern Oscillation (ENSO) (El Niño) shares the most variance with the incident oceanographic regime (e.g., significant wave

height, peak period), and although a causal relationship cannot be drawn, El Niño may contribute to the occurrence of erosive events on Wickaninnish Beach. Beyond El Niño, overall findings suggest climate variability signals are manifest in regional erosional water level regimes.

Table of Contents

List of Tables

List of Figures

Acknowledgements

I have many individuals and organizations to thank for the realization of this research and, best of all, the 'awesome' journey. Firstly, I would like to thank Ian for his direction, commitment, and realism over the past two years. It has been a joy to work with you. Thank you to Steve Wolfe and Nick Page for your constructive criticisms and insight throughout the process. Also Ole, thank you so much for all your help with the graphic feats of academia.

Thank you to the University of Victoria, MITACS, Parks Canada, the Clayoquot Biosphere Trust, and NSERC for funding various components of this project. Your financial contributions made this project logistically possible and are much appreciated. I would also like to acknowledge the Canadian Hydrographic Service for, in many instances, promptly providing essential data … pro bono.

I am incredibly indebted to the BLASTers. Jordan, thank you for the *rehab*ilitating field work adventures, rusty nail front porch ramblings, sunrise surf sessions, and … everything. I woman-heart you bra. Con-master-flex (Connie), "to be totally honest with you," "I'm not going to lie," you are lovely. I have truly appreciated our many moments of nerdy enthusiasm. D-crew (Derek), on a business note, thanks for your wicked airphoto work; it has been incredibly helpful throughout my research. And, more personally, I am grateful for your provision of endless entertainment(!), particularly in the struggles of year one. Darkness (Ian D.), thanks for your obvious 'hambre' for expanding various aspects of this research (e.g., DEEP, Geoindicators Monitoring Program). I am leaving you all with a heavy heart.

Melissa, Mary S., Andrea, Kara, Alice, Mary L., Katie M., Lisa, and Gemma, I am so blessed to have such amazing ladies in my life. Thank you for encouraging irresponsibility on *occasion* and supporting diligence when necessary. My friendship with each of you is truly invaluable to me. Keith, thank you so much for your support and understanding throughout first year, for generously allowing me to steal away in the Coho on numerous occasions, and for persuading two maniacal ladies faced with impending deadlines to keep their stick on the ice.

8-plex'ers. My heart is full thinking of you all. Thank you for the hilarious memories … the moth-trapping mission, 'walk-the-plank' party, Kennedy Lake surf wakeboarding, Mexican Fiesta, parking lot party … for the margaritas and Sailor Jerry's, the beach fires, and, generally, the wonderful community that you provided. I want to give special thanks to Sibylla. I could not have imagined to find a better roommate, colleague, and, most of all, friend. Many individuals at Parks Canada also made this research possible. Thank you so much Yuri, Danielle, Mike, Caron, Laura, Phil, and Dan for all your assistance with and enthusiasm for this project.

Lastly, but in no way a reflection of importance, thank you so much to my family. Particularly, thanks to Dad and Roger for the complimentary RTK survey, it was a life-saver. And to Grace & Alan for making sure I'm fed and for providing perspective. I love you guys.

1.0 Introduction

1.1 Background

Recent research shows that in the northeastern Pacific Ocean and coastal British Columbia (BC) extreme events (e.g., windstorms, storm surges) are increasing in frequency and/or magnitude with climate variability and change (Ruggiero *et al.*, 2001; Allan & Komar, 2006; Walker & Barrie, 2006; Cumming, 2007; Abeysirigunawardena & Walker, 2008; Walker & Sydneysmith, 2008). Variations in climate and sea level in the northeastern Pacific Ocean are often teleconnected to ocean-atmosphere phenomena including the El Niño-Southern Oscillation (ENSO), the Aleutian Low Pressure System, and the Pacific Decadal Oscillation (PDO) (Storlazzi *et al.*, 2000; Ruggiero *et al.*, 2001; Barrie & Conway, 2002; Allan & Komar, 2006; Walker & Barrie, 2006; Cumming, 2007; Abeysirigunawardena & Walker, 2008; Walker & Sydneysmith, 2008). These phenomena can cause annual to inter-annual changes in controlling regimes that are superimposed on longer-term trends in temperature, precipitation, storm frequency and intensity, and sea levels (e.g., Abeysirigunawardena & Walker, 2008; Walker & Sydneysmith, 2008). This has serious implications for coastal systems, which are expected to experience increased erosion and/or sedimentation, landward migration or loss of beach-dune and barrier systems, higher tidal inundation and flooding, and ecosystem and/or biome shifts (e.g., Allan & Komar, 2006). These impacts pose considerable challenges to coastal communities and agencies in managing infrastructure and in governing protected areas.

Sandy beach-dune ecosystems are proportionately rare in BC. Typically, beach-dune systems require a renewable supply of unconsolidated sediments and a shallow nearshore environment. However, most of coastal BC is typified by rugged, bedrock coastlines with narrow continental shelves and adjacent steep submarine slopes (Holland, 1976; Clague & Bornhold, 1980). Overall, less than 10% of the BC coast is comprised of beaches whereas greater than 80% is bedrock shoreline (Harper & Sawyer, 1983). Due to the limited occurrence of beach-dune ecosystems, little habitat is available to support specialized coastal dune fauna and flora. Consequently, these habitats support a number of species of concern (Tables 1.1 and 1.2) with high conservation significance (Page, 2003). Active or *dynamic* dunes (i.e., those on

which contemporary aeolian activity takes place) are important for all of the listed species given their early successional nature (Hillen & Roelse, 1995; Hugenholtz *et al.*, in press).

Table 1.1. Provincially and federally listed flora supported by beach-dune systems in BC (N. Page, personal communication, May 4, 2010; BC Conservation Data Centre, 2010). As classified by the BC Conservation Data Centre (BC CDC), blue listed species are species of special concern (formerly vulnerable) in BC, and red listed species are species that are extirpated, endangered or threatened in BC. As classified by the Committee on the Status of Endangered Wildlife in Canada (COSEWIC) species of special concern are species at risk of becoming threatened or endangered due to a combination of biological characteristics and identified threats, and endangered species are species facing imminent extirpation from Canada or extinction. Species marked with a star are found within Pacific Rim National Park Reserve.

Scientific Name	Common Name	Status according to BC CDC	Status according to COSEWIC
*Abronia latifolia**	yellow sand-verbena	Blue	Unlisted
*Abronia umbellata**	pink sand-verbena	Red	Endangered
Camissonia contorta	contorted-pod evening primrose	Red	Endangered
Cardionema ramosissimum	sandmat	Red	Unlisted
Carex pansa	sand dune sedge	Blue	Unlisted
*Convolvulus soldanella**	beach morning glory	Blue	Unlisted
Eleocharis kamtschatica	katmchatka spike-rush	Blue	Unlisted
*Glehnia littoralis**	beach carrot	Blue	Unlisted
Homalothecium arenarium		Blue	Unlisted
*Lathyrus littoralis**	grey beach peavine	Red	Unlisted
Lomatium dissectum	fern-leaved desert-parsley	Red	Unlisted
Mertensia maritime	sea bluebells	Blue	Unlisted
*Myrica californica**	California max-myrtle*	Blue	Unlisted
*Polygonum paronchyia**	black knotweed	Blue	Unlisted
Senecio pseudoarnica	beach groundsel	Blue	Unlisted

Table 1.2. Provincially and federally listed fauna supported by beach-dune systems in BC (N. Page, personal communication, May 4, 2010; BC Conservation Data Centre, 2010). See Table 1.1 for definitions of BC CDC and COSEWIC statuses. Species marked with a star are found within Pacific Rim National Park Reserve.

Scientific Name	Common Name	Status according to BC CDC	Status according to COSEWIC
*Anarta edwardsii**	Edwards' Beach Moth	Red	Endangered
*Branta bernicla**	Brant	Blue	Unlisted
*Cervus canadensis roosevelti**	Roosevelt Elk	Blue	Unlisted
Copablepharon fuscum	Sand Verbena Moth	Red	Unlisted
Eremophila alpestris strigata	Streaked Horned Lark	Red	Endangered
Hesperia Colorado oregonia	Western Branded Skipper	Blue	Unlisted
Limnodromus griseus	Short-billed Dowitcher	Blue	Unlisted
*Patagioenas fasciata**	Band-tailed Pigeon	Blue	Special Concern
Pooecetes gramineus affinis	Coastal Vesper Sparrow	Red	Endangered
*Sturnella neglecta**	Western Meadowlark	Red	Unlisted

Beyond their ecological value in providing key habitat for endangered fauna and flora, beach-dune systems, like dune fields outside of coastal settings, act as valuable corridors for wildlife movement (e.g., Barrows, 1996). They also offer natural coastal defenses, providing large stores of coastal sediments that buffer landward areas from extreme wave erosion and storm surge flooding events (Van der Meulen & van der Maarel, 1989).

1.2 Study Site and Rationale

Sandy beach-dune systems are proportionately rare in BC and consequently, many of the specialized species supported by these systems are species of concern (Tables 1.1 and 1.2). Thus, conservation efforts for listed species are very lucrative at the study site, Wickaninnish Beach (Figure 1.1), which is home to the largest beach-dune system on Vancouver Island, BC.

This study characterizes site morphology and improves understanding of site morphodynamics (e.g., wind, wave, and water level regimes). An understanding of site morphodynamics is vital to the development of effective habitat conservation strategies (e.g., approaches to the maintenance of system dynamism) and will assist in the understanding of other beach systems in the region. While extreme events (e.g., erosive water levels) are important to the maintenance of system dynamism in that they provide disturbance needed for the initiation of aeolian erosion, these same events may be responsible for habitat loss (e.g., shoreline retreat, salinization) and are of concern to parks management for the conservation of species at risk and the upkeep of infrastructure. Therefore, this research will also investigate the incidence of erosive events and the dune rebuilding potential, exploring possible linkages to known climate variability phenomena and climate change trends that may control site geomorphic processes. In addition to informing parks management strategies and infrastructure planning, this research broadens current understanding of the morphodynamics of mesotidal beach-dune systems in Western Canada and their potential responses to climate variability and change. To date, this has been an area of limited research.

Wickaninnish Beach, located in Pacific Rim National Park Reserve (PRNPR), is a high energy, mesotidal (i.e., tidal range of 2 – 4 m), embayed, prograding beach with a southwest aspect to the open Pacific Ocean. The beach is four kilometres long, extending from the southeastern headland of Wickaninnish Bay (Quisitis Point) to the outlet of Sandhill Creek. The transgressive dune field at Wickaninnish Beach (centred at UTM Zone 10, 304063 m E, 5433690 m N) is approximately 650 m in shoreline width and 200 m in landward depth. It is fronted by roughly 550 m of vegetated foredunes, of which only approximately 100 m is dominated by natural *Leymus mollis* plant communities and the remainder is dominated by non-native *Ammophila arenaria* plant communities. Within the dune field are saucer and trough blowouts, coppice dunes, and large precipitation ridges migrating into established forest. Aerial photographic evidence suggests the beach is prograding at 0.2 m a^{-1} (Heathfield & Walker, in review), although repeat scarping reveals the beach is exposed to erosive, high water events. South of the transgressive dune field, a smaller active blowout complex exists (centred at UTM Zone 10, 304390 m E, 5433297 m N). It is backed by a few relict dunes in the forest that front

the paleoshoreline. Dunes that extend north of the transgressive dune field to the outlet of Sandhill Creek are largely stabilized. Understanding of the morphodynamics of Wickaninnish Beach will assist in the understanding of other beach systems in the region exposed to similar wind, wave, and water level regimes (e.g., response to relative sea level fall).

Other beaches in the immediate vicinity of Wickaninnish Beach include Combers Beach, Long Beach, Schooner Cove, and Florencia Bay (Figure 1.1). Combers Beach is immediately north of Wickaninnish Beach. It is roughly two kilometres long and extends from the outlet of Sandhill Creek to Green Point. This beach exhibits a convex geometry versus the typically concave geometry of embayed beaches. The backshore is characterized by an erosive scarp and an extensive large woody debris (LWD) accumulation zone. Combers Beach transitions into Long Beach which is six kilometres long and extends from Green Point to Box Island. The larger embayment, Wickaninnish Bay, includes Wickaninnish Beach, Combers Beach, and Long Beach and is approximately 9.5 km wide from Quisitis Point to Box Island, with a total shoreline distance of 12 km. Beach sediments in Wickaninnish Bay are predominantly very well-sorted fine sands. North of Wickaninnish Bay is Schooner Cove, an embayed, moderately well-sorted sandy beach with a south aspect facing the open Pacific Ocean. The beach supports a well-developed foredune and a small, stabilizing dune complex. Beyond the southeastern end of Wickaninnish Bay is Florencia Bay. Like Wickaninnish Bay, Florencia Bay also has a southwest aspect towards the open Pacific Ocean. However, the shoreline of Florencia Bay is backed by an erosive coastal bluff system contrasting the prograding shoreline of Wickaninnish Bay. All of the beaches are exposed to a high energy, mesotidal regime.

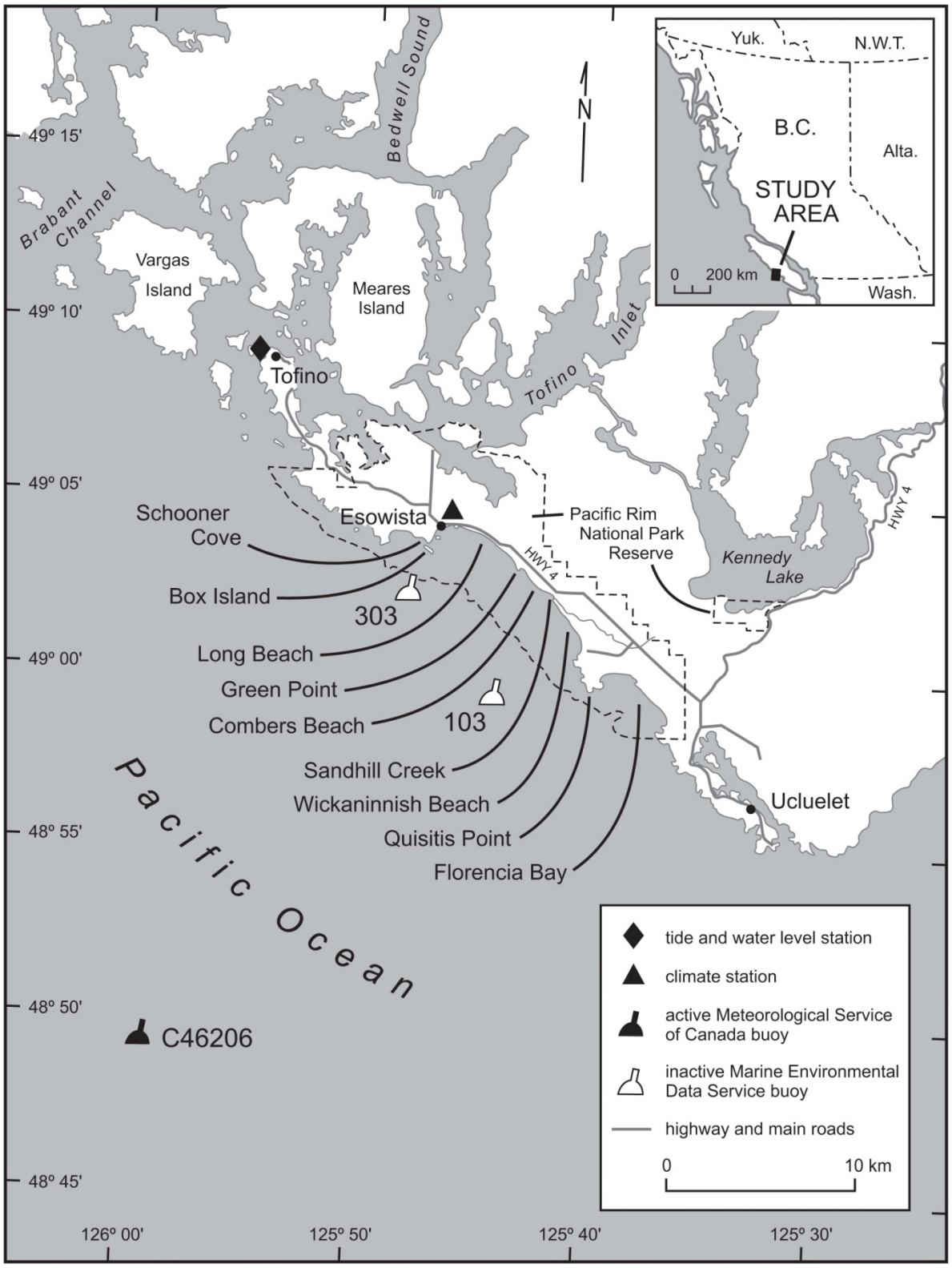

Figure 1.1. Map of study region also showing climate and tidal stations, and nearshore and offshore buoys (cartography by Ole Heggen).

1.3 Research Purpose and Objectives

The purpose of this research is to characterize the morphology of and improve understanding of beach-dune morphodynamics on Wickaninnish Beach and to investigate the erosional water level regime and its relationship with climate variability forcing. The following objectives directed this research:

i. To describe the beach-dune systems of Wickaninnish Beach and the factors (geological, climatological, oceanographic, and ecological) contributing to their present-day morphology;
ii. To characterize site morphodynamic processes by examining wave, tide, and wind regimes and their corresponding morphological impacts (e.g., erosion, dune migration);
iii. To assess the potential for onshore aeolian sediment transport responsible for the maintenance of current shoreline trends (i.e., progradation) and rebuilding following erosive events given the local wind regime and modal sediment grain diameter;
iv. To examine the erosion potential of beach-dune systems by superimposing calculated water levels (derived from observed water levels and calculated wave runup) on cross-shore beach profiles and, from this, develop a modern recurrence interval of erosive events where total water levels exceed the elevation of the beach-dune junction; and,
v. To explore correlations between regional climate variability signals (e.g., MEI, NOI, PDO, ALPI) and the total water level regime to investigate the possible relationships between climate variability and beach-dune erosion.

The significance of this research lies in improving our knowledge of morphodynamic responses of high-energy, wave-dominated, mesotidal beaches in BC to climate variability (e.g., increased storminess) and change (e.g., sea-level change) impacts. In addition, this research has direct relevance for protected areas management (e.g., developing mitigation measures for habitat preservation in areas host to listed species) and infrastructure planning.

1.4 Collaboration

This research was supported financially and logistically by Parks Canada Agency (PCA) and the University of Victoria (UVic) via a collaborative Mathematics of Information Technology

and Complex Systems (MITACS) Accelerate BC Graduate Internship. It was supplemented with funding from a NSERC Discovery Grant to Dr. Walker and a grant from the Clayoquot Biosphere Trust. The research was conducted, in part, to serve a PCA agenda to develop and implement a new geoindicators monitoring program for coastal erosion and shoreline dynamics in PRNPR. In response to recent directives, PCA has increased ecological monitoring efforts to provide information for regular State of the Park reporting and to improve understanding of the effectiveness of parks management actions (Parks Canada Agency, 2005). The coastal geoindicators monitoring program is part of a tri-park initiative involving Gwaii Haanas National Park Reserve and Haida Heritage Site (GHNPR), Gulf Islands National Park Reserve (GINPR), and PRNPR. The monitoring program aims to identify site morphological responses (e.g., shoreline retreat/progradation, dune stabilization) that result from different beach types, tide ranges, and water level regimes. Where possible, relations between driving wind, wave, and water level regimes are correlated to known climate variability signals. This information is useful for enhancing understanding of the vulnerability of coastal sites with key cultural and ecological value to climate variability and change and will aid in the development of mitigation strategies.

1.5 Thesis Outline

This thesis is organized into five chapters. Chapter 1 offers a brief introduction to the study area and presents the research objectives. Chapter 2 provides an overview of the regional geology, the prevailing wind, wave, and water level regimes, and gives a description of site morphology. Chapter 3 examines beach-dune morphodynamics (e.g., nearshore sediment transport, potential aeolian sediment transport). Chapter 4 analyses the interactions of the controlling processes of beach-dune morphodynamics with climate variability and change. Finally, Chapter 5 presents a summary and conclusion of the study and identifies areas for future research.

2.0 Beach-Dune Systems of Wickaninnish Beach

This chapter has two parts. First, it examines the factors that influence beach-dune morphodynamics on Wickaninnish Beach (e.g., regional tectonics, surficial and bedrock geology, modern climate, the wave and wind regime, typical vegetation, and non-native species). Second, it characterizes the general geomorphology of beach-dune systems along Wickaninnish Beach, giving consideration to the above factors. This chapter provides context for the study of beach-dune morphodynamics (Chapter 3) and the investigation of climate variability and change impacts (Chapter 4).

2.1 Tectonics

Tectonics affect longer-term processes on Wickaninnish Beach. Their most significant role is that they regulate sea levels relative to the land mass, where rising sea levels responding to tectonic subsidence may create erosive shorelines, and falling sea levels responding to tectonic uplift may create prograding shorelines. The study area is strongly influenced by a convergent plate margin (part of the larger Cascadia Subduction Zone), where the Juan de Fuca plate subducts beneath the North American plate (Figure 2.1). The average current convergence rate of the Juan de Fuca plate relative to the North American plate is 39.3 to 42.9 mm a^{-1} in a NE direction (Mazzotti *et al.*, 2003).

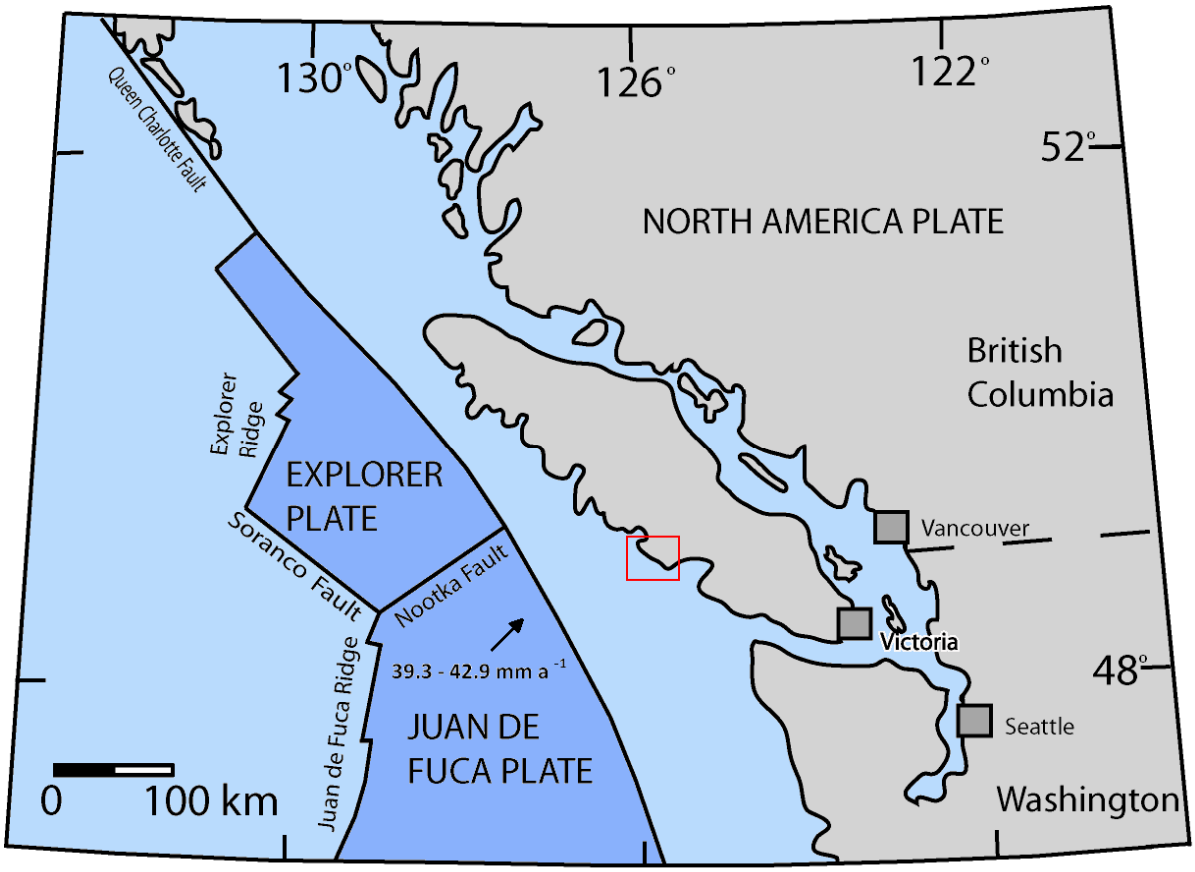

Figure 2.1. Tectonic setting of Western North America. The arrow indicates the direction of plate movement. The study region is within the red rectangle. Modified from Wolynec (2004).

Continual plate convergence during the interseismic stage, the stage in which elastic strain accumulates due to relative plate motions, results in elastic bending and buckling of the continental crust as its seaward edge is pulled down by the subducting slab (Ziv *et al.*, 2005). This stage generally lasts for a period of years and causes a vertical crustal deformation (bulge) on the seaward edge and a shortening of the crust across the margin as stress continues to accumulate. This bulge is responsible for regional crustal uplift and relative sea level changes and, correspondingly, is partially responsible for continued progradation of the Wickaninnish beach-dune system (see section 3.3.6). See Table 2.1 for published uplift rates calculated for the study area.

Table 2.1. Calculated uplift rates for the study region.

Study	Uplift (mm a^{-1})
Wigen & Stephenson, 1980[1]	2.50 ± 0.48
Wolynec, 2004[2]	2.92 ± 0.14
Mazzotti *et al.*, 2007[2]	2.7 ± 0.9
Mazzotti *et al.*, 2008[2]	2.6 ± 0.8

[1] Uplift rate calculated using annual mean sea level data from tidal gauges.
[2] Uplift rate calculated using continuous GPS data.

During the coseismic stage, the period in which elastic strain is abruptly released, an earthquake ruptures the locked portion of the fault, lifting the seaward portion of the continental crust, and causing a collapse of the bulge (Ziv *et al.*, 2005). This stage generally occurs over the period of seconds to tens of seconds and may cause sea levels to rise rapidly as the crust subsides. In the event of an earthquake of sufficient magnitude to rupture the locked portion of the fault, regional subsidence of anywhere from 0.5 to 2 m is predicted at Wickaninnish Beach (Hyndman *et al.*, 2004). This will cause rapid sea level rise on Wickaninnish Beach (and at all locations along the Cascadia margin that subside) and, in response, considerable shoreline retreat is expected. Stratigraphic research in the study area reveals the last large earthquake (moment magnitude $\geq$ 8) occurred approximately 300 years ago, where the interval of past great earthquakes is between 500 to 600 years (Clague & Bobrowsky, 1994).

2.2 Regional Surficial Geology

The surficial geology of the area surrounding Wickaninnish Beach is important as it supplies material to the beach and dune systems. Previous to the Late Wisconsin (Fraser) Glaciation of the Pleistocene Epoch, the physiography of western Vancouver Island reflected predominantly tectonic processes (e.g., insular mountains)(Harper & Sawyer, 1983). However, this physiography was modified significantly as glaciers advanced across the region about 25 ka ^{14}C BP (Lang & Muller, 1975; Harper & Sawyer, 1983, Clague & James, 2002). At the last glacial maximum (~14 ka ^{14}C BP), ice moved in a SW direction across the region, extending in places to the edge of the continental shelf (Clague & James, 2002) and reaching elevations of 1555 m relative to contemporary sea levels (Alley & Chatwin, 1979). This extent was maintained for approximately 200 to 300 years before the ice sheet began to decay (Clague & James, 2002).

During retreat of the ice sheet, glacial tills and outwash sediments were deposited over the Estevan Coastal Plain, a lowland extending 290 km along the SW coast of Vancouver Island that includes the study area (Harper & Sawyer, 1983). During deglaciation, sea levels rose as the rate of eustatic sea level rise surpassed the rate of isostatic rebound (Lang & Muller, 1975; Clague & Bornhold, 1980; Harper & Sawyer, 1983). This resulted in the submergence of the Estevan Coastal Plain and the deposition of a layer of marine clays in the study region. Around 12 ka ^{14}C BP the rate of eustatic rise slowed and the submerged coastline began to emerge due to isostatic rebound. As sea levels stabilized, sedimentary deposits were left exposed and vulnerable to wave erosion and removal by nearshore currents, which resulted in the formation of a steep wave-cut scarp on the backshore of Wickaninnish Beach. This feature is evident in recent LiDAR imagery (Figure 2.10) as discussed below. Harper and Sawyer (1983) suggest that at approximately 2 ka ^{14}C BP Grice Bay was connected to Wickaninnish Bay and the open Pacific Ocean through a tidal inlet that existed just north of Green Point. Due to continued isostatic and tectonic uplift and the corresponding regression of sea levels, the tidal inlet closed approximately 1 ka ^{14}C BP. With the continued regression of sea levels, erosion of the marine scarps backing Wickaninnish Bay ceased and the beach began to grow seaward. Materials eroded from Florencia Bay (an embayed coastal bluff system ~1.5 km SE of Wickaninnish Bay, see Figure 1.1) and the continental shelf began to accumulate on the beach face at Wickaninnish Bay via littoral and aeolian processes (Harper, 1980). In addition, both Sandhill Creek (in Wickaninnish Bay) and Lost Shoe Creek (in Florencia Bay) contributed to this accretion via fluvial sediment inputs. Sediments underlying Wickaninnish Beach and backing Florencia Bay are made up of outwash sands and gravels. North of Sandhill Creek, sediments are littoral in origin where marine drift sediments have been deposited in an unsorted, chaotic form directly on the seafloor by melting ice calved and/or rafted during a period of glacial retreat (Valentine, 1971). To date, Wickaninnish Beach continues to prograde and aeolian processes have transported sediments landward creating dune complexes in some places.

Sands on Wickaninnish Beach are derived from coastal, aeolian, and fluvially reworked outwash sands that are predominantly unimodal very well to well-sorted fine sands. They are composed mostly of quartz and potassium feldspar (Bremner, 1970).

2.3 Regional Bedrock Geology

Knowledge of the regional bedrock geology is important as it is revealing of the regional geological history (e.g., characterized by tectonics) and it contributes to present-day embayment and beach morphology as it influences the available sediment, location of beaches, and nature of morphodynamic processes (e.g., nearshore islets alter the character of the wave field). The study region is typified by a rocky shoreline, excepting the beaches found in the Long Beach Unit (Yorath, 2005). Bedrock backing the beach within Wickaninnish Bay is of the Pacific Rim Complex, which is a mélange of landslide material characterized by "severely deformed sandstone and mudstone turbidites, limestone, volcanic rocks, and chert" (Yorath, 2005, p.177). Lang and Muller (1975) suggest the Pacific Rim Complex is a subduction-mélange (a mixture of rocks of geologically distinct origin joined in the accretionary wedge above a subduction zone) while Brandon (1989) argues that the material more likely originates from submarine slides, rock falls, debris flows, and *in situ* liquefaction attributed to recurrent seismic events. Bedrock outcrops and headlands exist within Wickaninnish Bay and exert some control on nearshore currents, wave dynamics, and littoral sediment transport pathways. North of Wickaninnish Bay, rocky shorelines are predominant and are interspersed with pocket beaches. Several surf channels have been eroded into the bedrock along fault zones of weaker materials (Lang & Muller, 1975). Similar rocky shorelines exist south of Wickaninnish Bay, excepting Florencia Bay, which is an embayed, erosive shore backed with bluffs of glacial outwash sands and gravels.

2.4 Modern Climate

Climate governs a number of factors affecting beach-dune systems including available moisture, total sunlight, temperature, and wind speed and direction. These factors determine both vegetation growth and sediment transport potential which correspondingly have strong influence on resultant morphodynamic processes. According to the Köppen (1923) classification, the climate in the study region is *Cfb* (*marine West Coast cool*), where *C* indicates a moist, subtropical to mid-latitude climate, *f* indicates no period of precipitation deficiency, and *b* indicates a range of temperatures where summers are cool and winters mild. The longest climate record available in the region (1942 to 2009) is from Environment Canada's (EC) Tofino

Airport meteorological station (EC-ID 1038205). Therefore, average climate information presented here is based on the Canadian Climate Normals (1971-2000) for the Tofino Airport[1] (Figure 2.2). The average annual air temperature in this region is 9.1°C (average daily maximum of 12.8°C, average daily minimum of 5.4°C). Monthly mean air temperatures vary from a low of 4.5°C in January to a high of 14.8°C in August. On average, air temperatures fall below freezing only 0.87 days of the year. Extreme air temperatures over the period of record ranged from 32.8°C (July 12, 1961) to -15°C (January 30, 1969).

The region experiences high year-round precipitation with rainfall (> 0.2 mm) occurring, on average, 202.7 days of the year. The average total annual precipitation at Tofino Airport is 3305.9 mm, with 74.1% falling in the winter months (October through March) and only 25.9% falling during the summer months (April through September). The least monthly mean precipitation occurs in July (76.8 mm), while the greatest occurs in November (474.9 mm). Snowfall occurs infrequently, contributing only 1.3% to the total precipitation of the region.

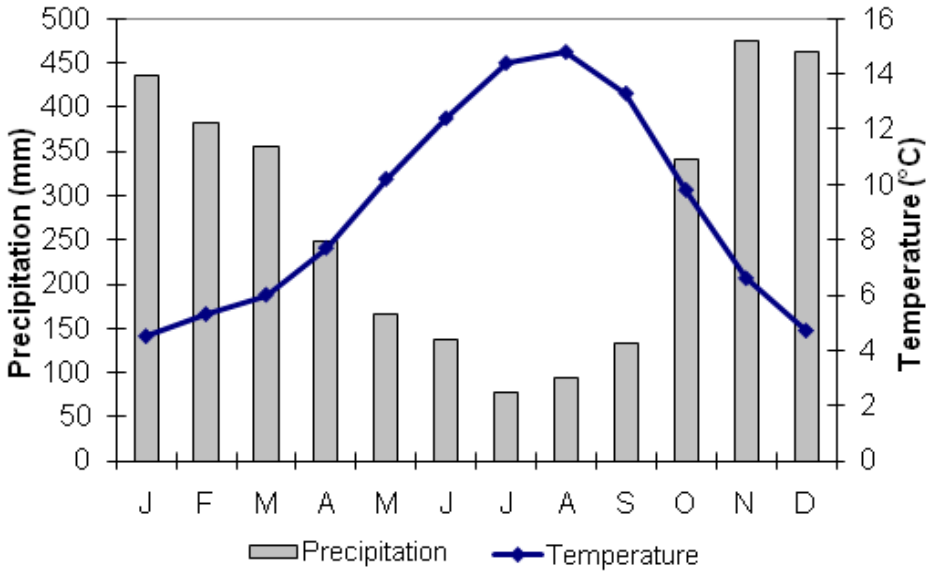

Figure 2.2. Regional precipitation and temperature averages from the Canadian Climate Normals (1971 to 2000) for climate station Tofino A (EC-ID 1038205). Precipitation is the water equivalent for all types of precipitation and is presented as the average accumulation for a given month (measured four times daily). Temperature represents a monthly average of mean daily temperatures derived by averaging the minimum and maximum temperatures measured over a 24-hour period.

[1] Available online from http://climate.weatheroffice.gc.ca/climate_normals/results_e.html

2.5 Wind Regime

The strength and direction of incident winds is determinant of fetch efficiencies, aeolian sediment transport potential, and the resultant alignment of surficial features (e.g., blowouts) in beach-dune systems. The wind regime also directs a variety of oceanographic elements including wave height and period that, along with other factors, govern beach type and shoreline trends. The west coast of Vancouver Island experiences primarily NW summer winds and SE winter winds (Clague & Bornhold, 1980; Eid *et al.*, 1993). During the winter season the jet stream shifts south and delivers strong SE winds from the offshore Aleutian Low pressure system, where the Aleutian Low is a semi-permanent low pressure system in the Gulf of Alaska. During the summer, the jet stream weakens and moves northward and, accordingly, calmer NW summer winds are delivered from the North Pacific High, a semi-permanent high pressure system in the eastern North Pacific Ocean (Clague & Bornhold, 1980; Lange, 2003). While SE and NW are the dominant wind vectors on the west coast of Vancouver Island, local land and sea breezes, in combination with secondary flow effects and topographic forcing along the shoreline (e.g., Walker *et al.*, 2009), may alter the direction and strength of sand-transporting winds on Wickaninnish Beach.

The regional wind regime was characterized using wind data from the Environment Canada meteorological station, Tofino A (EC-ID 1038205)[2]. Wind data are measured at 10 m above the surface, corresponding with World Meteorological Organization standards. Although data exist for 1960 to present, only data from 1971 to 1977 were used for this study as it is the only period where wind speed and direction measures were gathered every hour over a 24-hour period using 36-directional sectors. Using these data, one annual and twelve monthly wind roses were produced using WRPLOT[3] (Figure 2.3 & 2.4, respectively).

[2] Data from Environment Canada, Client Services and Outreach Section. Contact Giselle M. Bramwell (phone. 604.664.9067; e-mail. climatepyr@ec.gc.ca).

[3] Available online from http://www.weblakes.com/products/wrplot/index.html

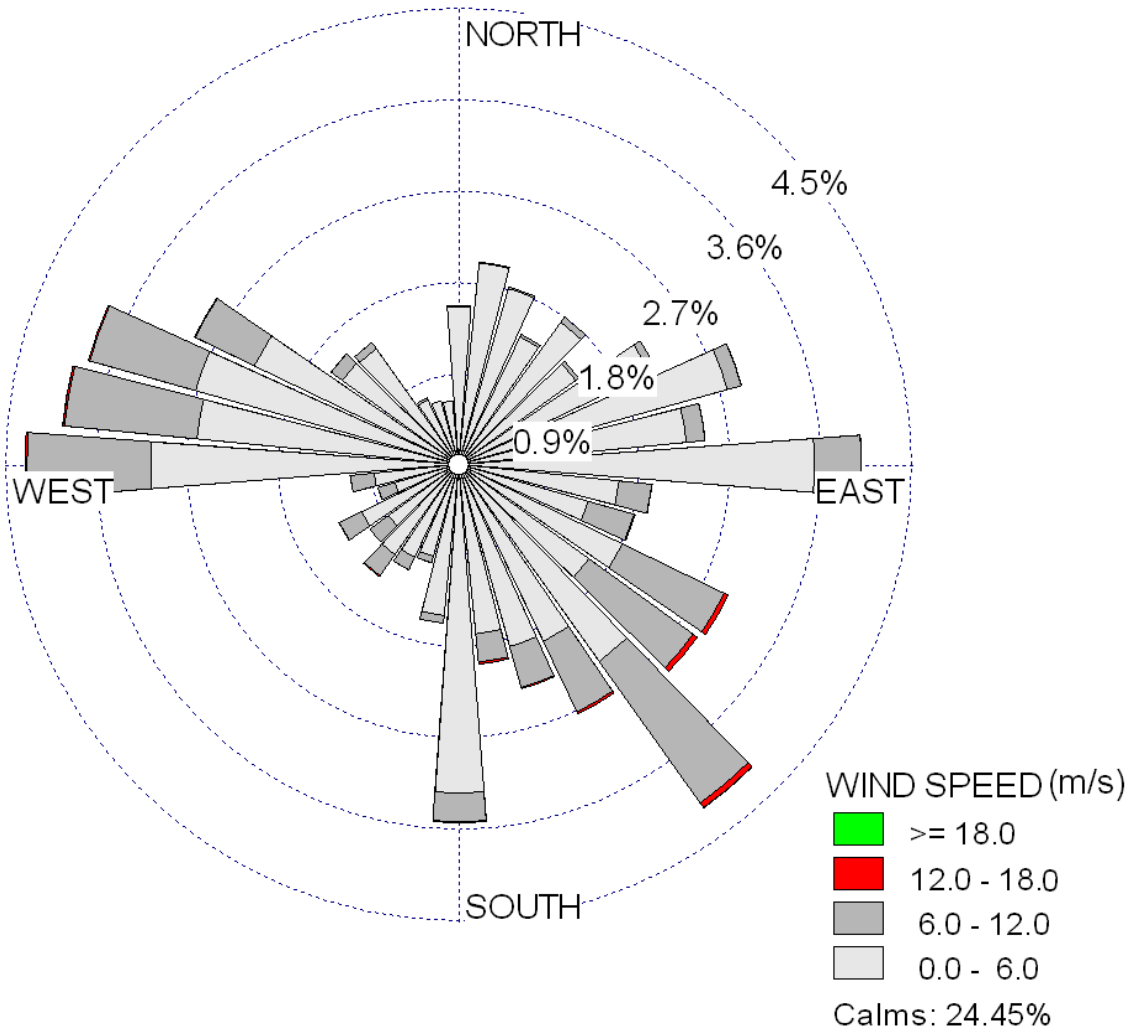

Figure 2.3. Annual wind rose for the study region. Data are from Environment Canada climate station Tofino A [EC-ID 1038205] for the period 1971 to 1977. Wind directions represent directions from which the winds are received. Wind directions represent the direction from which the winds are blowing. Calms indicate periods of no wind.

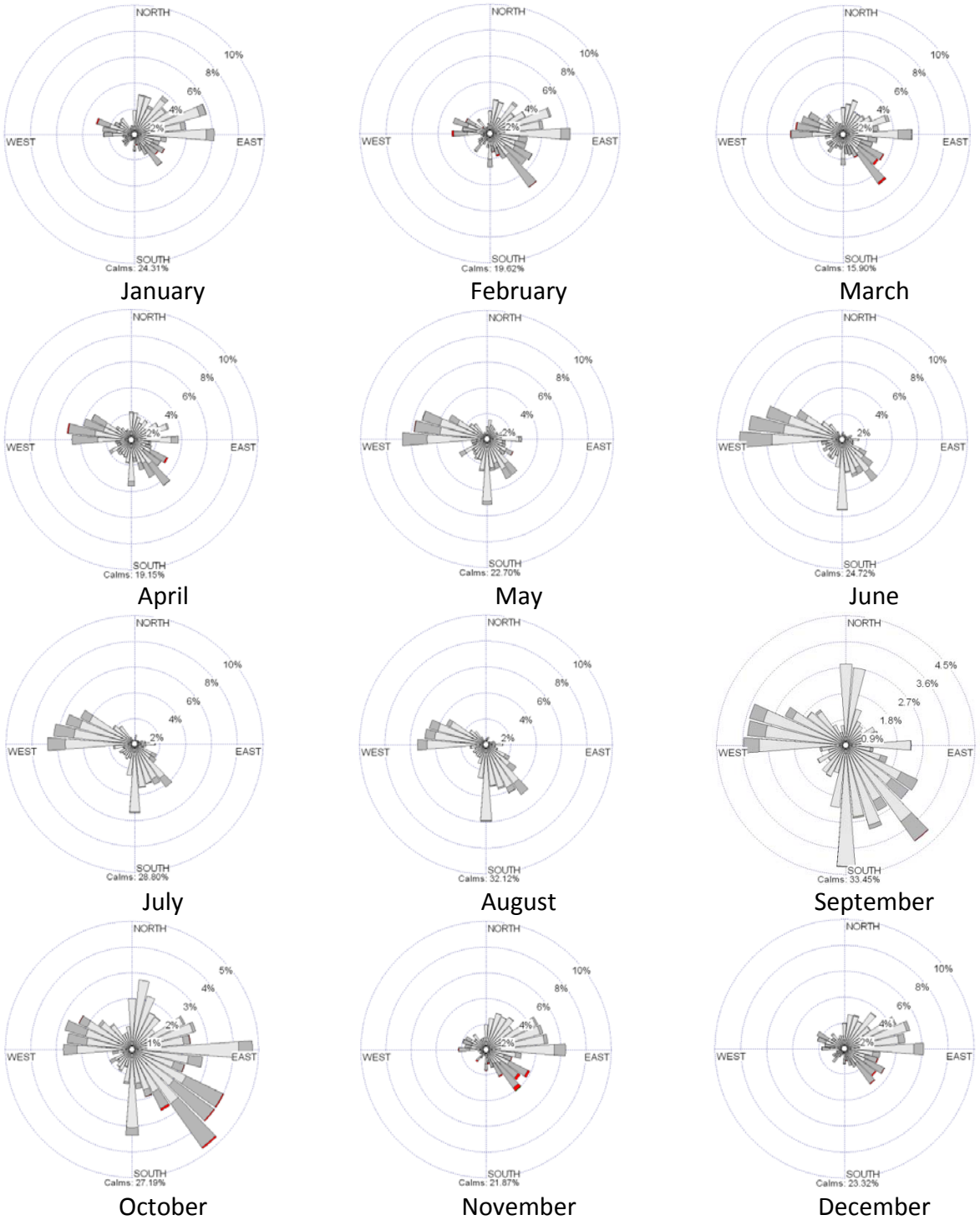

Figure 2.4. Monthly wind roses for the study region developed using wind data for the period 1971 to 1977 from Environment Canada climate station Tofino A [EC-ID 1038205]. Wind directions represent the direction from which the winds are blowing. Light gray indicates 0.0 to 6.0 ms^{-1}, dark gray 6.0 to 12.0 ms^{-1}, red 12.0 to 18.0 ms^{-1}, and green > 18.0 ms^{-1}. Calms indicate periods of no wind.

According to data from climate station Tofino A, the incident wind regime in the study region is bimodal. Frequent strong winter/spring winds ($\geq$ 12 ms^{-1}) are received from the SE with a less strong ($x < 12$ m s^{-1}) component from the E. Winter and spring winds also have a strong, but less frequent NW component. Field observations verify that strong SE winds are often followed by competent NW winds. Strong summer winds are received from the WNW with a less strong S and W component. While winter and spring winds demonstrate a considerable NW component (usually associated with summer months), the summer winds do not demonstrate a considerable SE component (usually associated with winter and spring months). Months of transition that express both wind modes include March and April (transitioning from winter to summer) and September and October (transitioning from summer to winter). Calms (periods of no wind) were experienced more often in summer months, specifically June, July, and August, and least in the winter months or months of transition, specifically February, March, and April.

The annual wind rose reveals that SE winds are the strongest and most frequent, followed by WNW winds. Less strong contributions come from the W, E, and S. While strong winds are more frequently received from the SE, the dunes exhibit a WNW alignment. This alignment can be contributed to embayment orientation, where effective SE winds are obstructed by Quisitis Point while WNW winds are received onshore. Implications for potential sediment transport are discussed further in section 3.3.3.

2.6 Vegetation and Non-native Species

2.6.1 Vegetation

Beach-dune systems support specialized flora that are adapted to cope with a number of environmental stresses including: low nutrient levels; unstable substrates with low moisture content and extreme pH levels; high winds; swash inundation; sand burial; high sunlight exposure; and, erosive sand scour (Hesp, 1991; Page, 2003). Defenses to these stresses, among many others, include leaf rolling, altered reproductive strategies, the modification of plant morphology, and growth in response to burial (Hesp, 1991). The beach-dune environment has

discrete zones within which specific plant associations are found. These zones are defined by the level of disturbance, available nutrients, and soil stability (Page, 2003). Kuramoto (1965) identified three distinct zones of vegetation on Wickaninnish Beach: the sparsely-vegetated lower beach (i.e., back beach), the grass-dominated upper beach (i.e., foredune), and the species-poor and sparsely-vegetated inter-dune. As per Page (2003), vegetation found in the lower beach zone is adapted to frequent swash inundation, high soil salinities, and deficient nutrient supplies. On Wickaninnish Beach, this zone is typified by the *Cakile edentula – Atriplex gmelinii* plant association (Table 2.2). Landward of the lower beach zone, is the upper beach zone, which, on Wickaninnish Beach, includes the foredune ridge. This zone is comparatively species rich and is characterized by greater available nutrients, higher substrate stability, and less frequent swash inundation. On Wickaninnish Beach, this zone is typified by both the *Leymus mollis* spp. *mollis – Lathyrus japonicus* and *Ammophila arenaria* plant associations (Table 2.2). Lastly, the inter-dune zone is species poor and sparsely vegetated. It is characterized by nutrient poor substrates and low moisture availability. On Wickaninnish Beach, this zone is typified by the *Poa macrantha* plant association (Table 2.2). The *Arctostaphylos uva-ursi* plant association (Table 2.2) also has a strong presence on Wickaninnish Beach. This plant association is found in both the upper beach and inter-dune zones, usually along the dune-forest margin or around the periphery of tree islands (Page, 2003).

Dune morphodynamics are directly impacted by dune ecology. Dune morphology varies according to plant canopy density and height, spacing, seasonality in density and distribution, and wind speed (Ranwell, 1972; Hesp, 1989; 2002). Both increasing canopy density and height decelerate near-surface flow, resulting in increased deposition from the leading edge of vegetation. Variability in plant distribution translates to variability in dune morphology along the shore, where erosion and accretion respond locally to surface roughness effects. Both density and distribution of plants vary seasonally and, correspondingly, this influences aeolian transport processes and deposition patterns. The wind regime not only determines transport potential but influences the aerodynamic behaviour of vegetation. Under increasing wind speeds, vegetation becomes streamlined, reducing roughness length (Hesp, 1989, 2002). For

the above reasons, vegetation type is a controlling factor of resultant dune morphologies. Thus, introduction of a non-native species that differs in life cycle, density, distribution, and morphology may not only alter the ecological beach-dune communities, but may also cause a change in dune morphology.

Table 2.2. Characteristic species of sandy beach-dune plant associations (Page, 2003).

Plant Association	Characteristic Species
Cakile edentula – Atriplex gmelinii	*Cakile edentula*, Cakile maritime*, Atriplex gmelinii, Honkenya peploides, Rumex maritimus, Leymus mollis* spp. *mollis.*
Leymus mollis spp. *mollis – Lathyrus japonicus*	*Leymus mollis* spp. *mollis, Latyhrus japonicus, Vicia gigantea, Rubus spectabilis, Fragaria chiloensis, Epilobium ciliatum, Eurhynchium oreganum.*
Ammophila arenaria	*Ammophila arenaria*, Aira praecox*, Leymus mollis* spp. *mollis, Hypochaeris radicata*, Lathyrus japonicus, Fragaria chiloenis, Cladonia* species, *Ceratodon purpurea, Ammophila breviligulata*, Peltigera* species.
Poa macrantha	*Poa macrantha, Polygonum paronychia, Abronia latifolia, Glehnia leiocarpa, Carex macrocephala, Convolvulus soldanella, Poa confinis, Tanacetum bipinnatum.*
Arctostaphylos uva-ursi	*Arctostaphylos uva-ursi, Ammophila arenaria*, Gaultheria shallon, Hypochaeris radicata*, Eurhynchium oreganum, Aira praecox*, Leptogium corniculatum, Cladonia* species, *Peltigera* species.

* indicates non-native species

2.6.2 Non-native Species

European beachgrass *(Ammophila arenaria*) and American beachgrass (*Ammophila breviligulata*), also known as marram grass, are introduced species that have become prevalent along the Pacific Coast of North America. Both species prefer colonization of the foredune region and have a considerable impact on dune morphology (Heyligers, 1985; Wiedemann & Pickart, 1996; Hilton *et al.*, 2005). *A. arenaria* is more established on Wickaninnish Beach and was planted historically for stabilization purposes. There are two hypotheses for its origin at the study site. First, it was introduced via marine dispersal from Clayoquot Island, ~24 km to the NW at the entrance of Clayoquot Sound near Tofino, where it was planted in the 1940s (Hubbard, 1969; Page, 2001). Second, it was introduced via marine dispersal from populations

introduced in Oregon and Washington (Page, 2001). Generally, *A. arenaria* is well-suited as an invasive species as it has the capability to endure long distance marine dispersal. *A. arenaria* maintains reproductive viability for up to 70 days via marine transport and survives longer in cooler water (e.g., viability retained for 40 days in 5°C seawater while only 35 days in 15°C seawater; Konlechner & Hilton, 2009). *A. arenaria* also thrives under conditions of extreme sand scour and burial, growing by both vertical and horizontal rhizomes (Van Hook, 1983). It is an effective species at dune building and is responsible for accretion and corresponding burial at rates that local dune species cannot tolerate (Heyligers, 1985; Wiedemann & Pickart, 1996; Hilton *et al.*, 2005). The capability of *A. arenaria* to withstand these rates of burial is its primary competitive advantage over native species (Hilton *et al.*, 2005). The species is also tolerant to a wide pH range and can survive in dry conditions (e.g., leaf inrolling occurs to prevent transpiration; Van Hook, 1983). However, *A. arenaria* is limited by local salt concentrations in the sand, withstanding concentrations of only 1 to 1.5% (Hilton *et al.*, 2005).

In Wickaninnish Bay, *A. arenaria* plant communities have displaced native *Leymus mollis* spp. *mollis* communities and non-native *A. arenaria* plant associations are now more abundant (Page, 2003). According to Page (2003), the native *Leymus mollis* community provides a mean percent cover of 40.5%, in contrast to the non-native *A. arenaria* community, which colonizes the foredune more densely with a mean percent cover of 61.6% (Figure 2.6). In addition, *A. arenaria* maintains rigid leaves throughout the winter, likely improving its ability to trap sand in winter transport events. Following *A. arenaria* colonization of the foredune, rapid and massive accumulations of sand result, considerably altering natural morphology and creating a steeper and relatively fixed foredune (Wiedemann & Pickart, 1996). In contrast, *Leymus mollis* communities support a more gradual, hummocky, and dynamic foredune. The development of a steeper and relatively fixed dune colonized more densely by *A. arenaria* has a notable impact on natural physical and biological dune processes. It causes an increase in the deceleration of competent winds and greater deposition of entrained aeolian sediments due to both an increase in gradient (i.e., steeper) and roughness (i.e., plant density) that creates flow separation and stagnation. Consequently, this may starve inter-dune regions of sediment inputs and, under these conditions, dune systems may trend toward stabilization (Wiedemann &

Pickart, 1996). According to Heathfield & Walker (in review), stabilization is implicated in a 27.8% loss of bare sand surface in the Wickaninnish dune system over the period 1973 to 2007 (see section 3.3.6). While encroaching plant communities are comprised of native species (such as *Arctostaphylos uva-ursi* or Kinnikinnick*),* their presence in dune ecosystems is undesired as they deprive native dune plant communities of available habitat that is limited in coastal British Columbia. More dynamic dune systems provide habitat to a number of provincially threatened species (Table 1.1) that are adapted to survive in nutrient poor sands and to tolerate salt spray, sand scour, and burial.

Efforts to restore aeolian sediment delivery to the backdune region and re-stimulate dynamism in the Wickaninnish beach-dune system began in September 2009. *Ammophila* spp. was removed both mechanically from the stoss slope of the foredune with a backhoe and specialized bucket (Figure 2.5), and manually on the lee slope and in backdune regions. Restoration efforts are planned to take place in the summer or fall over the next five years and will focus on the foredune from Combers Beach south to the small blowout complex. Some tree islands are also intended for removal.

Figure 2.5. Removal of *Ammophila* spp. from the foredune near transect 1 on September 21, 2009. Notice the specialized bucket design (i.e., finger-like appendages to sift through sands).

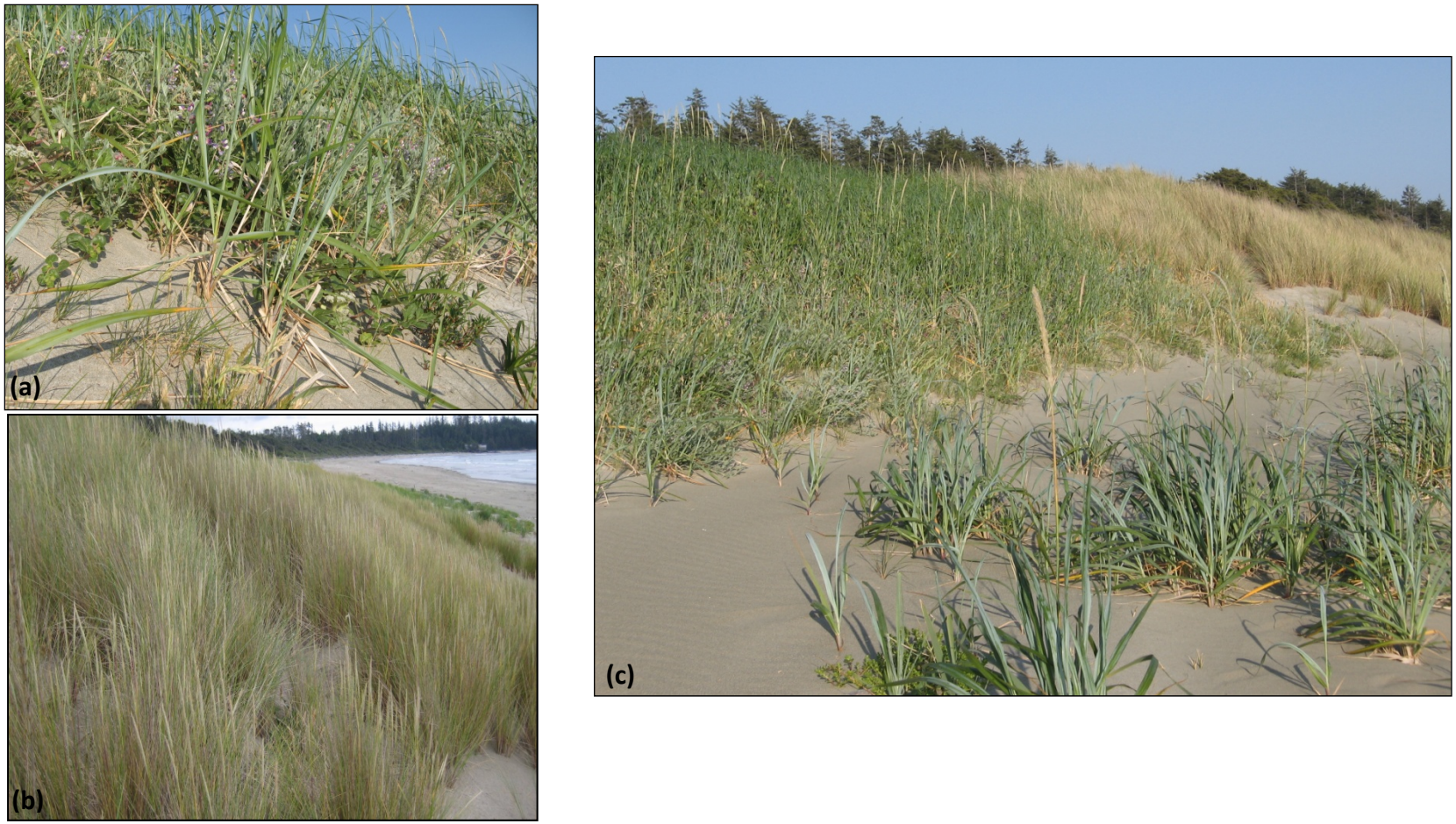

Figure 2.6. (a) Typical native Dunegrass (*Leymus mollis*) community in the Wickaninnish dunes, Pacific Rim National Park Reserve. Notice the variety of species within the community (e.g., *Lathyrus littoralis* or beach pea). Photo from Sibylla Helms, with permission. (b) Typical non-native European beachgrass (*Ammophila arenaria*) community. Notice there are few species present beyond European beachgrass. (c) Transition between native *Leymus mollis* community (darker green on left side of image) and non-native *Ammophila* community (lighter green to brown on right side of image). Photo from Sibylla Helms, with permission. All photos taken in July 2009.

2.7 Tides, Wave Regime, and Nearshore Currents

Wickaninnish Beach is exposed to energetic wave conditions (i.e., modal significant wave height of 1.14 m and peak wave period of 14.29 s) and a mesotidal regime (i.e., 2 to 4 m tidal range), where the maximum tidal difference in Tofino is 4.2 m. A wave buoy, Marine Environmental Data Service (MEDS) buoy 103, was located offshore of Wickaninnish Bay (UTM Zone 10, 299588 m E, 5429953 m N), 5.2 km WSW of Quisitis Point in 40 m of water. While it is no longer operational, it maintains the longest available record of significant wave height and period (1970 to 1998). According to MEDS 103 (disabled in 1998), over the period of record the average significant wave height entering Wickaninnish Bay was 1.97 m. The maximum significant wave height on record entering Wickaninnish Bay was attained in February 1979 reaching 11.44 m (Table 2.3) and the maximum peak period attained was in March 1997 at 28.57 s. Average winter significant wave height and peak period values are greater (2.47 m, 12.07 s respectively) than average summer values (1.49 m, 10.89 s respectively). Typically, the greatest modal values for significant wave height are measured in November (2.33 m), while the smallest modal values are measured in August (0.92 m). The greatest modal values for peak period are obtained in May through September (15.38 s) and the smallest modal values are obtained in October (11.76 s)[4].

[4] Available online from http://www.meds-sdmm.dfo-mpo.gc.ca/isdm-gdsi/waves-vagues/search-recherche/list-liste/data-donnees-eng.asp?medsid=MEDS103

Table 2.3. Mean, mode and maximum significant wave heights and peak periods from MEDS buoy 103 measured over the period 1970 to 1988. Significant wave heights are four times the square root of the first moment of the wave spectrum. Peak period is the period associated with the most energetic waves in a total wave spectrum, where period is the time elapsed between two successive wave crests.

	Significant Wave Height (m)			Peak Period (s)		
Month	**Mean**	**Mode**	**Max**	**Mean**	**Mode**	**Max**
January	2.67	2.33	7.92	12.49	13.33	22.76
February	2.51	1.78	11.44	12.49	12.50	22.76
March	2.30	1.58	8.75	12.15	14.29	28.57
April	2.09	1.60	7.43	11.51	12.50	25.00
May	1.61	1.16	5.43	11.20	15.38	27.31
June	1.45	0.95	7.83	10.70	15.38	22.76
July	1.19	0.92	3.35	10.26	15.38	22.22
August	1.18	0.84	4.34	10.68	15.38	22.76
September	1.41	0.90	6.77	10.96	15.38	22.76
October	1.97	1.61	9.43	11.34	11.76	22.76
November	2.59	2.73	10.56	11.56	12.50	22.76
December	2.79	2.25	9.20	12.38	13.33	25.00
Annual	1.97	1.14	11.44	11.45	14.29	28.57

Average sea surface temperature and salinity for the period 1934 to 2009 measured at Amphitrite Point (UTM Zone 10, 313843.64 m E, 5421793.55 m N) is 10.83°C and 3.03%, respectively[5]. Offshore currents are influenced by a NW flowing tidal flood. The velocity of winter currents is augmented by SE winter winds that align with this tidal flow direction. However, the velocity of SE flowing summer currents that respond to NW summer winds are reduced as they oppose the direction of the tidal flood (Thomson, 1981).

2.8 Beach-Dune Systems

As above, Wickaninnish Beach supports the largest beach-dune system on Vancouver Island. According to the Masselink and Short (1993) classification model Wickaninnish beach is classified as low tide bar/rip beach (see section 3.3.1). Although longshore currents were

[5] Available online from http://www.pac.dfo-mpo.gc.ca/science/oceans/data-donnees/lighthouses-phares/index-eng.htm

identified to be significant using the methods of McLaren and Bowles (1985), rip cell circulation operates in the nearshore and is evident in aerial photographs and through observation (Figure 3.9). Low amplitude bar topography is present in the nearshore, with some bars revealed at low tide (Figure 2.7). In extreme wave conditions, an outer bar is obvious from breaking waves. Further characteristics of beach morphodynamics (e.g., direction of longshore currents) are provided in Chapter 3.

Figure 2.7. Intertidal bar revealed at low tide on Wickaninnish Beach looking from the smaller dune complex to Quisitis Point. Wickaninnish Interpretation Centre visible on far left. Photo taken in August 2009.

Incipient dunes are present on the upper beach fronting the foredune and are formed principally in the lee of large woody debris (LWD) (see Walker and Barrie, 2006; Eamer and Walker, 2010) and around American beachgrass (*Ammophila brevilgulata*), European beachgrass (*Ammophila arenaria*), Dune wildrye (*Leymus mollis*), Sea rocket (*Cakile edentula*), and Seabeach sandwort (*Honkenya peploides*). Although LWD is evident in scarped foredunes in the study area, its density in the backshore is relatively low in the central portion of the study area near the transgressive dunes (i.e., between transects 1 to 3, see Figure 3.6). LWD does not seem to contribute significantly to the system morphology. However, it may play a role in

backshore morphodynamics toward the Wickaninnish Interpretive Centre and around Sandhill Creek near Combers Beach where it accumulates.

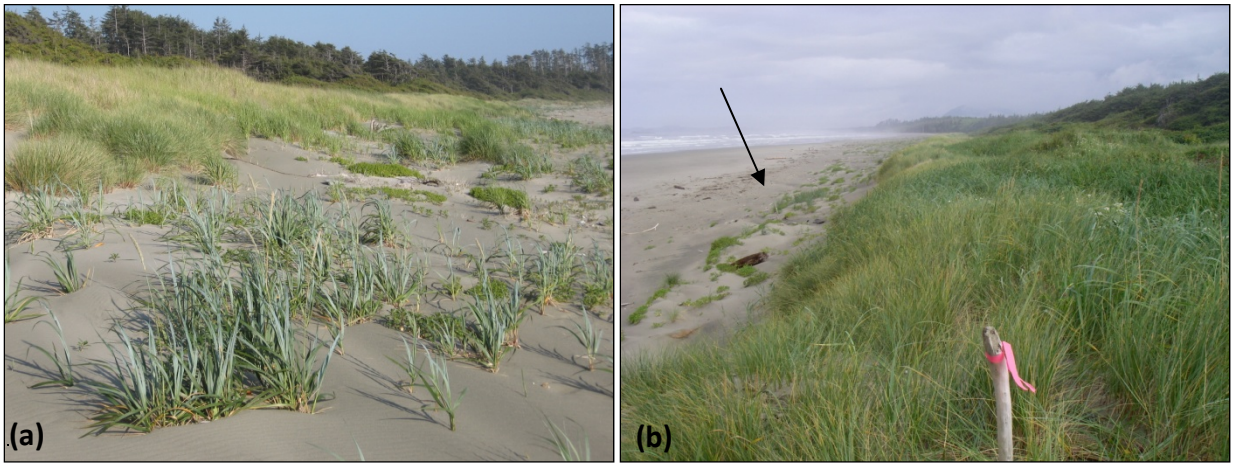

Figure 2.8. (a) Incipient foredunes fronting the large transgressive dune system. Photo taken in August 2009. Photo from Sibylla Helms, with permission. (b) Incipient foredunes (indicated by arrow) north of large transgressive dune system. Photo taken in August 2008.

A distinct foredune ridge is present on Wickaninnish Beach beginning at the small blowout complex and extending northward to the outlet of Sandhill Creek (see Figure 2.9). Over this distance the foredune ridge is continuous and relatively uniform in height (~9 to 10 m above Chart Datum [aCD]). It reaches its highest, steepest form in the NW portion of the large transgressive complex where it is ~12 m aCD. Over its southern extent, the foredune ridge is vegetated predominantly by *Ammophila arenaria*, with few remaining natural *Leymus mollis* dominated areas. North of the large transgressive dunefield the dominant foredune vegetation shifts to *Ammophila breviluglata.*

Three dune complexes exist on Wickaninnish Beach as identified in Figure 2.9 ([b], a stabilizing transgressive dune system, [c], a large, active transgressive dune system, and [d], a smaller blowout complex), in addition to an incipient dune plain [a] that extends from the established foredune plain adjacent to the migrating outlet channel of Sandhill Creek.

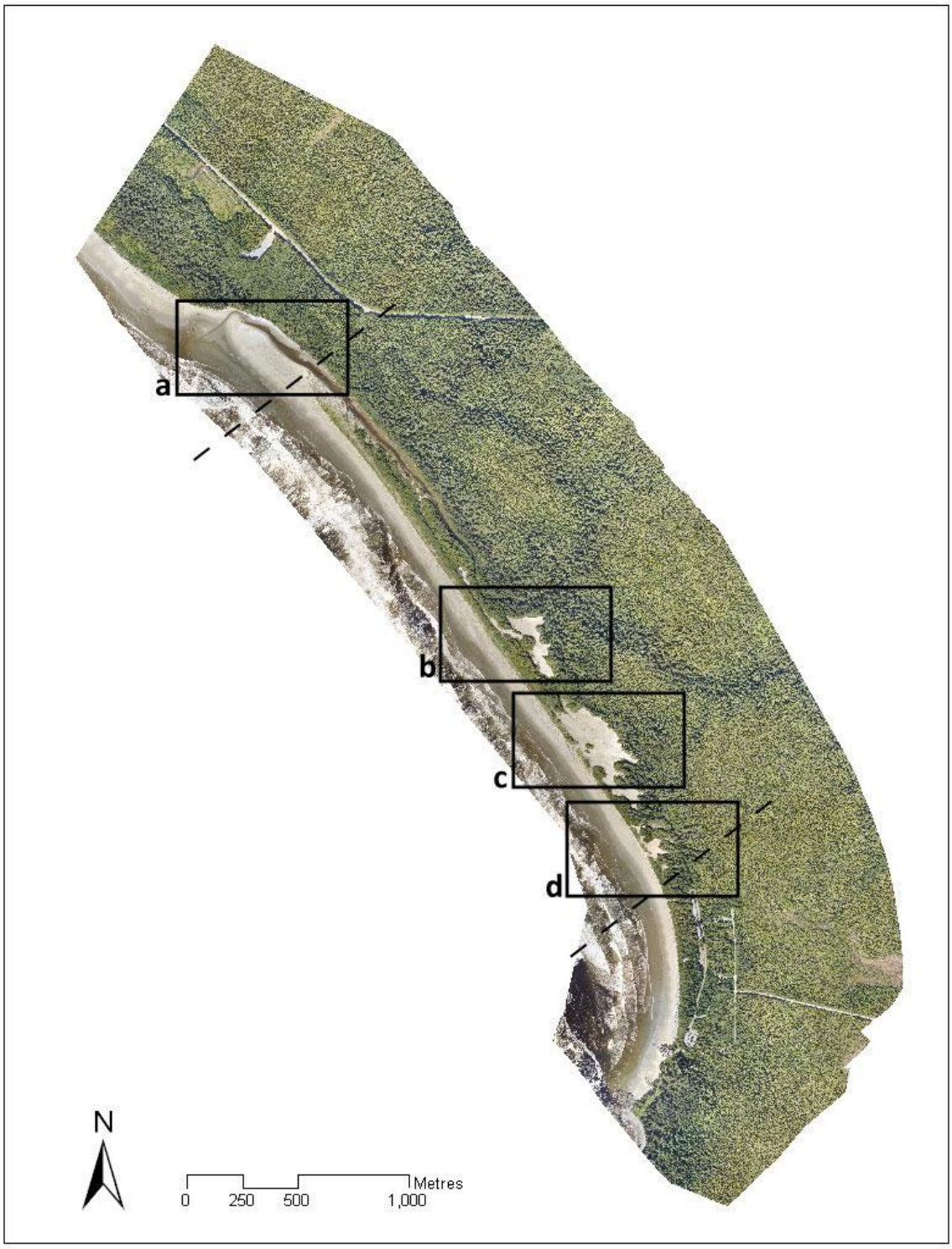

Figure 2.9. Aerial photomosaic of Wickaninnish Beach. Aerial photographs obtained August 27, 2009. (a) Sandhill Creek outlet and incipient dune plain; (b) Stabilizing transgressive dune complex; (c) Large active transgressive dune system; and, (d) Smaller blowout complex. The extent of the established foredune is indicated by dashed lines.

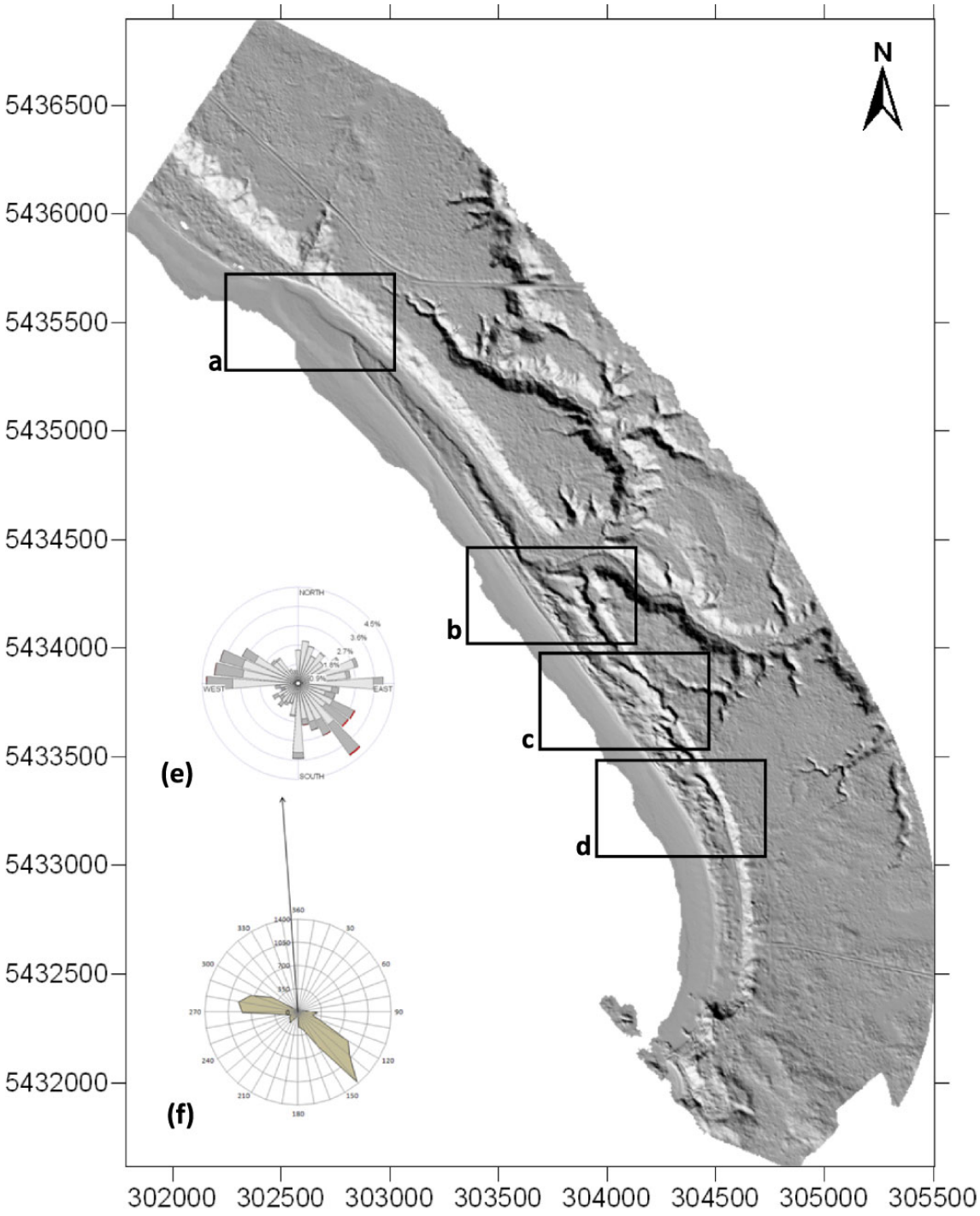

Figure 2.10. Shaded relief model of Wickaninnish Beach derived from LiDAR imagery gathered August 27, 2009. The image extends from Sandhill Creek mouth in the north, to Quisitis Point in the south. (a) – (d) described in Figure 2.9. Regional wind (e) (light gray 0.0 to 6.0 ms^{-1}, dark gray 6.0 to 12.0 ms^{-1}, red 12.0 to 18.0 ms^{-1}, and green greater than 18.0 ms^{-1}) and aeolian sediment drift (f) roses (solid brown areas represent potential transport from corresponding directions and the arrow represents the resultant transport direction) shown as insets, described in more detail in sections 2.5 and 3.3.3, respectively.

A bare earth digital elevation model (DEM) of Wickaninnish Beach was produced from LiDAR data gathered August 27, 2009 (Figure 2.10). See section 3.2.5 for details of LiDAR processing. This DEM reveals a relict coastal bluff system ~300 m behind, and parallel to, the modern coastline. This erosive paleoshoreline speaks to past sea level transgression (rise) and provides evidence for subsequent sea level regression (fall) and corresponding progradation of the beach-dune system. In addition, an extensive network of well-incised river channels is apparent backing Wickaninnish Beach. Denudation and incision of the channels most likely occurred in response to continued tectonic and isostatic uplift in the region.

Sandhill Creek, part of the larger Kennedy Lake watershed, has a dendritic drainage network. Its outlet flows north along the paleoshoreline and delivers reworked sediments to the nearshore. Some of these sediments are then available to be reworked by nearshore currents and winds onto the supratidal reaches of the beach. In response to regional tectonic uplift, additional sediments may be supplied to the river systems due to continued channel incision and increasing channel gradient.

The DEM also reveals that the large transgressive dune complex is, in places, transgressing onto the paleoshoreline (Figure 2.10, inset c). Generally, the beach appears flat and featureless. However, nearer the outlet of Sandhill Creek, cuspate features are apparent on the beach face. The cusps are ~10 m in cross-shore depth and occur at a ~20 m spacing interval. These may due to refracted waves propagating off Sea Lion Rocks and/or Green Point or created from the interactions of incident waves with the morphology of, and flow from, the outlet of Sandhill Creek. These refracted or altered waves may interfere with progressive longshore wave energy from Wickaninnish Beach, creating edge waves that are believed to be primarily responsible for the formation of swash cusps on the beach face (Guza & Inman, 1975) and may explain their presence in the study area, although this is beyond the scope of this study.

The following sections describe Wickaninnish Beach geomorphology as shown in units (a-d) identified on the orthophoto (Figure 2.9).

2.8.1 Sandhill Creek Outlet & Incipient Dune Plain (A)

The morphology of this area is complex. The outlet of Sandhill Creek at the northern extent of Wickaninnish Beach is migrating in a NW direction, which has caused continual erosion of the backshore on the outer (northern) bank of the final channel bend (Figure 2.11a). This migration compromised the structural integrity of a parking lot backing Combers Beach in 1978, leading to its eventual removal in 2003 (B. Campbell, personal communication, May 21, 2009). Coincident with channel migration, the foredune complex has extended in a NW direction via prograding, recurved dune ridges at the tip of the complex. Relict foredune ridges reveal the former position of the creek outlet and provide evidence to this progradation (Figure 2.12, 2.13).

Leading the NW extension of the foredune complex is a supratidal beach plain (~41,950 m^2 from the high tide line (HTL) to the edge of the seaward creek bank; Figure 2.11b). At the time of the aerial photo survey, this plain consisted of individual shadow dunes anchored by Sea rocket (*Cakile edentula*) nearer the channel and seaward margins, to more hummocky and linear forms closer to the foredune anchored by LWD, *Cakile edentula*, Seabeach sandwort (*Honkenya peploides*),and dune grasses (*Ammophila* spp., *Leymus mollis*). Extension of the beach plain is enabled via materials continually delivered by littoral and aeolian action onto the NW extent of the plain. Littoral studies suggest a NW flowing nearshore current (see section 3.3.2), which may cause continual deposition of sediments on the SE edge of the creek outlet, encouraging the NW extension of the beach plain. The orientation of individual dune forms within the beach plain also reflect of differing aeolian transport directions, including both WNW summer winds and SE winter winds (see drift rose, Figure 2.10f). In general, the net migration of this complex, and the larger established foredune complex, corresponds well with the dominant aeolian transport modes, WNW and SE (see section 3.3.3).

Extension may also be encouraged by rapid stabilization of the foredune complex by *Ammophila* spp. The vigorous colonization by the non-native grasses may act to reinforce the foredune complex, creating a barrier more rigid than of that experienced under natural conditions (Wiedemann & Pickart, 1996). In response to dune migration and extension, the creek mouth is forced to migrate northward in an attempt to reach a quasi-equilibrium state (e.g., adjusting channel slope, width, depth, etc. to reach the least energy intensive state).

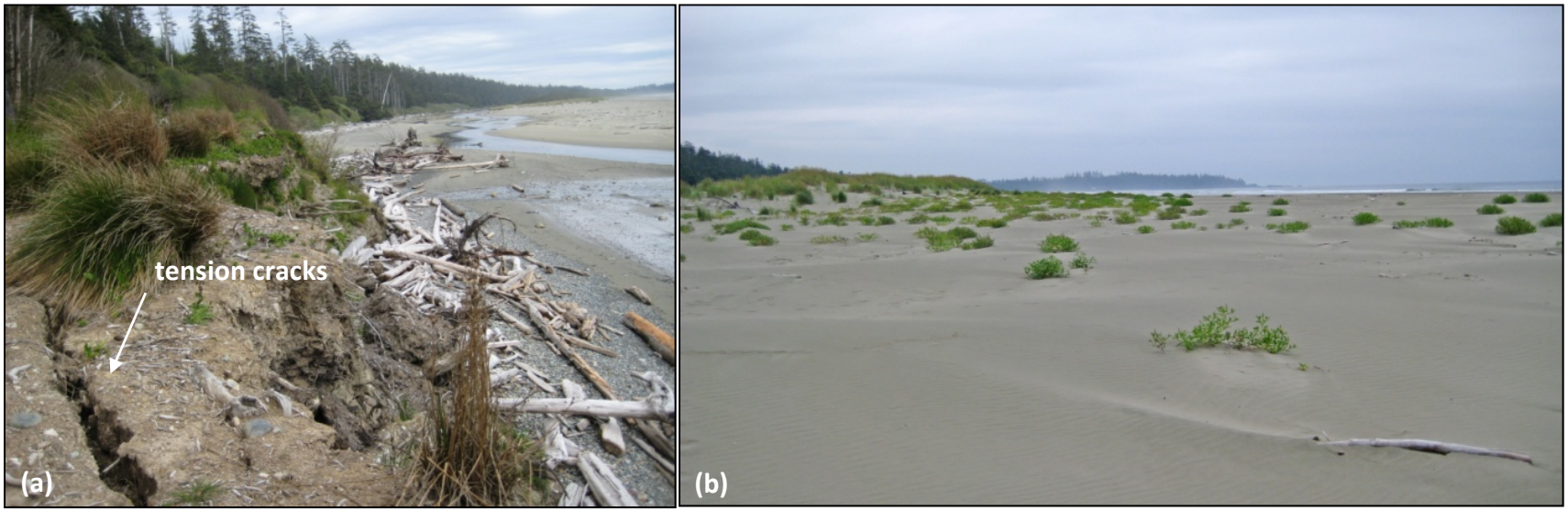

Figure 2.11. (a) Tension cracks of the eroding channel bank of Sandhill Creek. Photo taken in May 2009 from the eroding channel bend of Sandhill Creek looking south. (b) Incipient dune plain extending from the tip of the established foredune complex near Sandhill Creek (see Figure 9a). Photo taken in July 2009 from the middle of the dune plain looking SSW towards Quisitis Point. Note that shadow dunes are aligned with the SE winds.

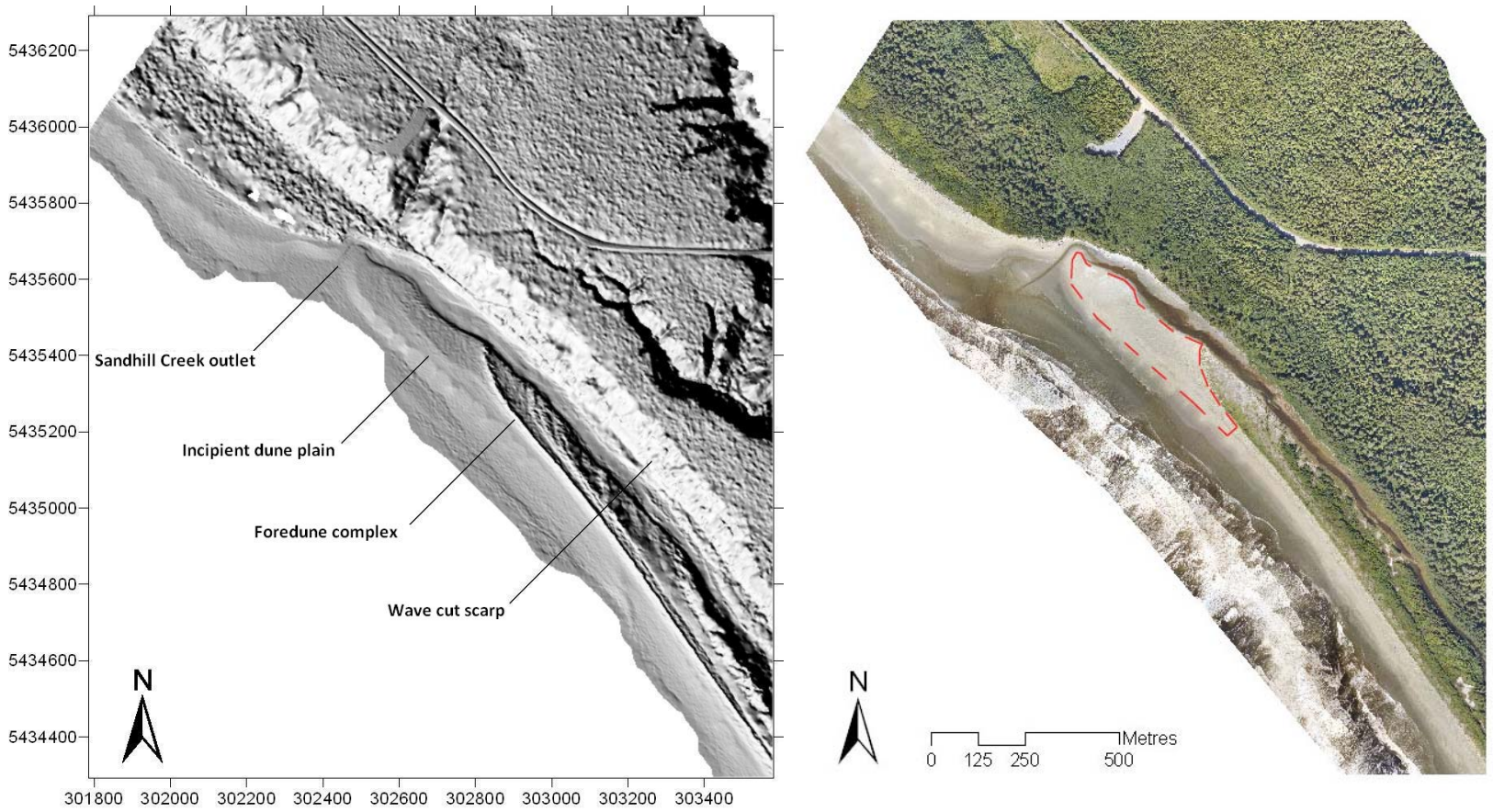

(a) **(b)**

Figure 2.12. (a) DEM of the outlet of Sandhill Creek. Notice wave cut scarps (i.e., paleoshoreline and relict foredune ridges). (b) Aerial photograph of the outlet of Sandhill Creek. Dashed red line indicates area of incipient foredune plain. Aerial photograph obtained August 27, 2009.

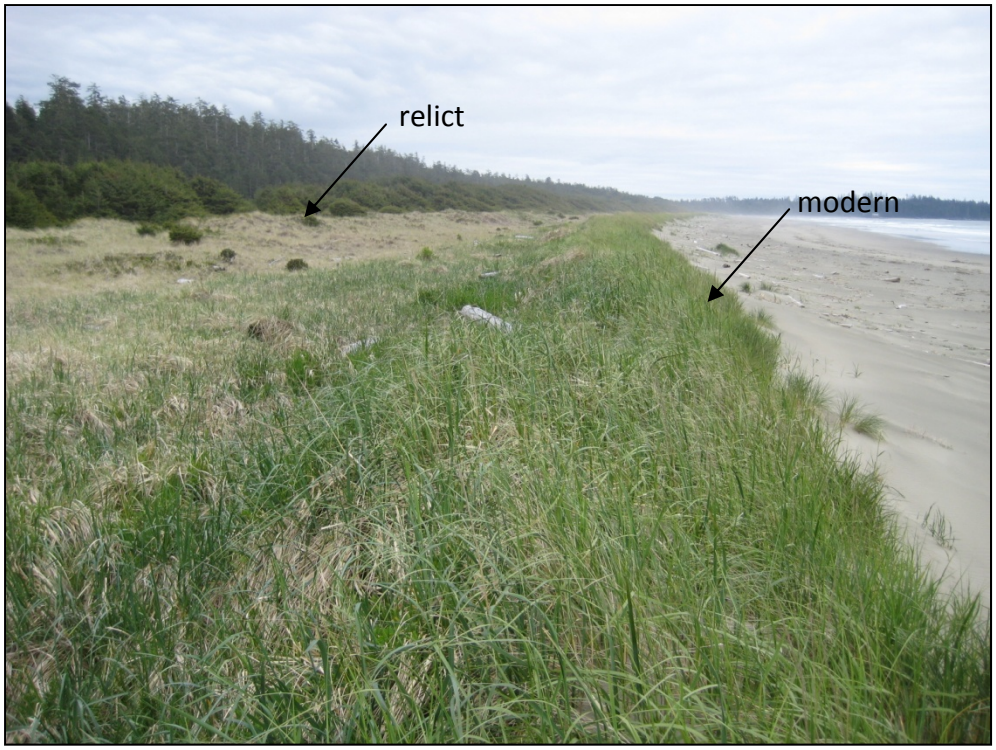

Figure 2.13. Relict and established modern foredune ridges near the outlet of Sandhill Creek. Photo taken in July 2009 looking south from foredune ridge at outlet of Sandhill Creek .

During the summer field seasons in 2008 and 2009, Sandhill Creek presented an unobstructed, free flowing channel. However, following storms in the winter of 2010, the creek became dammed by a LWD jam and, in response, the waters backed up creating a backshore swale. It is assumed this occurs periodically and influences the system morphology through limiting available sediment for transport and through rapid drainage following wave attack and removal or breaching of the barrier (Pearce, 2005; Walker & Barrie, 2006).

2.8.2 Stabilizing Transgressive Dune Complex (B)

South of the outlet of Sandhill Creek are a number of stabilized foredune ridges and blowouts (Figure 2.14a, 2.15a). Behind these stabilized dunes is a large (~21,500 m^2) transgressive dune complex (Figure 2.14b) that is essentially severed from aeolian inputs due to the dense succession of conifers along a NW-SE axis landward of the foredune. Though speculative, sand supply within this system is likely limited to the remaining deflation basin and a large blowout in the NW region of the system (Figure 2.15b). North of this system Sandhill

Creek enters the backshore from its incised valley and the backshore landscape consists predominantly of prograding foredunes that have extended northward (as discussed above). Over this same stretch *Ammophila breviluglata* begins to become more prevalent as compared to more southerly reaches of Wickaninnish Beach.

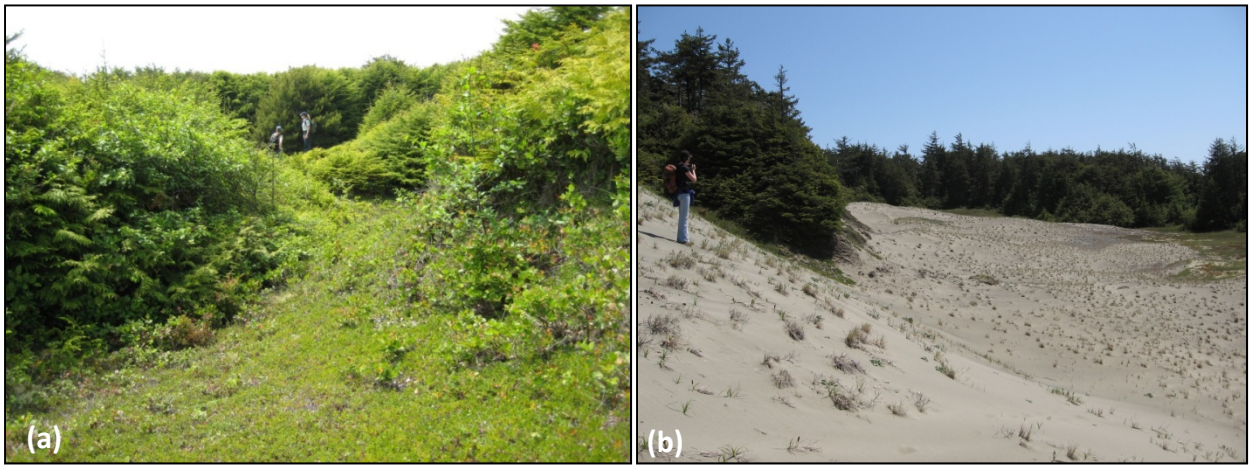

Figure 2.14. (a) Stabilized dunes on the backshore south of Sandhill Creek directly west of the stabilizing dune complex. Photo taken in July 2009. This photo corresponds to site *a* identified in Figure 2.15. (b) SE arm of the stabilizing dune complex. Photo taken mid-complex looking SE in July 2009. Photo from Sibylla Helms, with permission.

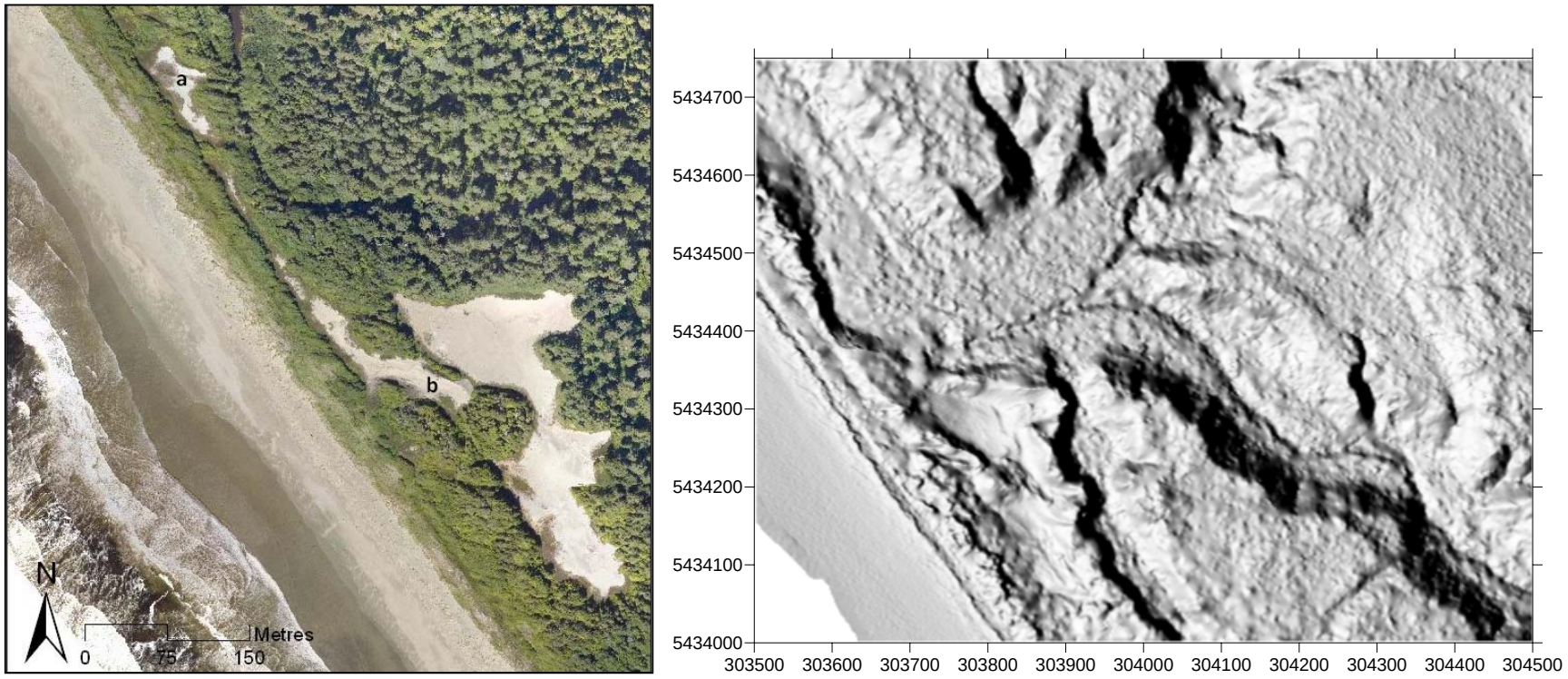

(a & b) **(c)**

Figure 2.15. Aerial photograph of stabilizing transgressive dune system. (a) Stabilized dunes on backshore corresponding to Figure 2.14a. (b) Large, active blowout feeding into the stabilizing complex. Aerial photograph obtained August 27, 2009. (c) DEM of the stabilizing transgressive dune system.

2.8.3 Transgressive Dune System (C)

The large (~62,000 m^2) transgressive dune system (Figure 2.9c and 2.10c) has a well-developed, densely vegetated foredune, fronted by small incipient dunes (Figure 2.16a). The foredune is dominated by the non-native *Ammophila arenaria,* however, a relatively intact native *Leymus mollis* community exists on the foredune on transect two and just south of transect three (for transect locations see Figure 3.6). Within the larger, active transgressive dune system are saucer and trough blowouts, erosional remnants, large tree islands, deflation plains, and large precipitation ridges migrating into established forests (Figure 2.16b). Three NE-SW aligned linear ridges intersect the dominant NW-SE dune alignments and are artifacts of ridges built for military training exercises during World War II (B. Campbell, personal communication, June 8, 2009). A number of spruce tree islands are found in the lee of the foredune ridge and within the transgressive dune complex. These features exhibit a Krumholtz formation, wind-sculpted in form with sloped upwind faces modified by aeolian abrasion. The margins of the complex are colonized predominantly by kinnikinnick (*Arctostaphylos uva-ursi*), salal (*Gaultheria shallon*), shore pine (*Pinus contorta*), Douglas fir (*Pseudotsuga menziesii*), and Sitka spruce (*Picea sitchensis*).

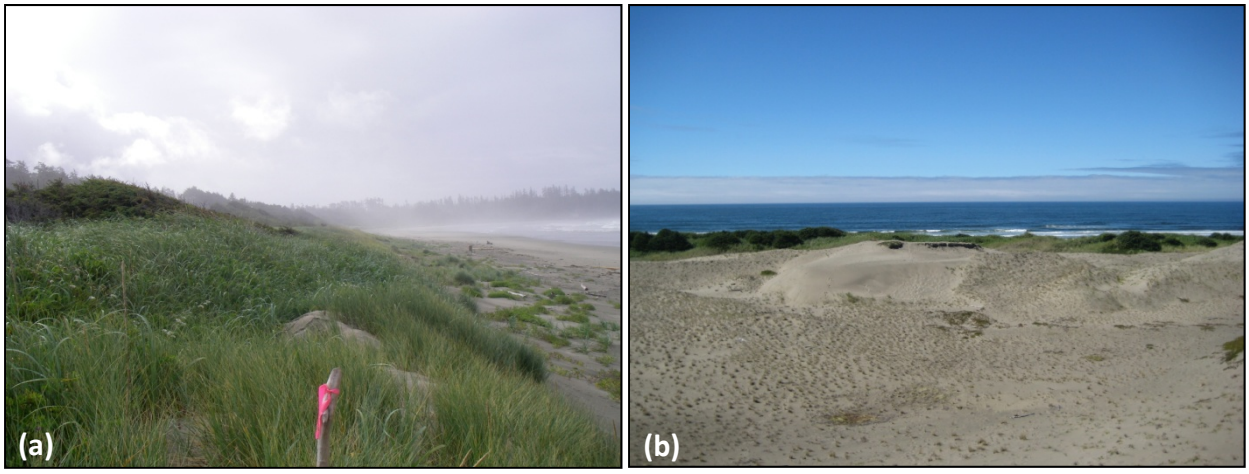

Figure 2.16. (a) Looking south along the foredune ridge from the northern extent of the system. Photo taken in August 2008. (b)Large transgressive dune system looking west from the precipitation ridge in the northern extent of the system. The depositional lobe of an active trough blowout is visible in the centre of the photo, with the vegetated foredune complex in the background. Photo taken in August 2008.

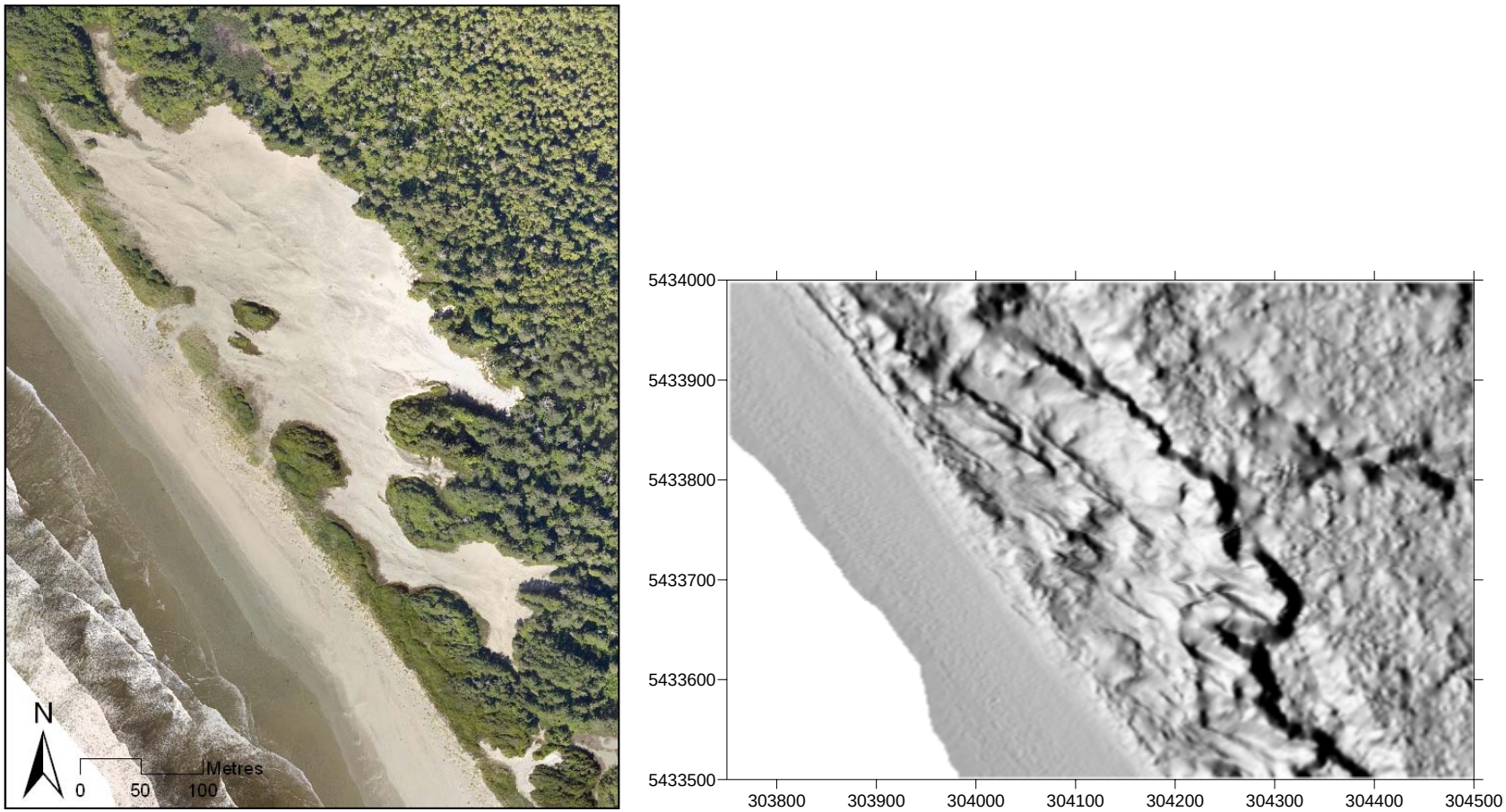

(a) **(b)**

Figure 2.17. (a) Aerial photograph of large transgressive dune system. Aerial photograph obtained August 27, 2009. (b) DEM of the large transgressive dune system.

2.8.4 Blowout Complex (D)

South of the large transgressive dune system is a smaller (~6,500 m^2) active blowout complex (Figure 2.18). It was noted in the 2008 field season that the foredune ridge fronting the blowout complex was severely scarped. However, by 2009 infilling of the scarp created a more gradual foredune fronted by incipient dunes (Figures 3.14b and 3.14c). A few tree islands exist on the foredune but none within the complex. A stabilizing arm of the blowout complex extends inland in the NE corner of the dune (Figure 2.19). Immediately south of stabilizing arm, backing the blowout complex, is a scarped ridge experiencing active aeolian erosion. In the lee of this scarp, a depositional lobe has formed and is transgressing into the forest. Both this scarping and deposition may be responsible for the death of a number of trees on the forests edge (see snags in Figure 2.18a).

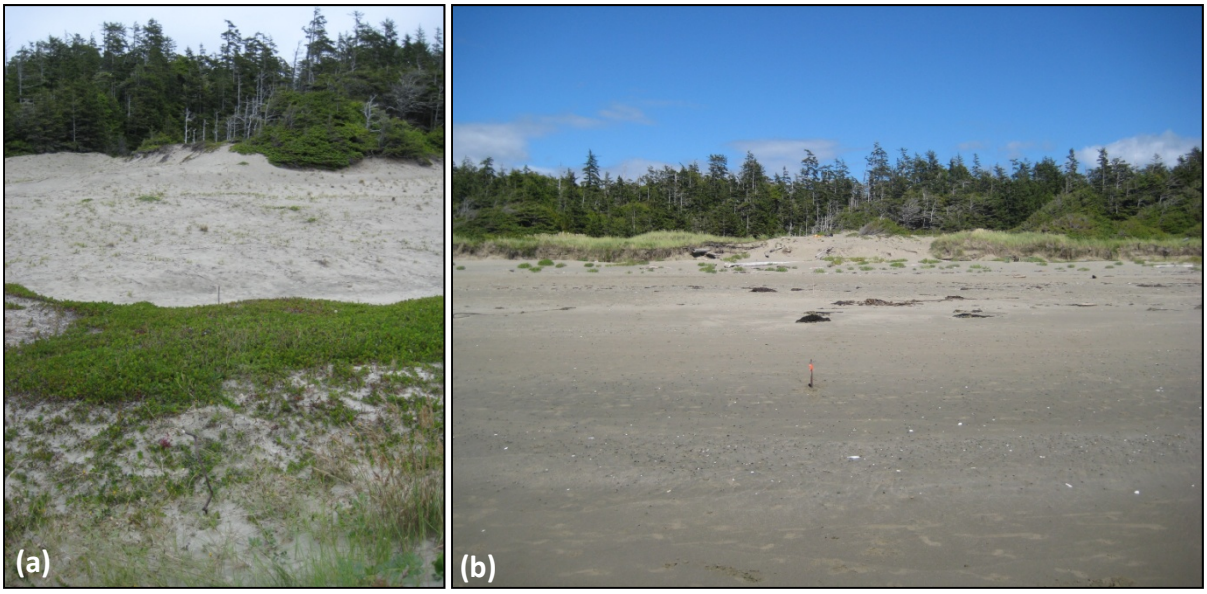

Figure 2.18. (a) Smaller blowout complex at site d. Photo taken in August 2008 from the middle of the foredune ridge looking east. (b) Foredune ridge of the smaller blowout complex. Photo taken from the beach looking east in July 2009. The denuded gap in the middle of the foredune is a result of manual removal of *Ammophila arenaria* in 2005.

An effort to restore a portion of the foredune at this site was conducted in 2005 by hand pulling of *Ammophila arenaria* along a 20 m swath of the foredune. This increased aeolian activity on the foredune slope and crest and, coupled with human foot traffic, promoted early stage blowout development. Restorative actions have been successful to date, compared to

unrestored areas directly north of the restored foredune section, in that dynamism and native species populations are returning to the site.

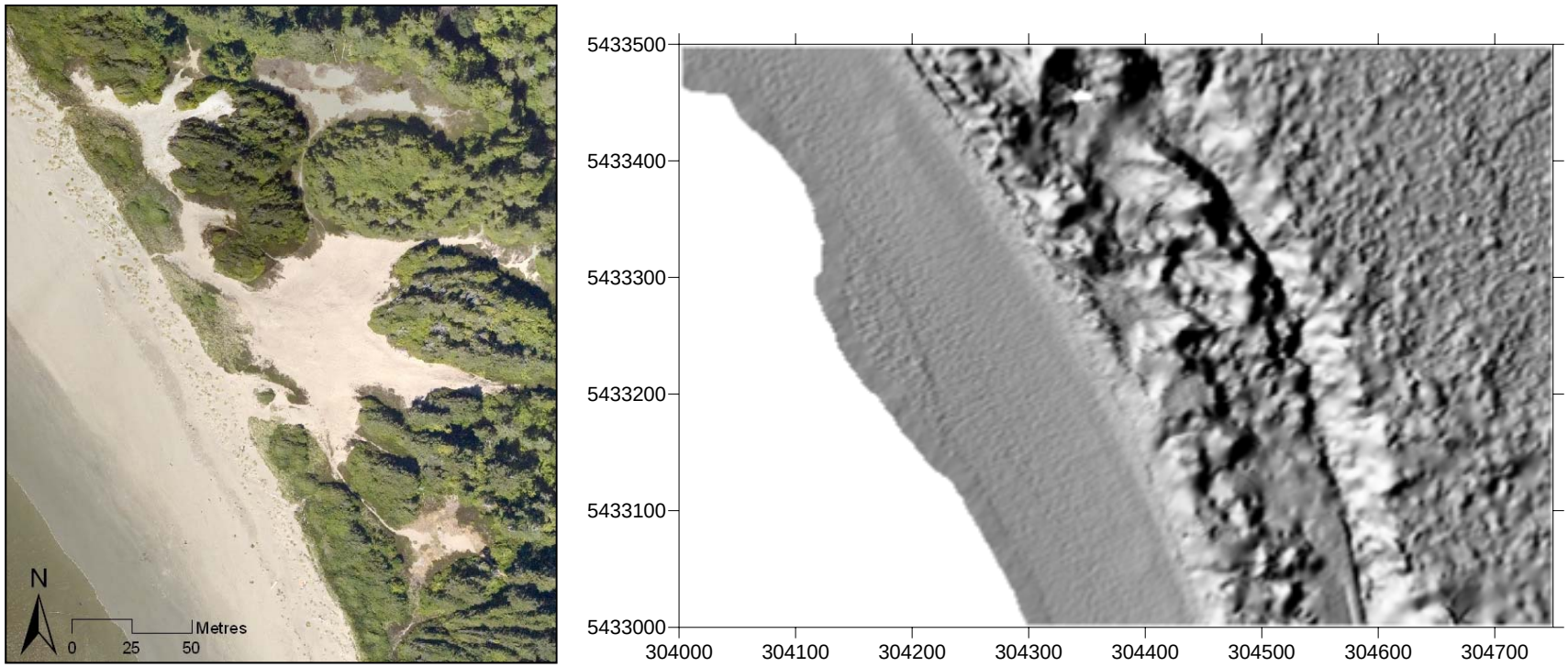

Figure 2.19. (a) Smaller blowout complex nearer the southern extent of Wickaninnish Beach. Aerial photograph obtained August 27, 2009. (b) DEM of the smaller blowout complex.

3.0 Morphodynamics of Wickaninnish Beach

3.1 Introduction

This chapter examines the morphodynamics of Wickaninnish Beach. Morphodynamics inform our understanding of the rebuilding capacity of beach-dune systems, the relationship between ecology and geomorphology, the influence of the oceanographic and climatic regime, and both event-based and longer-term beach-dune and shoreline processes. Understanding of these processes aids in our predictive ability and, correspondingly, aims to direct effective coastal management approaches (e.g., restoration approaches, infrastructure planning). This chapter provides a classification of Wickaninnish Beach (per Battjes, 1974; Wright & Short, 1983; Masselink & Short, 1993; Short & Masselink, 1999), examines the contemporary beach-dune processes (i.e., nearshore sediment pathways, aeolian sediment transport potential, temporal volumetric change), and examines historical shoreline trends (i.e., retreat/progradation).

3.2 Literature Review

This section provides a theoretical foundation to the morphodynamic assessments made in this study through a review of literature addressing beach-dune classification schemes and morphodynamics. A detailed review of beach classification models is provided including examination of the equilibrium beach profiles of Bruun (1954) and Dean (1977) and the morphodynamic models of Wright and Short (1983) and Masselink and Short (1993). The inclusion of the equilibrium beach profile is important as this theory guided the development of the more complex morphodynamic models. In addition, a general review of aeolian processes is provided and, more specifically, methods available to calculate potential aeolian sediment transport are explored, including Bagnold's (1941) equation, the Fryberger and Dean (1979) approach, and the Arens *et al.* (2004) approach. Lastly, the factors controlling dune morphodynamics are examined and Hesp's (2002) model of foredune evolution is presented.

3.2.1 The Equilibrium Beach Profile

The equilibrium beach profile was first qualitatively described in 1889 by Cornaglia (1889/1977) who hypothesized a neutral point on the beach profile where the shoreward and seaward flux of sediments are in equilibrium. The position of this neutral point is dependent on beach slope and the specific weight and grain size of the sediment. Since Cornaglia's initial work, the equilibrium beach profile has been the focus of much research. Defined, more contemporarily by Larson (1991), the equilibrium beach profile is a beach of specific grain size, when if exposed to constant forcing conditions (normally assumed to be short-period breaking waves) will develop a profile shape that displays no net change over time. Dean (1991) suggests the equilibrium beach profile is characterised by four key attributes: (i) an upward, concave form; (ii) a more gradual slope corresponding to smaller grain sizes; (iii) a planar beach face; and, (iv) a more gradual slope resulting from steeper waves. While in reality the equilibrium beach profile is rarely realized, equilibrium theory has provided a useful heuristic from which reference conditions can be drawn to gauge beach change and form (Cowell *et al.*, 1999).

Bruun (1954) and Dean (1977) were among the first to attempt to quantitatively characterise the equilibrium beach profile. They identified three possible governing mechanisms of the equilibrium beach profile: (i) a uniform average longshore shear stress; (ii) a uniform average energy dissipation rate per unit area; and, (iii) a uniform average wave energy dissipation rate per unit water volume. Based on previous work by Bruun (1954) and Dean (1976), Dean (1977) found the equilibrium beach profile to be of the form:

$$h = Ax^m \tag{1}$$

Where h is the water depth at a distance x from shore (m), and A and m are scale and shape constants, respectively. The values of these constants were determined through empirical analysis of 504 profiles from the Atlantic and Gulf coasts of the United States. Depending on the destructive agent responsible for offshore transport, m was either 0.4 (based on uniform stress or average energy dissipation across the surf zone) or 0.67 (based on uniform average wave energy dissipation rate per unit volume across the surf zone). Of the 504 cases analysed, the m value of 0.67 occurred most frequently and Dean (1977) concluded that fixing the m at 0.67 was most representative. This finding suggested the dominant mechanism governing the

equilibrium beach profile was the stability of the sediment under a certain level of turbulent water particle fluctuations. It allowed for the calculation of equilibrium beach profiles from sediment characteristics (fall velocity and/or diameter). This work provided a foundation for more contemporary beach models.

3.2.2 The Beach-Dune Profile

Categorization of the beach-dune profile is important as it breaks down the beach profile into organized units of analysis that are defined by the processes that operate within them. As per the categorization scheme of Short (1999), a cross-sectional beach profile is made up of essentially four morphodynamic zones, the shoaling, surf, and swash zones (Figure 3.1) and the backshore and dunes. Each zone is typified by distinct morphology and geomorphic processes. The shoaling zone defines the seaward edge of the beach system and is marked by the point where the wave base begins to interact with the seabed. Typical shoaling zone morphology includes an upward, concave, and gradually sloping profile with rippled bedforms. As interaction with the seabed increases, wave orbital motions begin to elongate, steepening the wave until breaking point, which defines the beginning of the surf zone. The surf zone is the most dynamic zone due to the interaction of breaking waves and currents with the seabed. Surface morphology may include bars, troughs, ripples, and channels. The surf zone extends from the breaking point to the point of final wave collapse, where swash begins to form. Swash is the wave-induced oscillation of the water's edge across the beachface (Hughes & Turner, 1999). The swash zone extends from the final point of wave collapse to the upper limit of swash action and is typified by a steeper seaward sloping profile. The upper limit of swash action is largely a function of profile slope, wave type (i.e., plunging, surging, or spilling) and height, tidal range, and sediment properties (Short, 1999). Tide range transfers these three morphodynamic zones and the shoreline across the beach profile with each tidal cycle and resultantly, intertidal morphology is defined by a mixture of hydrodynamic processes (Masselink & Turner, 1999). Tides also contribute geomorphically effective energy to the beach system through tidal currents (Short, 1999).

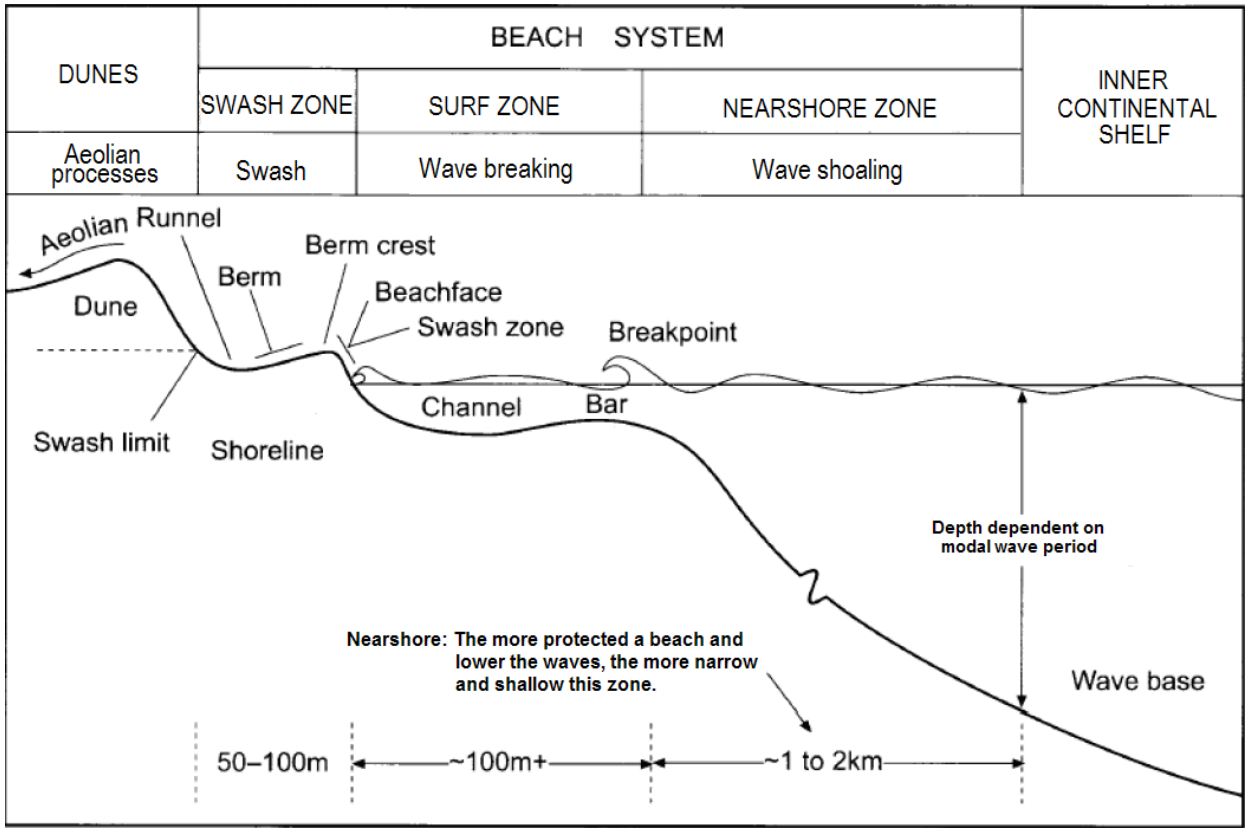

Figure 3.1. Categorization of a high energy beach-dune profile. Modified from Short (1999).

Landward of the swash zone is the subaerial beach and backshore. The width of the backshore is dependent on beach type (e.g., reflective, dissipative), tidal range (e.g., microtidal, mesotidal), sediment supply, and beach-dune mobility (i.e., prograding, eroding, stable) (Short & Hesp, 1982; Hesp, 1999). Microtidal beaches range from wide, dissipative forms lacking berms to moderately wide with some berm morphology to narrow, steep, and reflective with pronounced berm morphology. Meso- to macrotidal beaches are typically wider, with a gradual sloping lower to mid-intertidal zone and a steeper upper-intertidal zone. As wave energies and tidal range increase non-barred, ultra-dissipative beaches are more common (Hesp, 1999).

On the sub-aerial beach and backshore, aeolian processes begin to dominate, transporting sediments from the beach to the backshore and into the dunes. Aeolian transport varies depending on beach and backshore/dune morphology, gradient, and available sand surface (i.e., beach width, fetch). In general, potential aeolian transport is greatest on wide dissipative beaches, moderate on intermediate beaches, and least on reflective beaches.

Accordingly, foredunes are largest on dissipative beaches, moderately sized on intermediate beaches, and smallest on reflective beaches (Short & Hesp, 1982). Landward of the foredune typical coastal dune morphologies include blowouts, transgressive dunefields (may contain barchans, transverse, oblique, etc.), and parabolics. Backshore dune extent ranges from very small to hundreds of kilometres in extent (Hesp, 1999).

Overall, as per the wave, beach, and dune classification by Short & Hesp (1982), dissipative beaches are characterized by a high energy wave regime, wide, low gradient surf zone with bar and trough morphology, high potential aeolian sediment transport and large foredunes which display a variety of morphodynamic states. Intermediate beaches are characterized by moderate wave energies and have a complex surf zone that displays rhythmic three-dimensional topographies. Rip circulation is prevalent on intermediate beaches. As beach gradient increases, potential aeolian sediment transport decreases and, accordingly, foredune size decreases. Finally, reflective beaches are characterized by lower wave energies, a small surf zone, and a steep nearshore with a narrow beach. Potential aeolian sediment transport is limited and resultantly foredunes are small.

3.2.3 Beach Morphodynamic Models

Morphodynamic models are important as they enable both characterization of a beach based on select measureable components (e.g., mean wave breaker height) and, provided they are evaluated according to the same criteria, allow comparison between beach systems. As above, theory surrounding the equilibrium beach profile led to the development of these more complex morphodynamic models. Thus, building on the equilibrium beach profiles of Bruun (1954) and Dean (1977), Wright and Short (1983) pioneered the integration of hydrodynamic and morphologic variables in their conceptual beach model. They found existing and pre-existing beach topography affects surf zone processes, and fluid motions beyond storm waves (e.g., edge waves, longshore currents) play a significant role in determining beach character. Six morphodynamic states were recognized in this research: (i) dissipative; (ii) intermediate longshore bar-trough; (iii) intermediate rhythmic bar and beach; (iv) intermediate transverse bar and rip (normal or skewed); (v) intermediate ridge-runnel or low-tide terrace; and, (vi)

reflective. Each state supports its own distinct morphology, hydrodynamic regime, and sediment characteristics. Wright and Short (1983) distinguish between dissipative and reflective beaches, the two extreme morphodynamic states identified in their model, using the surf-scaling parameter (ε) (Guza & Inman, 1975):

$$\varepsilon = \frac{4\pi^2 H_b}{gT^2 \tan^2 \beta} \tag{2}$$

Where H_b is breaker height (m), g is the acceleration of gravity (9.81 m s^{-1}), T is wave period (s), and β is beach gradient. When $\varepsilon > 30$ dissipative morphology can be expected and when $\varepsilon < 2.5$ reflective morphology can be expected. Four intermediate morphologies are identified: longshore bar-trough; rhythmic bar and beach; transverse bar and rip; and, ridge-runnel or low tide terrace. These morphologies are more difficult to classify as they experience both dissipative and reflective conditions and, resultantly, ε is more variable. As this model was primarily derived using data from microtidal beach systems it is limited in application for beaches with larger tidal ranges (Masselink & Short, 1993).

A subsequent model by Masselink and Short (1993) incorporates relative tide range (*RTR*) and a dimensionless sediment fall velocity (Ω) to classify beach type (Figure 3.2). Masselink and Short (1993) found that a large relative tide range indicates a tidal dominance in the beach system, whereas small values indicate wave dominance. Parameters required for use of this model are: (i) breaker height (H_b); (ii) sediment fall velocity (w_s); (iii) wave period in seconds (T); and, (iv) spring tide range (*MSR*). Overall, using these parameters the dimensionless fall velocity (Ω) and relative tide range (*RTR*) can be calculated using the following equations:

$$\Omega = \frac{H_b}{WsT} \tag{3}$$

and,

$$RTR = \frac{MSR}{H_b} \tag{4}$$

Dimensionless fall velocity (Ω) and relative tide range (RTR) values are then input to the conceptual beach model to determine the beach state. Masselink & Short (1993) identify nine beach types in their model: (i) reflective; (ii) low tide terrace with rips; (iii) low tide terrace without rips; (iv) barred; (v) low tide bar/rip; (vi) barred dissipative; (vii) non-barred dissipative; (viii) ultra-dissipative; and, (ix) tide-dominated tidal flats. Masselink and Short (1993) recognize the following limitations of their model (per Cumming, 2007): (i) it was developed primarily using empirical data from macrotidal beaches of Queensland, Australia and should be applied carefully in other locations; and, (ii) it may predict bar morphology in low energy environments ($H_b < 0.25$ m) where infragravity waves and corresponding bar morphologies are absent. In addition, Masselink and Short (1983) acknowledge their criteria for differentiating between reflective and low tide terrace beaches is rather arbitrary as the formation of low tide terraces is a function of the drainage capacity of the beach, a parameter that is not considered in this model.

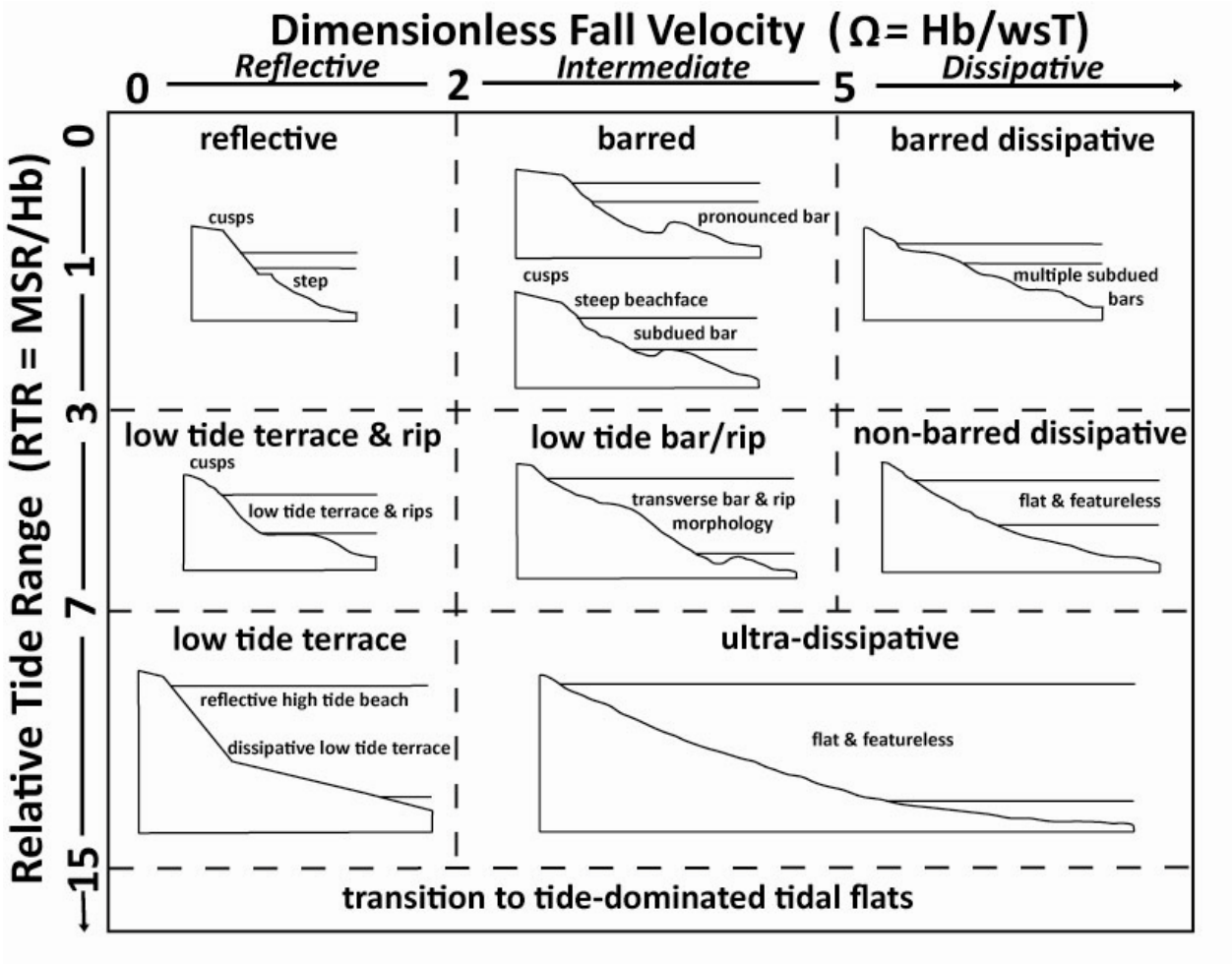

Figure 3.2. Conceptual beach model showing the nine morphodynamic states of the beach. The horizontal axis represents dimensionless fall velocity ($\Omega=Hb/w_sT$) and the vertical axis represents relative tide range (RTR=MSR/Hb; modified from Masselink & Short, 1993).

3.2.4 Aeolian Sediment Transport

Aeolian sediment transport is a key component of the rebuilding potential and morphodynamics of beach-dune systems. In broadest terms, it is the movement of sediments by the force of the wind. Aeolian sediment transport results when shear stress (τ) exerted by near-surface flow exceeds the resisting forces of sediment weight and cohesion, and grains are lifted into transport (Sarre, 1987). Near-surface flow is affected by the nature of the underlying surface and can be explained using boundary layer theory. The lower 10 to 20% of the boundary layer is characterised by a log-linear increase in velocity with height above the surface (Oke, 1978). The Law of the Wall describes this log-linear increase in velocity (see Equation 11).

Particles in transport are moved in four main ways: creep; saltation; modified saltation; and, suspension. Creep is the rolling or sliding of particles along the surface when shear is not competent enough to lift the particle from the surface. Saltation is the sporadic bouncing of sediment along the surface where the winds are competent enough only to transport particles a short distance. The force of impact of out fallen particles often dislodges stationary sediment into transport. Modified saltation occurs when the trajectory of saltating grains is modified by turbulent eddies. Lastly, suspension occurs when winds are competent enough to lift grains to high elevations and may result in transport over kilometres (Ritter *et al.*, 2002).

Aeolian sediment transport is determined by aeolian sediment supply, sediment availability, and transport capacity (Kocurek & Lancaster, 1999). These three components are distinct and interact to define a system's aeolian sediment transport regime (Kocurek & Lancaster, 1999). Aeolian sediment supply is the amount of contemporary sediment of suitable transport size delivered that provides a source to a system (e.g., originating via rock deflation, or fluvial, alluvial, and/or coastal delivery). Sediment availability determines the capability of near-surface airflow to transport sediments. Sediment availability is a function of moisture content (e.g., Sherman & Namikas, 1998; Walker & Barrie, 2006; Bauer *et al.*, 2009), surface conditions (e.g., surface roughness, ground freezing; e.g., Hugenholtz *et al.*¸2009), and vegetation type and density (e.g., Hesp, 2002). Lastly, transport capacity is the capability of a wind regime to transport sediments and is primarily a function of wind speed (e.g., Sarre, 1987) and direction (e.g., Hesp, 2002).

Bagnold (1941) was among the first to attempt to quantify potential aeolian sediment transport (see Equation 10). However, Bagnold's (1941) equation did not recognize a threshold term and thus, estimates transport for velocities lower than those required to entrain sediments. Since Bagnold's (1941) original research a number of methods for estimating potential sediment transport have been created. The current convention for estimating regional aeolian sediment transport potential is Fryberger and Dean's (1979) model, which uses a modified sand transport equation from Lettau and Lettau (1978) to calculate sand drift potential (DP) and resultant drift potential (RDP) in dimensionless vector units and a resultant drift direction (RDD). Fryberger and Dean's (1979) model assumes that the available transport

surface is dry, quartz sand with no bedform roughness greater than ripples and is absent of vegetation. In addition, the model is limited as it presents drift potential in dimensionless units whereas a method that presents dimensional units would be more informative.

A more recent model by Arens *et al.* (2004) calculates aeolian sand transport potential using the Kawamura (1951/1964) equation, which is a modified version of Bagnold's (1941) equation, and produces sediment transport values in $m^3\ m^{-1}$ over the period of investigation (Hugenholtz *et al.*, 2009). As such, the Arens *et al.* (2004) model provides sediment transport potential (TP) values similar to Fryberger and Dean's (1979) DP values but produces a dimensional and arguably more useful output.

Arens *et al.* (2004) acknowledge the calculation of potential transport is very sensitive to the value of the roughness length and warn potential sediment transport calculations should provide more of a relative versus absolute measure. In addition, this model assumes that the surface is dry, lacking surficial crusts, and absent of vegetation. In coastal environments these assumptions are not likely to be met. However, to date, these parameters remain to be successfully incorporated into a universal sediment transport model.

3.2.5 Dune Morphodynamics

Dune morphodynamics are controlled by several factors including beach type, surface moisture content, wind regime (speed and directionality), sand supply and sediment characteristics, and vegetation (type and density). The interaction of all the above components defines the aeolian sediment transport regime and the resultant beach-dune morphology. Beach type (product of geometry and form, tide range, sediment size, system energy, etc.), surface moisture content, and wind regime interact to effectively control the available surface for sediment entrainment and transport (i.e., fetch) on the beach. As above, on coasts with ample sediment supply, dune systems on steep and relatively narrow reflective beaches are typically smaller due to limited available fetch distances and, correspondingly, limited sand delivery to the backshore. In contrast, on wide and flat dissipative beaches, dune systems are largest due to a greater available surface for sediment entrainment and, correspondingly, greater sand delivery to the backshore (Short & Hesp, 1982; Hesp, 1999; Hesp, 2002). Surface

moisture content influences effective fetch by increasing the sediment entrainment threshold. Surface moisture content and aeolian sediment transport are inversely related where, with increasing amounts of surface moisture content, there are decreasing rates of transport (e.g., Bauer *et al.*, 2009). In-depth studies of aeolian sand transport across beaches on Prince Edward Island (PEI) show that moisture content in surface sediments reduces transport potential significantly except in intense wind conditions, like those common to the Queen Charlotte Islands (Sherman *et al.*, 1998; Walker & Barrie, 2006; Bauer *et al.*, 2009). Research shows short-term fluctuations in aeolian sediment transport over beaches with high moisture content could contribute to episodic stripping of dry sand veneers and subsequent exposure to underlying moist sand patches, which then must dry before further entrainment occurs. Wind speed and directionality are critical components of transport distribution across beaches. Together they define the approach angle of transporting winds and thereby determine the extent of surface exploitation (see Figure 3.3). As the angle of wind approach becomes more oblique, potential sediment transport increases to some threshold when it becomes negligible for highly oblique winds (Bauer *et al.*, 2009).

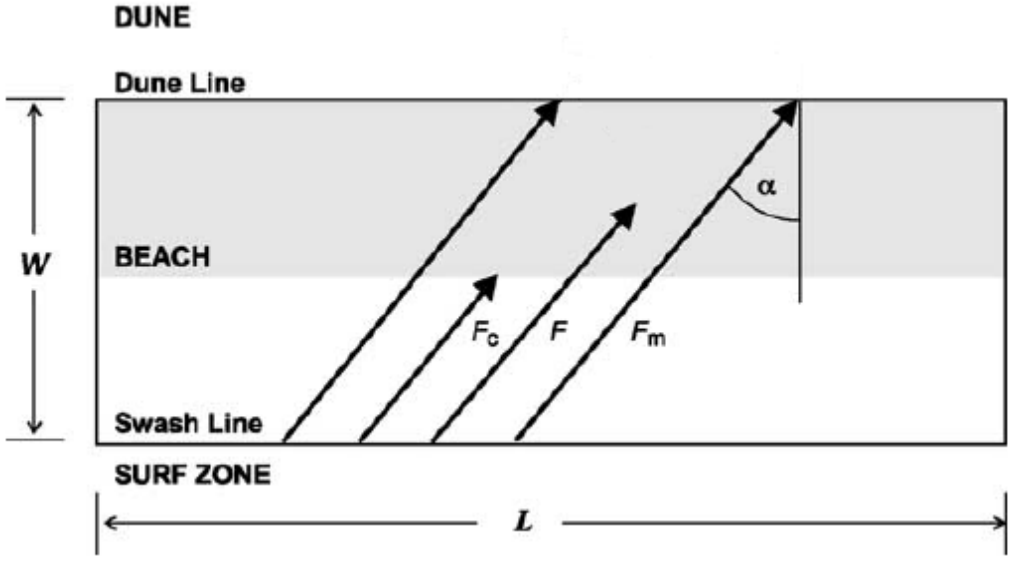

Figure 3.3. Illustration of the fetch effect over a beach surface, where the beach is defined at its seaward boundary by the swash line and at its landward boundary the limit of dune vegetation. *L* is beach length and *W* is beach width. *F* notates fetch more generally, F_c is the critical fetch length, and the grey zone indicates where aeolian transport is at a maximum. F_m is maximum fetch as a function of beach width and wind approach angle α. Modified from Bauer & Davidson-Arnott (2002).

Overall, sediment transport is minimal in the lower swash zone (high moisture content), highest in the mid-beach as sand transport exceeds the critical fetch distance (and perhaps reaches maximum sediment transport velocities), and decelerates nearing the foredune due to the development of an internal beach boundary layer as a function of beach topography and increasing surface roughness attributed to the presence of vegetation. This boundary layer was shown to expand vertically with downwind distance, causing near-surface wind speeds to decrease and the total shear velocity to be distributed across a thicker layer of atmosphere causing an outfall of suspended sediment (Bauer *et al.*, 2009). Generally, efficacy of transport on beaches is not only dependent on local controlling factors (e.g., wind speed, grain size and sorting, surface moisture content) but also on contextual factors (e.g., slope, fetch geometry) that collaboratively produce site-specific morphological results (Bauer *et al.*, 2009).

Two main types of foredunes exist on the beach: incipient foredunes and established foredunes. Incipient foredunes are newly developing foredunes and are formed in the lee of pioneer plant communities, large woody debris, flotsam, etc. Their morphological development depends primarily on plant density, distribution, height and cover, incident wind regime, and aeolian sediment transport rates. Other factors influencing the development of incipients includes frequency of swash inundation (corresponding to high water level events), storm wave erosion, and overwash. Incipients form due to changes in surface roughness (e.g., pioneer plant communities versus bare sand) and topography (e.g., approach to established foredune) that generate altered flow conditions (e.g., flow stagnation, flow separation, drag) compared to those conditions over the flat beach (Hesp, 2002). Consequently, near surface shear stresses and grain transport trajectories are altered, resulting in the deposition of some entrained sediments (Arens, 1996).

Established foredunes are formed from incipient foredunes and are distinguished by a greater morphological complexity, height, age, and width. The development of established foredunes is dependent on available sediments, vegetation (type, cover, height, etc.), aeolian transport rate, frequency and magnitude of erosive water levels, beach-dune mobility (i.e., stable, accreting, or eroding), water level trends, and human impacts. Hesp (2002) identifies five morpho-ecological stages of foredunes (Figure 3.4). Stages one to three suggest

foredunes are still able to prograde whereas stage five foredunes are highly erosional and suggest landward retreat or slow disappearance of the foredune ridge. Foredune stages are indicative of the form a foredune may assume for most of its existence, but also are insightful to the evolutionary sequence through which a foredune may progress given an increase in aeolian erosion, a decline in vegetation cover, and an increase in the frequency of erosive high water events. This progression may be reversed given an increase in vegetation cover, reduction in aeolian erosion, and/or a decline in the frequency of erosive high water events. Accordingly, stage five foredunes do not revert to stage one foredune but rather shift along a continuum from stage one to stage five. This model is particularly functional as it considers both event-based and longer-term coastal foredune evolution. However, it is limited in that it simplifies a complex system and controlling variables may combine constructively or destructively to produce several end scenarios not captured in the model (Hesp, 2002).

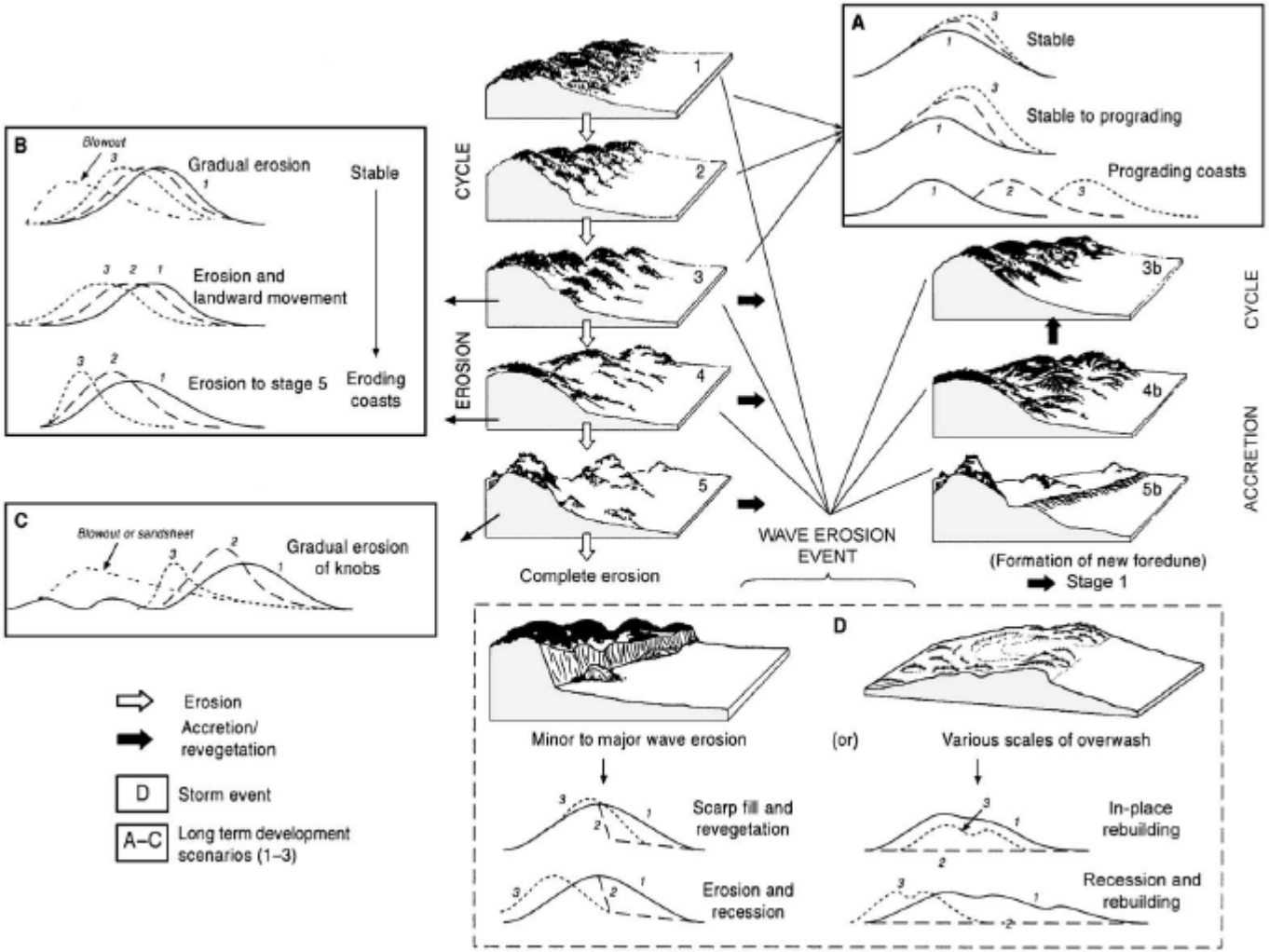

Figure 3.4. Morpho-ecological model of established foredune evolution. Foredunes may remain static in their evolutionary stage or may shift from stage one to stage five along a continuum. Boxes A – C indicate longer-term scenarios and Box D indicates event-based scenarios (Hesp, 2002, with permission).

3.3 Methods

3.3.1 Morphodynamic Classification

Quantitative morphodynamic insight to Wickaninnish Beach was provided by the non-dimensional scaling embayment scaling parameter (Equation 5), Wright and Short's (1983) surf-scaling parameter (Equation 2), Battjes (1974) surf similarity parameter (Equation 6), and Masselink and Short's (1993) conceptual beach model (Equations 3 and 4). The non-dimensional embayment scaling parameter (*δ'*; Equation 5) provides insight to surf zone circulation within an embayment. The embayment scaling parameter is calculated as follows (per Short and Masselink, 1999):

$$\delta' = \frac{S_l^{\,2}}{100 C_l H_b} \tag{5}$$

Where S_l is the length of the embayment shoreline (m), C_l is the width of the embayment from headland to headland (m), and H_b is breaker wave height (m). Where $\delta' > 19$ normal beach circulation prevails, where $19 \geq \delta' \geq 8$ transitional circulation prevails, and where $8 > \delta'$ cellular beach circulation prevails. 'Normal' circulation is when no longshore transport occurs and all waves arrive obliquely to the shore. This type of circulation exists on beaches with no headlands. Transitional circulation occurs when embayment morphology (i.e., size and shape) causes a shift in longshore currents, directing some flow against headlands while maintaining some normal circulation. Lastly, cellular circulation results when headlands dominate surf zone circulation, causing strong seaward rip circulation at the ends of the embayment (Short & Masselink, 1999).

Battjes (1974) surf similarity parameter (*ξ*), or the Iribarren number, is a dimensionless parameter used to characterise the incident wave regime (e.g., breaking or non-breaking waves). Spilling waves are characterised by $\xi_o \leq 0.8$, plunging waves by $0.8 < \xi_o \leq 1.0$, surging waves by $1.0 < \xi_o \leq 1.1$, and no waves by $1.2 < \xi_o$. The surf similarity parameter can be calculated as follows:

$$\xi = \frac{S}{(H_o / L_o)^{1/2}} \tag{6}$$

Where β is the beach gradient, H_o is the offshore significant wave height (m), and L_o is the deep water wave length (m) calculated by:

$$L_o = \frac{gT^2}{2\pi} \tag{7}$$

Where g is the acceleration of gravity (9.81 m s^{-2}) and T is the offshore wave period (s).

The beach at Wickaninnish Bay was classified using the Masselink and Short (1993) model. As above, parameters required for this model include: (i) breaker height (H_b); (ii) sediment fall velocity (w_s); (iii) wave period in seconds (T); and, (iv) spring tide range (MSR). Short and Masselink (1999) present the following equation to calculate breaker height (H_b) in an embayed beach:

$$H_b = \sqrt{H_o^2 (\frac{C_l}{S_l})} \tag{8}$$

Where Ho is deep water significant wave height (m), C_l is embayment width measured as the distance between headlands (m), and S_l is embayment shoreline length (m). Sediment fall velocity can be determined empirically using a settling tube, or calculated theoretically using Stokes' Law (Ferguson & Church, 2004):

$$Ws = \frac{RgD^2}{C_1 v} \tag{9}$$

Where Ws is representative of sediment fall velocity (m s^{-1}), R is the dimensionless submerged specific gravity (1.65 for quartz in water), g is the gravitational constant (9.81 m s^{-2}), D is sediment diameter (m), C_1 is a constant with a theoretical value of 18 (representative of the asymptotic value of the drag coefficient for a settling spherical particle), and v is the kinematic viscosity of water at 20°C ($1.0 \bullet 10^{-6}$ kg m^{-1} s^{-1}). The dimensionless fall velocity for sediments on Wickaninnish Beach was obtained experimentally using sediments from the high tide swash line, and theoretically, using Stokes' Law (Equation 9). Using experimental methods, sediments from the high tide line were released into a graduated cylinder and their fall rate was calculated (distance over time). While this experiment is typically done using a settling tube, this resource

was not available. Therefore, the theoretical fall velocity using Stokes' Law was also calculated for comparison to see if the experimental results yielded the same classification.

For classification purposes Stokes' Law was used. The kinematic viscosity of seawater was determined using mean water temperature at Amphitrite Point Lighthouse, located on the south-western periphery of Ucluelet (UTM Zone 10, 313934.53 m E, 5421669.46 m N). Mean water temperatures over the period of record (August 1934 to December 2009) were 10.8°C. Therefore, the kinematic viscosity for seawater at 10.8°C and 3.5% salinity ($1.3 \bullet 10^{-6}$ kg m^{-1} s^{-1}) was used versus the kinematic viscosity for water at 20°C and 3.5% salinity (International Towing Tank Conference, 1999). Offshore peak wave period and deep water significant wave height values were taken from the Marine Environmental Data Service buoy (MEDS 103) located ~5.2 km offshore of Wickaninnish Bay (UTM Zone 10, 299588.68 m E, 5429953.93 m N) (see Figure 1.1). MEDS 103, although no longer operational, has the longest period of record for the region and is most representative of the wave conditions on Wickaninnish Beach. It operated from 1970 to 1998, with a total of 10218 days of measured data, 8958 of which provided reliable data. Beyond MEDS 103 the nearest buoy is La Perouse Bank (UTM Zone 10, 279840.62 E, 5412894.33 N), positioned roughly 32 km offshore of Wickaninnish Bay. The modal wave breaker height for Wickaninnish Bay was calculated using deep water significant wave heights from MEDS 103, shoreline length, and embayment width as per Equation 8.

3.3.2 Nearshore Sediment Transport

Nearshore sediment transport pathways were explored using the McLaren Method (McLaren & Bowles, 1985; Gao & Collins, 1991). This one-dimensional model estimates net sediment transport pathways by analysing spatial variation in the mean grain size (μ), the sorting coefficient (σ^2), and the distribution skewness (Sk) (McLaren & Bowles, 1985). This model assumes that the sediment is of a unique source and, while mean grain size and skewness may vary, sorting always improves in the direction of transport. McLaren and Bowles (1985) predict two trends indicative of net transport from site one (d_1) to site two (d_2) (per Gao

& Collins, 1991)[6]; case *i* where sediments become finer, better sorted, and more negatively skewed; and, case *ii* where sediments become coarser, better sorted, and more positively skewed. Mean grain size, sorting, and skewness are compared between all samples along a transect and the relationship between each sample pair is recorded in a sediment trend matrix as per McLaren (1981). The number of pairs that demonstrate either case *i* or case *ii* above are tallied for each transport direction and results are tested for statistical significance using a one-tailed Z-score technique (Spiegel, 1961). Statistical significance suggests transport occurs in a preferred direction.

In some cases transport is significant in both directions due to the presence of more than one sediment source (e.g., fluvial sediment inputs) (McLaren, 1981). Additionally, while net longshore transport trends may exist, these trends may be confounded by rip currents. McLaren and Bowles (1985) recognize that, in application, their model is limited due to variance in the original sediment source, local and temporal variability in transport processes, and sediment sampling issues (e.g., choice of representative sample intervals). Gao and Collins (1991) criticize the one-dimensionality of this model as well as its unweighted representation in the comparison of transect samples, where the comparison of two neighbouring samples does not share the same meaning as the comparison of two samples that are some distance apart. Gao and Collins (1991) suggest that a two-dimensional analysis (i.e., two or more sampling transects) would provide results more representative of true nearshore processes. They also suggest a smoothing operation to remove noise in the data resulting from unweighted comparisons between samples. Regardless, the McLaren Method, while it has notable limitations, provides meaningful insight to nearshore transport trends on beaches characterised by longshore current processes or 'normal' circulation.

In Wickaninnish Bay, 24 surface sediment samples of a 15 cm by 15 cm area to 1 cm depth were taken at approximately 500 m intervals along the high tide line from Box Island in the north to Quisitis Point in the south (Figure 3.5). Each sample was sieved mechanically using sieves of 0.00 to 3.50ϕ and separated in quarter phi intervals. Sediment moment statistics were

[6] Grain size is expressed using the logarithmic phi scale where the real size of particles decreases with increasing phi values. Therefore, $\mu_2 > \mu_1$ indicates fining.

generated using GRADISTAT (Blott & Pye, 2001). A sediment trend matrix was created using the sediment moment statistics to investigate if a preferred transport direction existed.

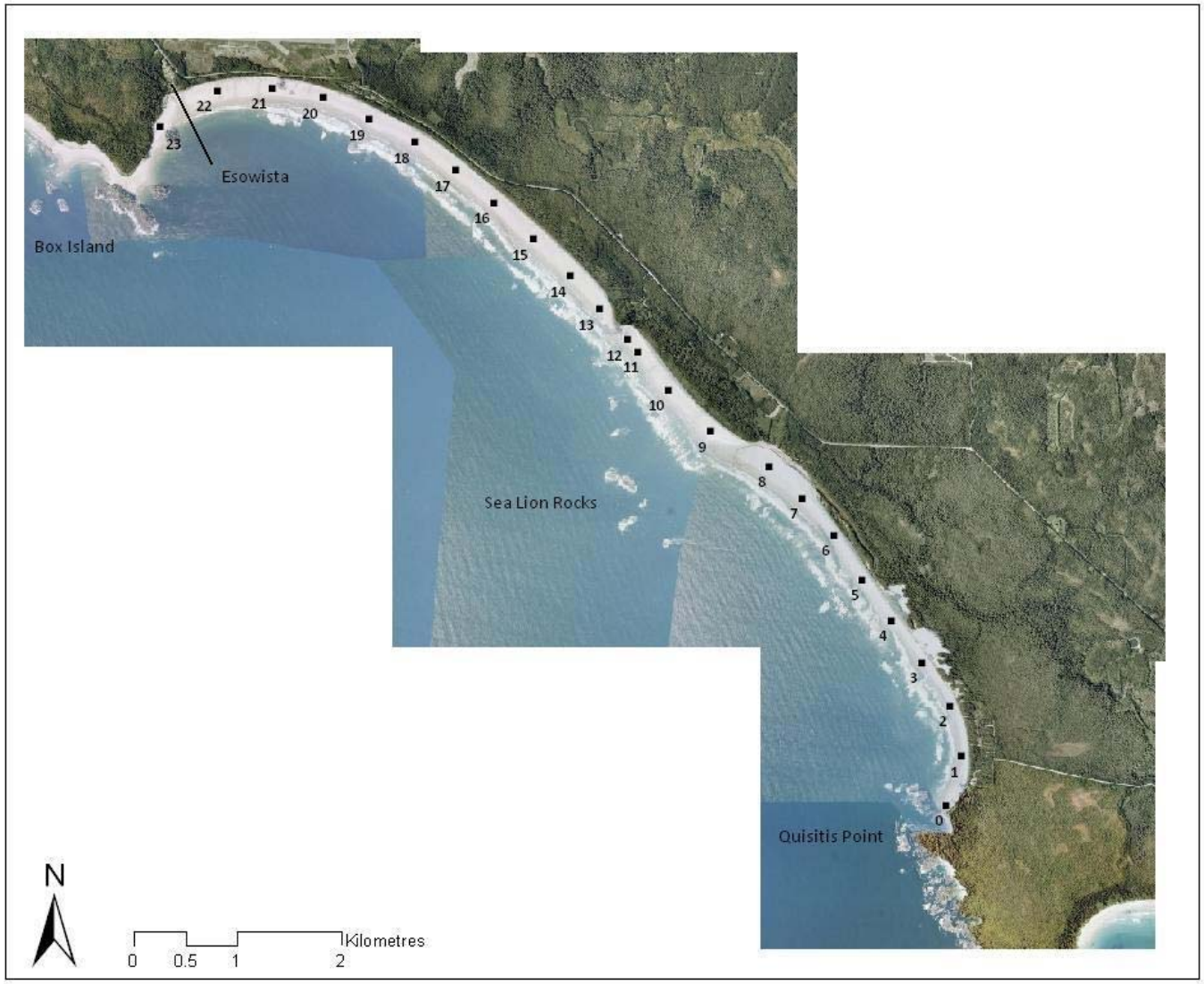

Figure 3.5. Locations of sediment samples used to characterise nearshore sediment transport pathways in Wickaninnish Bay (per McLaren & Bowles, 1985). Airphotos obtained May 24, 2007.

3.3.3 Aeolian Sand Transport Potential

Aeolian sediment transport potential of the Wickaninnish beach-dune system was calculated per the methods of Arens *et al.* (2004) and Hugenholtz *et al.* (2009). This method uses vector analysis to determine a dimensional ($m^3\ m^{-1}$) sediment transport potential (TP), resultant transport potential (RTP), and resultant transport direction (RTD).

First, the threshold velocity for transport (U_{*t}) is determined using Bagnold's (1941) equation:

$$U_{*t} = A\sqrt{\frac{(\rho_p - \rho_a) - gd}{\rho_a}} \tag{10}$$

Where A is an empirical coefficient (0.08 for impact threshold), ρ_p is the density of quartz sand particles ($2.65 \bullet 10^3$ kg m^{-3}), ρ_a is the air density (1.22 kg m^{-3} at STP), g is the gravitational constant (9.81 m s^{-2}), and d is the sand grain diameter at the study area (dune sand grain diameter of $1.65 \bullet 10^{-4}$ m). Next, the threshold normal velocity ($u(z_a)$) at both the anemometer height (10 m for station *Tofino A*) and the focal height (0.01 m for normal dune sand) are determined using the Law of the Wall:

$$u(z_a) = \frac{U_{*t}}{\kappa}\ln(\frac{z}{z_0}) \text{ if } z > z_0 \tag{11}$$

Where κ is the von Karman constant (0.41), z is the measuring height, and z_0 is the roughness length (equivalent to $1/30^{th}$ of the sand diameter). Then, shear velocity (U_*) is calculated from (Bagnold, 1941; Craig, 2000):

$$U_* = \kappa\frac{u(z_a) - u_t(z_f)}{\ln(z_a / z_f)} \text{ if } U_* > U_{*t} \tag{12}$$

Where $u(z_a)$ is the observed wind velocity at the anemometer height and $u_t(z_f)$ is the threshold normal velocity at the focal height. Next, the Kawamura (1951/1964) equation is used to calculate potential transport (*q*):

$$q = C\kappa \frac{\rho_a}{g}(U_* - U_{*t})(U_* + U_{*t}) \text{ in kg m}^{-1}\text{ s}^{-1} \quad (13)$$

Where *Cκ* is an empirical constant (2.78) introduced by Kawamura (1951/1964). The transport potential per hour (*qi*) is calculated as follows:

$$qi = 3600q \quad (14)$$

The transport potential is assigned to the corresponding wind sector of the measured winds. The transport potential for each wind sector is totalled for the period of measurement. This yields total transport *Qj* per wind sector *j* in $m^3\ m^{-1}$:

$$Qj = \frac{1}{1600}\sum_{i=1}^{nj} qi \quad (15)$$

Where *nj* is the total number of hours *i* for wind sector *j* assuming a bulk density of sand 1600 kg m^{-3}. Transport potential in each wind sector is then combined to create wind direction classes (*TP_Q*):

$$TP\_Q = \sum_{i=1}^{36} Qj \quad (16)$$

This creates 36 wind direction classes of 10˚ each. Finally, the resultant transport potential (RTP) (similar to Fryberger's RDP) is determined by calculating the cardinal vectors per wind direction class *ddj* and the summation of the vectors of all sectors:

$$RTP\_Qjx = Qj \bullet \sin[ddj] \tag{17}$$

$$RTP\_Qjy = qj \bullet \cos[ddj] \tag{18}$$

$$RTP = \sqrt{\left(\sum_{j=1}^{36} RTP\_Qjx\right)^2 \left(\sum_{j=1}^{36} RTP\_Qjy\right)^2} \tag{19}$$

The resultant angle of transport potential (αRTP) is then calculated by:

$$\alpha RTP = \arctan\left[\frac{\sum_{j=1}^{36} RTP\_Qjx}{\sum_{j=1}^{36} RTP\_Qjy}\right] \tag{20}$$

These data are illustrated using a sediment transport rose where vectors show directions from which sand is transported. The RTP is the vector sum of all TPs and is illustrated by an arrow with a length proportionate to the resultant transport quantity and a direction toward which sand is transported. Wind data are from Environment Canada's meteorological station Tofino A (EC-ID 1038205) and represent the period of 1971 to 1977, the only period of 24-hour data with 36 directional sectors. Results were calculated for the entire period and arbitrarily divided by six to provide per annum values. Data were also aggregated according to month and arbitrarily divided by six to provide average monthly potential transport values. Grain diameter was determined via empirical analysis of sediment from the Wickaninnish dunes.

3.3.4 Bathymetric Profile

A bathymetric profile for Wickaninnish Beach was derived from field sheet data (Parizeau *et al.*, 1931) to provide data on the nearshore. While the field sheet data are dated, these are the only nearshore bathymetric data that exist for Wickaninnish Beach (M. Ward, personal communication, December 11, 2008). Bathymetric data are extended from transect 3 (Figure 3.6) from 0 m above Chart Datum (aCD) to -11 m aCD. This contour was chosen as it

extends from headland to headland and was considered to be most relevant to analysis. While it is meaningful to extend the profile to the depth of the wave base (-79.70 m aCD), soundings were not collected to this depth along the transect. Only one bathymetric profile for Wickaninnish Beach was created due to the small scale of the field sheet.

Wavelength and wave base (half of the wavelength [L_o]) were calculated to determine where typical waves start to shoal. The wave base calculation intended to inform the length of the bathymetric profile, where the bathymetric profile would extend to the depth of the wave base.

3.3.5 Topographic Surveys of Cross-Shore Profiles

Profiles were established to provide data on the character and dynamics of nearshore to backdune topography. General regions of interest on cross-shore profiles include the nearshore, surf zone and intertidal beach, supratidal beach, foredune, and transgressive dune complex. The nearshore region is defined by the initiation of wave shoaling. The nearshore profile is typically concave and bedforms range from wave ripples to a plane bed. The limit of breaking waves defines the surf zone. The surf zone and the intertidal beach (region from the lowest low water large tide elevation to the highest high water large tide elevation) typically have a number of surficial morphological features including bars, troughs, channels, and ripples. Berms, accretionary features formed at the upper limit of swash action, are one of the last wave-driven morphological features on the beach (excepting morphology influenced by erosive high water events) (Short, 1999).

Morphological features of the supratidal beach zone are no longer influenced by hydrodynamic processes (except in cases of extreme water levels) and are a function of aeolian processes. Incipient foredunes are one of the first morphological features found in this zone. They are small, newly developing foredunes and form at the base of the modern foredune around flotsam and pioneer plant communities (e.g., sea rocket or *Cakile edentula*)(Hesp, 2002). Incipient foredunes may be ephemeral if they rely structurally on annual plants and/or are exposed to erosive high water events. Incipient foredunes mark the initial stage of foredune development. Foredunes are shore-parallel dune ridges. They are aligned shore-parallel as an

increase in slope and roughness at the land/sea interface creates a change in the wind field, steering it onshore. Flotsam and pioneer plant communities cause a deceleration of flow responsible for aeolian sand transport, causing the deposition of some entrained sediments. Deposited sediments contribute to the development of incipient and/or modern foredunes (Hesp, 1999). Landward of the foredune is the transgressive dunefield. These dunefields migrate alongshore over vegetated or semi-vegetated terrain. Active transgressive dunefields are characterized by deflation plains oriented alongshore, a mobile to partially vegetated sand sheet, and a sinuous precipitation ridge, demarcating the landward edge of the system (Hesp, 1999).

Three cross-shore topographic profile locations were established and surveyed on Wickaninnish Beach, one in the blowout complex in the south and two in the larger transgressive dune complex (see Figure 3.6). These profiles were established to capture the various dynamics of nearshore to backdune topography on Wickaninnish Beach. Transect 1 was situated in the blowout complex in the south. *Ammophila arenaria* was removed from the foredune at this site in 2005. This profile was established to provide insight to the morphodynamics of the blowout complex as well as the dynamics of a recently restored dune. Transect 2 traverses one of the few remaining foredunes that supports an intact *Leymus mollis* plant community. In addition, a backdune blowout ramp is captured by this profile. This profile was established to provide insight to beach-dune morphodynamics under the natural foredune vegetation regime. Transect 3 intersects a portion of foredune stabilized by a tree island. This profile was established to provide insight to beach-dune morphodynamics under a stabilized foredune. The stoss side of the foredune on all transects was restored (i.e., *Ammophila arenaria* was removed) in September 2009 following the field season.

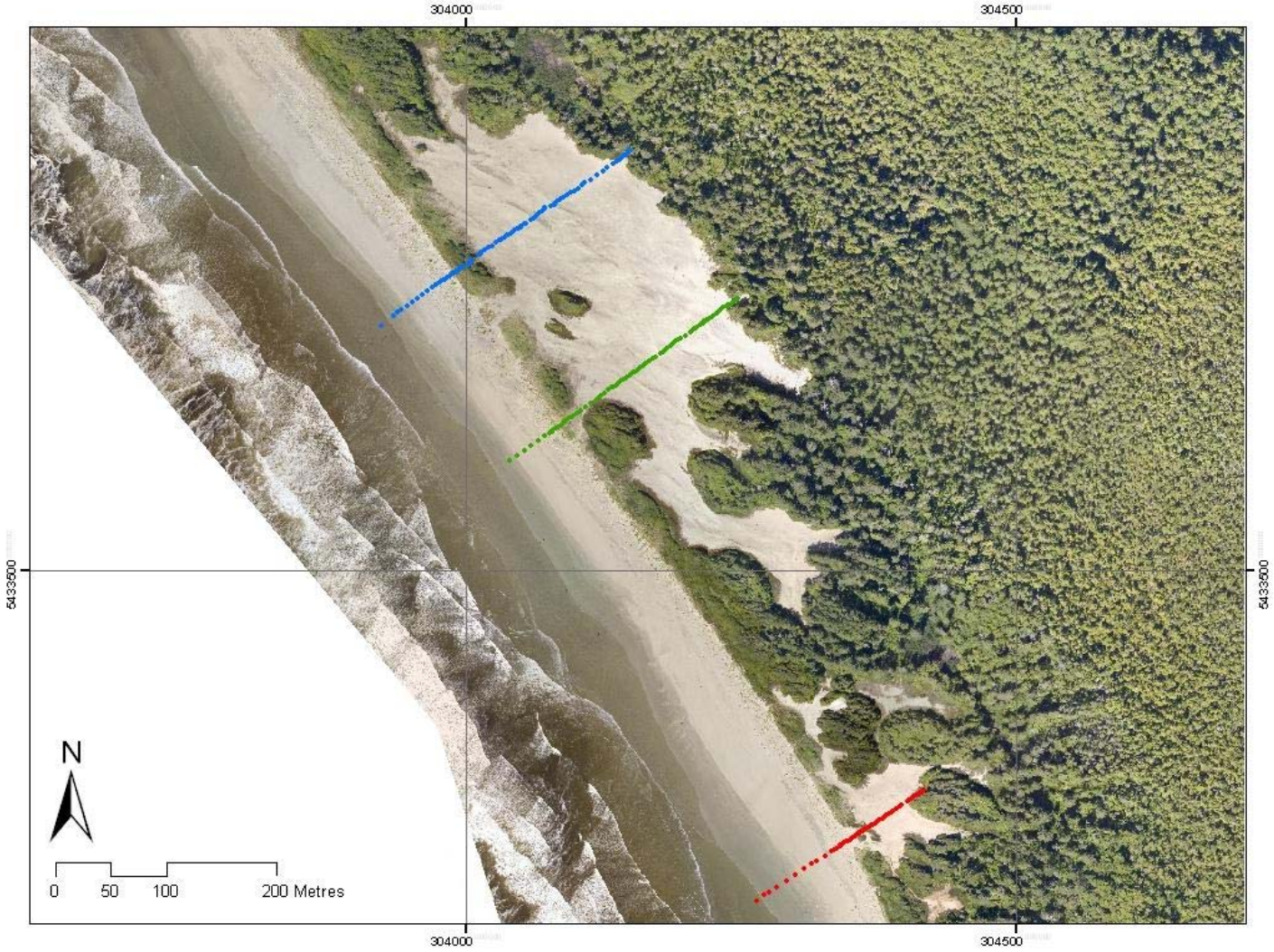

Figure 3.6. Location of the three repeat cross-shore transects in the Wickaninnish beach-dune system. From right to left: transect 1 (red), transect 2 (green), and transect 3 (blue). Airphoto obtained August 27, 2009.

Each transect was marked using two semi-permanent benchmarks (3' rebar rods), where the first benchmark was installed just within the forest edge and the next installed approximately five metres seaward, aligned along a shore-normal bearing. A shore-normal bearing was determined via sighting the shoreline orientation from the foredune crest, then turning landward 90 degrees. This bearing informed the placement of benchmarks and was used to extend the cross-shore profile from the benchmarks (BMs) to the swash line. Declinations were confirmed immediately prior to field surveys.[7] Survey BMs were georeferenced to the Geodetic Reference System 1980 (GRS1980) using six control points (Table 3.1) installed by Roger Leeman of the Marshall Macklin Monaghan Group using real time kinematic (RTK) methods. To minimize error in the survey layout, the control points were installed so the enclosed angle between points was within 45˚ and 180˚ (optimal is within 45˚ and 150˚). Issues of vandalism had to be considered in control point installation and resultantly, 'hidden' control point locations were chosen. Profiles were corrected to Chart Datum (CD) using conversion rates established for Tofino by the Canadian Hydrographic Service (GRS1980 to CD = +2.095 m). These conversion rates were determined using VDatum[8], a software that interpolates known water levels across a grid enabling the transformation between CD and ellipsoidal datums. Accordingly, following conversion to CD, profiles could be meaningfully compared to water levels.

[7] Available online from http://geomag.nrcan.gc.ca/apps/mdcal-eng.php

[8] Available online from http://vdatum.noaa.gov/download.html

Table 3.1. Control point coordinates and elevations in the Wickaninnish dune system surveyed using RTK methods and Reference Ellipsoid GRS 1980. Elevation is according to GRS 1980 not local Chart Datum. All coordinates are an average of two measurements. All horizontal accuracy is sub centimetre. Survey conducted July 23, 2009.

Control Point	Easting (UTM Zone 10)	Northing (UTM Zone 10)	Elevation (m)	Vertical Accuracy (cm)
1	304401.2132	5433235.6474	10.0292	1
2	304337.4506	5433323.6544	10.8855	1
3	304053.0264	5433714.6339	8.0718	1
4	304085.9403	5433741.9868	12.8995	1
5	304048.4959	5433908.2557	14.2461	4
Transect 1 BM1	304411.5502	5433298.6116	10.7806	1
Transect 1 BM2	304415.6184	5433300.7607	9.8425	2

Profile measurements were collected in both the 2008 and 2009 field seasons along the transect using a total station (TOPCON GTS 226, TOPCON GTS 229, or Leica TCR405 Power), pole, and prism at points of topographic inflection and at intervals appropriate to the beach width and morphology (i.e., fewer measurements were collected over featureless terrain that maintained a consistent gradient). All surveys were conducted during a low spring tide window to capture as much of the intertidal beach as possible. Repeat vantage photos were taken systematically (i.e., in the same directions and locations) to provide a qualitative complement to these topographic surveys.

Benchmark elevations were recorded three times each survey using the total station and averaged to estimate both positional and vertical survey accuracies. Maximum, minimum, and average differences in benchmark position were determined for northing, easting, and elevation measures using data from both 2008 and 2009 (Table 3.2). Instrument accuracies were within approximately two centimetres for northing, three centimetres for easting and four centimetres for elevation.

Table 3.2. Assessment of within instrument accuracies through repeat capture of the benchmark position and assessment of the discrepancy between measures.

Differences in Positional Measurements	Northing (m)	Easting (m)	Elevation (m)
Max	0.019	0.032	0.043
Min	0.002	0.004	0.001
Average	0.008	0.011	0.013

To improve survey confidence, all positional measurements were corrected using least squares regression. This enabled any slight digressions from the bearing to be corrected to the appropriate bearing. In theory, this should improve the capability to compare profiles over time. To assess the accuracy between surveys, UTM points were plotted in plan view to determine if the same transects were established between the years (Figure 3.7). Analysis in plan view reveals no transect established exactly the same line between the two years. Error was expected to an acceptable degree given the methods used to re-establish the transect. However, the scale of error was greater than anticipated. Error ranged from 0.06 m m^{-1} (transect 2) to 0.08 m m^{-1} (transect 3). Furthermore, error is compounded over distance and resultantly, longer surveys reveal greater discrepancy between surveys. In future, different methods should be employed to re-establish the survey line in order to improve between year survey accuracies. For example, three to four points along the known transect could be determined using *stakeout*, a total station feature that allows you to reposition over a point of known location, and the survey line could be re-established between these points.

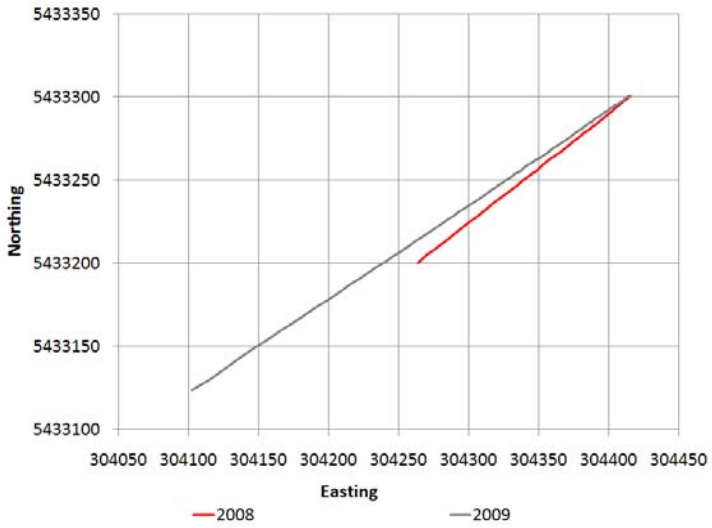

Transcript 1 (error 0.07m m^{-1})

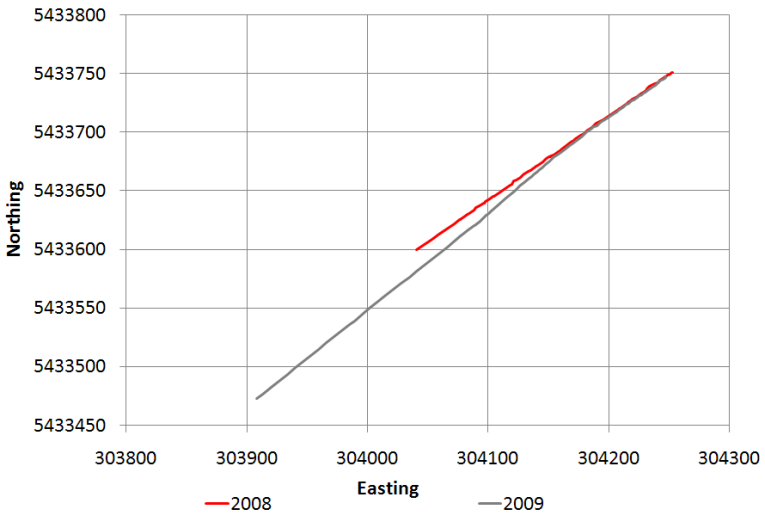

Transcript 2 (error 0.06m m^{-1})

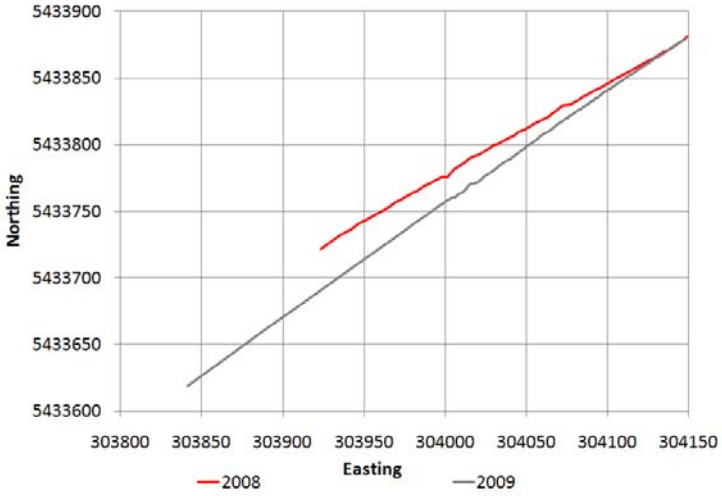

Transcript 3 (error 0.08 m m^{-1})

Figure 3.7. Plan view of the 2008 and 2009 *in situ* surveys.

The 2009 *in situ* surveys were not used in comparative analyses due to a failure to re-establish the same transect. Instead 2009 and 2010 profiles were extracted from DEMs. The 2009 DEM was produced from LiDAR data flown August 27, 2009 (15 cm accuracy). LiDAR data were classified in MicroStation© to identify ground points. The 2010 DEM was produced using data from a full topographic field survey in March. DEMs for both LiDAR data (2009) and field survey data (2010) were created in Arc GIS©. They were created using ordinary kriging techniques. A variable search radius was used that considered the nearest 12 points in the creation of the DEM surface (default settings). A 1 m cell size was output from the analysis. See Swales (2002) for details on this method. DEMs were opened in ENVI© to extract the profile. All coordinates from the 2008 *in situ* survey for were used to extract the same profile in 2009 and 2010.

3.3.6 Profile Volumetric Change Estimation

Profile volumetric change estimation exposes morphological changes (i.e., accretion or erosion) that may not be evident when viewing a two-dimensional profile. While the topographic profiles are two-dimensional, representative volumes can be calculated by assuming a uniform profile width of one metre and a reference depth of 0 m aCD for closure. Thus, volumes can be estimated by multiplying the total trapezoidal area (m^2) under the profile curve between two data points by a profile width of 1 m. Trapezoidal area (A) is calculated as per the trapezoidal rule:

$$A = \frac{1}{2} h(a + b) \tag{21}$$

Where *h* is the height of the trapezoid, and *a* and *b* are the lengths of the parallel sides (Figure 3.8). After volumes were calculated, the total volume under the curve in the previous year(s) was subtracted from the total area under the curve in following year to determine the change between the years.

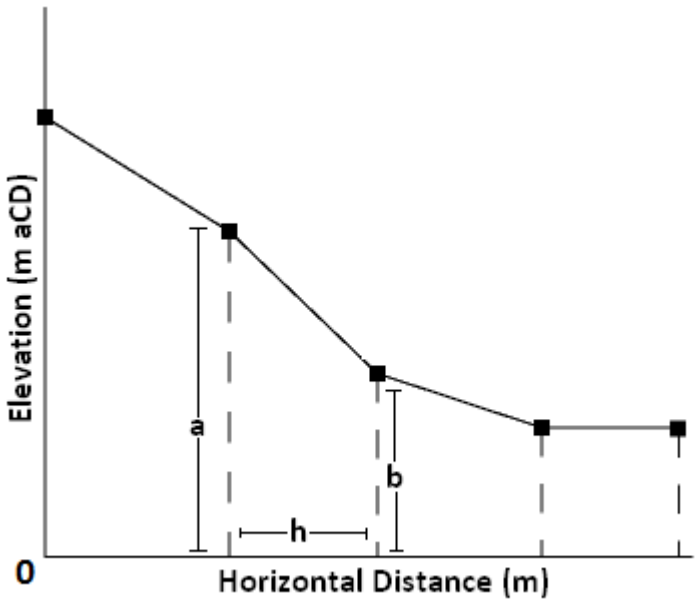

Figure 3.8. Illustration of the trapezoidal rule, where *h* is height and *a* and *b* are the lengths of the parallel sides. The trapezoidal rule was used to calculate the area under the cross-shore transect. The base elevation was arbitrarily set to 0 m aCD.

Profiles deconstructed into meaningful analytical units (e.g., backdune, beach) are particularly insightful to understanding the trends of different regions of the beach-dune system. Thus, each profile was examined for volumetric change over the entire profile, from the foredune to the beach, and from the foredune to the backdune.

3.3.7 Airphoto Analysis

Aerial photographs from 1973, 1996, and 2007 (Table 3.3) were analysed to reveal historical trends of the beach-dune system (i.e., progradation/erosion, stabilization/mobility). Non-digital airphotos from 1973 and 1996 were digitized and orthorectified using PCI Geomatica©. All geometric corrections for the 2007 digital airphotos were conducted by Integrated Mapping Technologies© on contract for the Parks Canada Agency. Additional airphotos exist for the area (1930, 1938, 1950, 1954, 1967, 1969, and 2005) but are of poor resolution and/or features of interest are indistinguishable. Each feature of interest (area of open sand surfaces and mean shoreline position) was demarcated by a digitized arc and the

position of this arc was compared throughout the time series using PCI Geomatica©. Relative shoreline position was defined by the seaward extent of vegetation and change was estimated in m a^{-1}. A polygon was drawn around bare sand surface in the backshore dune complex of each airphoto to estimate change in dune sand surface extent (m^2). Vegetation islands in the dune complex were also digitized and subtracted from total change calculations. See Heathfield and Walker (in review) for further details of analysis.

Table 3.3. Acquisition date, format, scale, resolution, and source of airphotos used in analysis of temporal change on Wickaninnish Beach.

Date	Format	Scale	Resolution (m)	Source
1973	Non-digital	1:15000	0.30	BC Airphoto Library
July 6, 1996	Non-digital	1:15000	0.30	BC Airphoto Library
May 24, 2007	Digital	n/a	0.30	Parks Canada Agency

3.4 Results and Discussion

3.4.1 Beach and Embayment Classification

According to the Masselink and Short (1993) model, Wickaninnish Beach is a low tide bar/rip beach (RTR = 3.79 m, where MSR = 3.75 m and Hb = 0.99 m; and, Ω = 2.02, where Ws = 0.03 m s^{-1} and T = 14.29 s). Stokes' Law was used to determine sediment fall velocity values (Ws = 0.034 m s^{-1}) in the Masselink and Short (1993) model. For comparative purpose, average empirical sediment fall velocity values (Ws = 0.033 m s^{-1}) were explored and yielded the same classification. Low tide bar/rip beaches fall into the intermediate beach classification, characterized by beaches with distinct bar morphologies and cellular rip circulation. They have a relatively steep upper intertidal zone that is met with a lower gradient mid-intertidal zone where swash bars may form. Around low tide levels bar and rip morphology is present. Corresponding to the varied zonal morphology (i.e., steeper upper intertidal and gradual mid-intertidal zones) these beaches may exhibit reflective, intermediate, and dissipative conditions throughout the tidal cycle.

Wickaninnish Beach corresponds well with this classification. The mid-intertidal zone is gradually sloped (0.78°) and leads into a steeper high intertidal zone (1.46°). Bar morphology is

present in the mid-intertidal zone. However, in place of swash bars in the mid-intertidal zone ridges and runnels were present (Figure 3.13). As suggested by the model, rip circulation cells operate in the nearshore system at Wickaninnish Beach and are apparent in aerial photographs (Figure 3.9) and from the beach under certain conditions.

Figure 3.9. Rip current in the nearshore fronting the Wickaninnish dunes. Photo taken in 1984.

The surf scaling parameter (Guza & Inman, 1975) for Wickaninnish beach (ξ = 44.71) indicates a dissipative form. While this does not correspond completely with the classification provided by the Masselink and Short (1993) model, the beach arguably assumes a dissipative form under certain incident sea conditions (e.g., lower energy summer swell) and nearshore morphologies (e.g., nearshore bars; see Figure 3.12). As suggested by the earlier classification schemes of Wright and Short (1983), intermediate beaches experience both dissipative and reflective conditions and are accordingly more difficult to classify.

The surf similarity parameter (ξ = 0.35) suggests Wickaninnish Beach primarily receives spilling breakers (Battjes, 1974). However, personal observation throughout the study period

suggests that plunging breakers are more common. This disagreement may be due to a shorter period of observation (2008 to 2010) versus period of wave record (1970 to 1998) and perception may therefore be influenced by anomalous or cyclical climatic forcing that is responsible for more extreme wave conditions, leading to a misleading assessment of the regions average wave regime.

The embayment scaling parameter (per Short & Masselink, 1999) classifies beach circulation on Wickaninnish Beach as 'normal' ($\delta = 156.53$). 'Normal' circulation occurs when an embayment is in equilibrium and all waves arrive obliquely onshore creating no net longshore transport. Weak longshore transport may occur from regions of higher wave energies to those of lower. In addition, rips may be present at the bounding headlands of the embayment (Short & Masselink, 1999). This classification counters local knowledge, personal observation, and classification under other schemes. The embayment scaling parameter may be misleading as it does not account for the influence of rocky outcrops in the nearshore (e.g., Sea Lion Rocks, Figure 3.5) or headlands within the larger embayment (e.g., Green Point). These may interfere with the predicted 'normal' circulation and contribute to the observed rip current circulation. Embayment scaling parameter is also highly sensitive to estimates of embayment width (C_I) and length of the embayment shoreline (S_I). These variables are used directly in embayment scaling parameter calculations (Equation 5) and are used to calculate breaker wave height in an embayed beach (0.99 m; Equation 8), another variable in the embayment scaling parameter calculation. In Wickaninnish Bay, C_I and S_I values may vary dependent on the measurement parameters chosen. Where analysis above considered the distance between Box Island and Quisitis Point, a more accurate classification of beach circulation might be obtained by considering the distance between Green Point and Quisitis Point. However, to date no studies have shown that Green Point is a dominant headland and/or have investigated the influence of nearshore islets (i.e., Sea Lion Rocks) with the incident wave field and corresponding currents. Thus, to determine if a better classification is possible by restricting the embayment width and shoreline length, a much more detailed study is required which is beyond the scope of this study.

3.4.2 Nearshore Sediment Transport Pathways

Both case *i* and case *ii* net transport trends recognized by McLaren and Bowles (1985) were identified to be statistically significant in Wickaninnish Bay (0.01 level of significance, one-tailed test). See Appendix 1 for sediment moment statistics. Case *i* (trending towards finer, better sorted, and more negatively skewed deposits) was significant in the NW direction (Z = 16.472), and case *ii* (trending towards coarser, better sorted, and more positively skewed deposits) was significant in the SE direction (Z = 3.003). Z-score strength suggests that NW net swash-driven sediment transport trends are prevalent. This trend aligns with the WNW extension of the foredune complex and supratidal beach plain fronting Sandhill Creek and may contribute to its extension through littoral sediment inputs. While Z-score strengths suggest that case *i* is the predominant trend, significant transport in both directions was revealed. This is expected as it is known that oscillating flows operate in Wickaninnish Bay that may confuse evidence for net littoral sediment transport directions. Oscillating flows may be created by a number of factors including wave refraction around headlands and islets, variable bathymetry and submerged surficial morphology, and/or current interactions at the fluvial-marine interface of Sandhill Creek. The model is also sensitive to the spatial scale analysed. While legitimate nearshore net sediment transport pathways may exist within the area chosen, they may not be identified by the McLaren Method as conflicting nearshore flow directions (e.g., rip cell circulation) may confound legitimate signals. For example, in Wickaninnish Bay it may be more appropriate to examine transport trends from Schooner Cove to Green Point, and Green Point to Quisitis Point in consideration of the potential hydrodynamic influence (e.g., wave refraction and attenuation) of the rocky headlands at Green Point and the nearshore islets (e.g., Sea Lion Rocks). In addition, the McLaren Method assumes a single sediment source. Sediment inputs from Sandhill Creek may violate this assumption.

General beach-face sediment characteristics were also derived from the above analysis. Sediments sampled from the high tide line (HTL) across the greater Wickaninnish Bay have a mean grain size of 2.542 ϕ (174.65 µm) and a modal size of 2.605 ϕ (165.0 µm). Sediments in the dunes along Wickaninnish Beach have a mean grain size of 2.295 ϕ (203.7 µm) and a modal size of 2.605 ϕ (165.0 µm), the latter being the same as that on the beach. All but one sample was negatively skewed, and the greater proportion (70.8%) were strongly negatively skewed.

Samples taken from the HTL immediately north of the large transgressive dune system and near the outlet of Sandhill Creek were less negatively skewed. Skewness is reflective of both grain size and sorting and can provide insight to direction of transport. Reworked fluvial sediment inputs and/or influence by complex surf zone circulation processes near the outlet of Sandhill Creek may be responsible for the atypical grain characteristics found at this location.

3.4.3 Aeolian Sediment Transport Potential

The annual average total sediment transport potential (TP) on Wickaninnish Beach is 9984.31 m^3 m^{-1} a^{-1} and the resultant transport potential (RTP) is 3268.28 m^3 m^{-1} a^{-1} at a resultant transport direction (RTD) of 356° in relation to true north (as per Arens *et al.*, 2004 and Hugenholtz *et al.*, 2009) Due to a bi-modal, high energy wind regime, potential aeolian sediment transport is bimodal. The resultant transport direction shifts seasonally (Table 3.4) with dominant transport from September to March in a NW direction in response to winter winds from the SE. From April to August, dominant transport is in an ESE direction in response to summer winds from the WNW. Both TP and RTP are appreciably greater in winter months and, in general, transport is more unidirectional. This finding can be attributed to the strength and directional consistency of winter storms. However, winter aeolian sand transport may actually be less than predicted due to high amounts of precipitation compared to summer months, which would effectively increase the sediment entrainment threshold wind speed. In most conventional models the influence of moisture content in potential sediment transport calculations is unaccounted. In addition, given the NW alignment of Wickaninnish Beach, and the obstruction created by Quisitis Point, the predominantly SE winter winds are not expected to be as effective as the WNW summer winds in onshore sediment transport. In fact, offshore sediment transport has been observed under strong SE winter wind events. The WNW alignment of the long axes of the transgressive dunes in the backshore supports the interpretation that, while SE winter winds are stronger and have greater aeolian sediment transport potential, the WNW summer winds appear to be more effective in terms of sediment transport within the Wickaninnish dune system. While this is true for the transgressive dune

complex, the SE winter winds likely contribute to the WNW extension of the foredune complex and incipient dune plain fronting Sandhill Creek (see Figure 3.21 and section 2.8.1).

Table 3.4. Monthly and annual calculated aeolian sediment transport potential (TP), resultant transport potential (RTP), resultant transport direction (RTD), ratio of resultant transport potential to overall transport potential (RTP/TP), and percent annual transport potential, calculated as per the methods of Arens *et al.* (2004).

Month	TP ($m^3m^{-1}a^{-1}$)	RTP ($m^3m^{-1}a^{-1}$)	RTD (° to true north)	RTP/TP	% Annual TP
January	960.09	319.17	344.70	0.33	9.62
February	1128.47	418.12	350.70	0.37	11.30
March	1397.65	504.73	343.53	0.36	14.00
April	1060.03	299.08	18.97	0.28	10.62
May	739.48	289.59	57.30	0.39	7.41
June	698.43	360.57	77.55	0.52	7.00
July	430.43	189.07	75.85	0.44	4.31
August	319.72	102.94	19.25	0.32	3.20
September	289.60	109.17	351.97	0.38	2.90
October	787.37	410.07	322.70	0.52	7.89
November	1117.80	651.70	328.88	0.58	11.20
December	1055.27	481.12	330.76	0.46	10.57
Annual	**9984.31**	**3268.28**	**356.12**	**0.33**	**100.00**

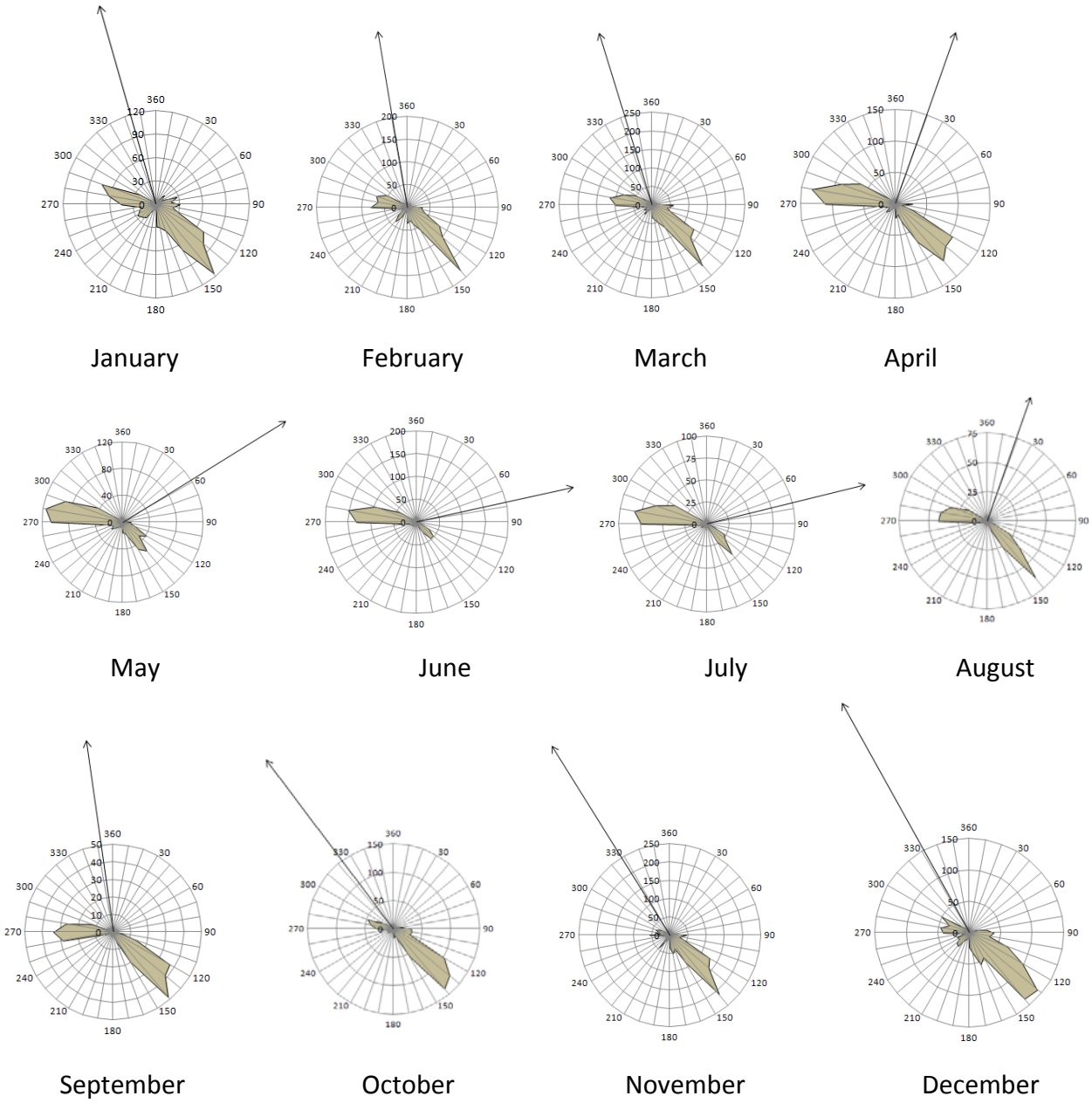

Figure 3.10. Monthly predicted sediment transport roses for the Wickaninnish beach-dune system (1971 to 1977). Brown regions represent the direction sediment transport is from while the arrow (resultant transport direction [RTP] vector) indicates the direction where sand is transporting towards. The length of the RTP vector is proportional to the magnitude of potential sediment transport.

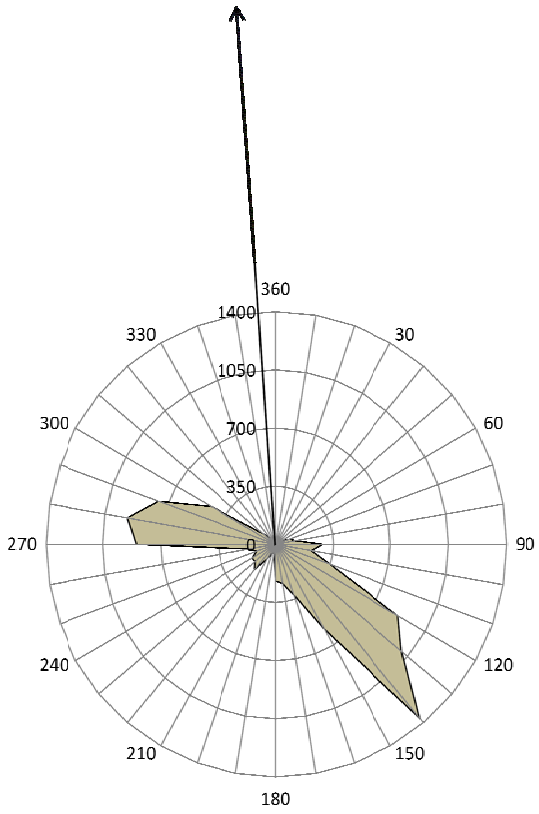

Figure 3.11. Annual predicted sediment transport rose for the Wickaninnish beach-dune system (1971 to 1977). Brown region represents the direction sediment transport is from while the arrow (resultant transport direction [RTP] vector) indicates the direction where sand is transporting towards (356°). The length of the RTP vector is proportional to the magnitude of potential sediment transport.

3.4.4 Bathymetric Profiles

Bathymetric data extended from the transect 3 show a bar approximately 250 m wide (i.e., horizontal distance) and 0.5 m to 1 m in height at approximately -6 m aCD (Figure 3.12). This bar is evident from the beach as a wave breaking point approximately 500 m offshore under big swell conditions. This bar may serve to store sediments during the winter season until they are returned to the beach face in the summer.

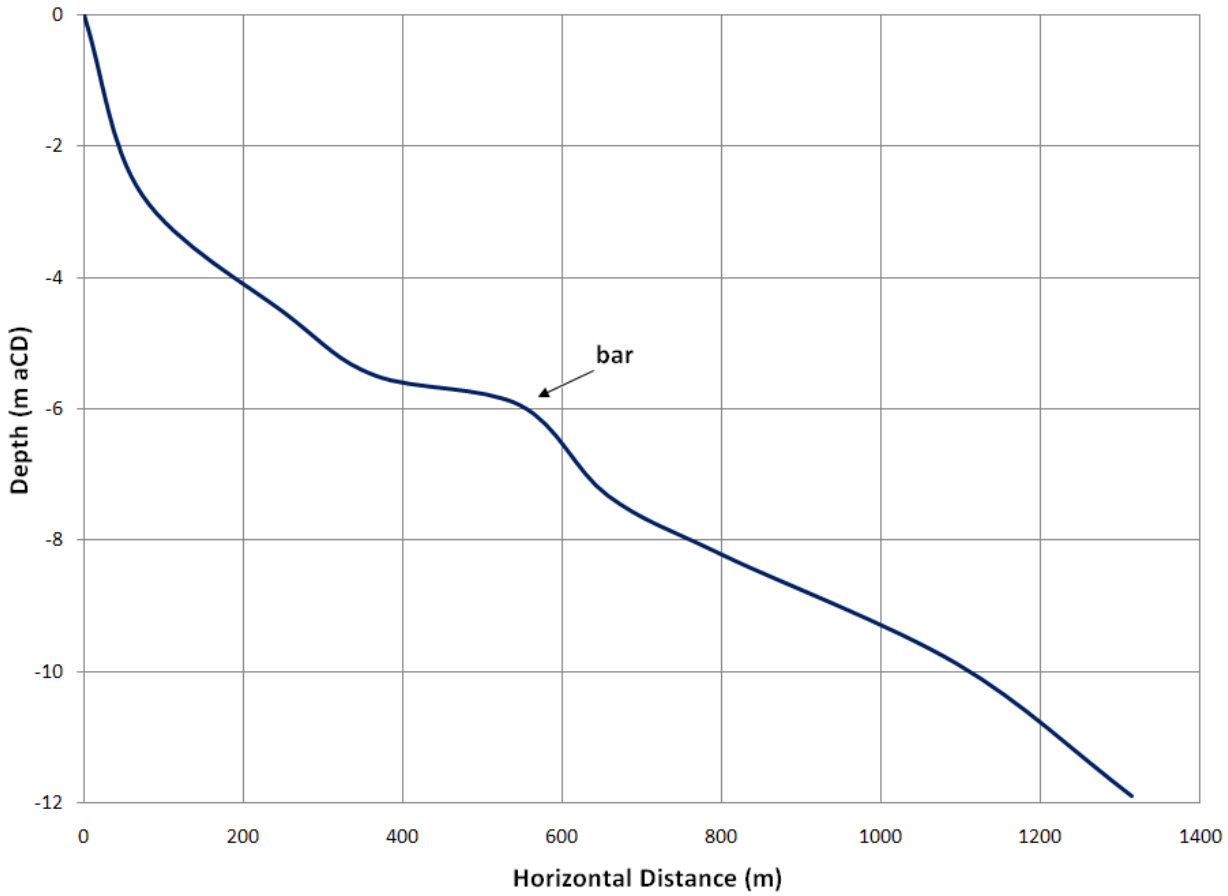

Figure 3.12. Bathymetric profile (an extension of transect 3) derived from Canadian Hydrographic Service field data sheets (Parizeau *et al.*, 1931). Vertical exaggeration of the profile is 560 times.

3.4.5 Morphological Responses from Cross-Shore Topographic Profiles

Three cross-shore profiles exist for each transect on Wickaninnish Beach (July/August 2008, August 2009, March 2010). Profiles from 2008 were gathered *in situ* using a total station, 2009 profiles were extracted from LiDAR data, and 2010 profiles are extracted from a DEM created from a full topographic survey of the beach-dune system. Both 2009 and 2010 profiles were extracted using the same coordinates from the 2008 survey. See Appendix B for data required to reproduce these transects.

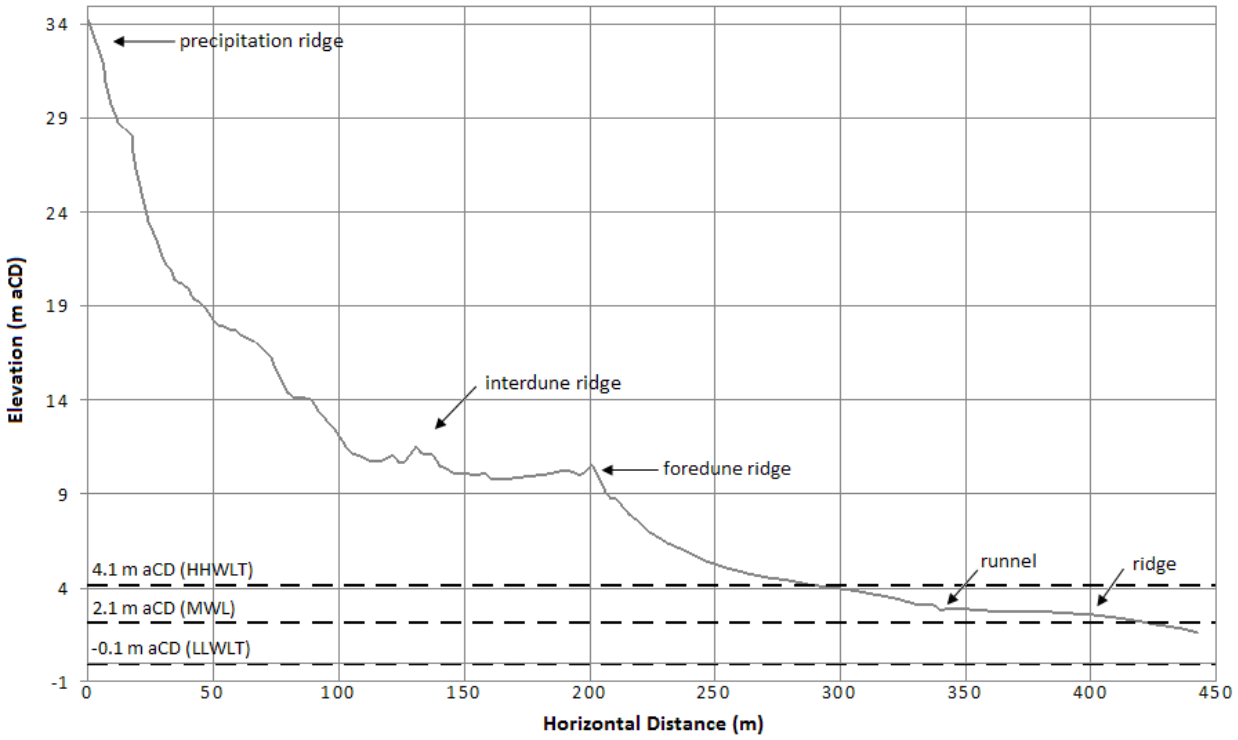

Figure 3.13. Transect 2 from 2009 field survey. This profile was not included in the comparative study below as the same transect was not established between the years.

The profile of transect 2 surveyed *in situ* in 2009 (Figure 3.13) captured more of the intertidal zone than any other survey. It is not comparable with 2008 profiles as benchmark loss and the establishment of an incorrect bearing created positional discrepancies between the years. However, it provides a good example of intertidal morphology. Ridges and runnels are evident in the intertidal zone and, as above, the mid-intertidal zone assumes a more gradual slope than the upper-intertidal zone.

An obvious berm exists on transect 1 in the 2008 profile (Figure 3.14a), a small berm is present on transect 2 in its 2008 profile (Figure 3.15a), and berms are absent on transect 3 (Figure 3.16a). Berms may be seasonal as sediment moves onshore from bar systems and contributes to berm development under calmer summer wave conditions (mean significant wave height of 1.49 m). With the return of stormier winter conditions (mean significant wave height of 2.42 m), sediments stored in the berm are removed from the shoreface and returned to bar systems (Hughes & Turner, 1999).

In 2008 and 2010, following the loss of the berm on transect 1, the upper intertidal beachface smoothed and its slope assumed a more gradual form (2.28° to 1.21°, respectively). In 2010, a considerable amount of sediment was removed from the upper intertidal beachface (Figure 3.14a). The berm was also removed on transect 2 but, as above, the upper intertidal zone exhibited more trends of accretion than erosion (Figure 3.15a). On transect 3, while 2008 and 2009 profiles exhibited much the same form in the upper intertidal zone, in 2010 there was considerable accretion in this region (Figure 3.16a). Build up of the upper intertidal zone in the winter (March) seems anomalous as sediments are theoretically moved seaward under higher wave conditions and stored in bar systems. While this cycle of seasonal sediment movement is conventionally accepted, Aagard *et al*. (2004) claim that onshore sediment transport is possible under high energy storm conditions when wave-induced sediment transport is dominant versus offshore sediment transport associated with undertow. This scenario is most likely on gently sloping, dissipative beaches as the strength of the undertow is proportional to beach slope (Aagard *et al.*, 2004). Wickaninnish Beach is an intermediate beach, assuming both dissipative and reflective conditions. While assuming a dissipative morphology, according to the findings of Aagard *et al.* (2004), onshore sediment transport during the winter season is probable if conditions are such that wave-driven onshore sediment transport is greater than undertow.

Incipient dunes are present in all 2008 and 2009 profiles and absent in all 2010 profiles. Both the 2008 and 2009 profiles were surveyed during the summer season, exposed to lower mean water levels, whereas the 2010 profiles were surveyed during the winter season, with relatively higher mean water levels. Seasonal differences in mean water levels are a function of both differences in wave runup, extreme tides, and storminess, where all are greater on average in the winter season. As above, incipient dunes are ephemeral features and can be removed by high water levels or in association with the senescence and death of annual pioneer plant species. Thus, it is rational that incipient dunes are absent in the 2010 winter survey.

The stoss and lee foredune slopes on transect 1 did not change considerably between 2008 to 2010, whereas the foredune ridge accreted (Figure 3.14a). On transect 2 the foredune changed little, except for deposition on the leeward side of the ridge (Figure 3.15a). On transect

3, consistent erosion of the foredune ridge and deposition on the leeward slope occurred between 2008 and 2010 (Figure 3.16a). The stoss slope, however, remained unchanged between 2008 and 2009, but accreted considerably in 2010.

All profiles suggest aeolian activity in the inter-dune area. Transect 1 indicates the erosion of an inter-dune feature from 2008 to 2010 (Figure 3.14a). Transect 2 is relatively uniform in the backdune region. However, the slow landward migration (0.55 m a^{-1}) of an inter-dune ridge is apparent (Figure 3.15a). Transect 3 reveals a lot of dynamism in the inter-dune region with the vertical accretion of an inter-dune ridge. In addition, considerable accretion at the toe of the precipitation ridge occurred (Figure 3.16a). In all profiles the precipitation ridge is relatively uniform. Interpolation of the LiDAR and full topographic survey data to create DEMs led to the loss of some edge data, particularly data on the precipitation ridge. Thus, volumetric calculations only included data shoreward of major discrepancies between the profiles on the precipitation ridge.

According to vantage photography, qualitative change in foredune morphology is most evident on transect 1. Erosional scarps are obvious in the 2008 photograph (Figure 3.14b) and are infilled in the 2009 photograph (Figure 3.14c). This suggests rebuilding of the beach-dune system over this interval. Other vantage photographs are not revealing of obvious morphological changes (besides variability in annuals, flotsam, and incipient foredune position).

While surveys show seasonal and/or shorter-term morphological changes, they are not yet revealing of contemporary trends in beach-dune form and shoreline position.

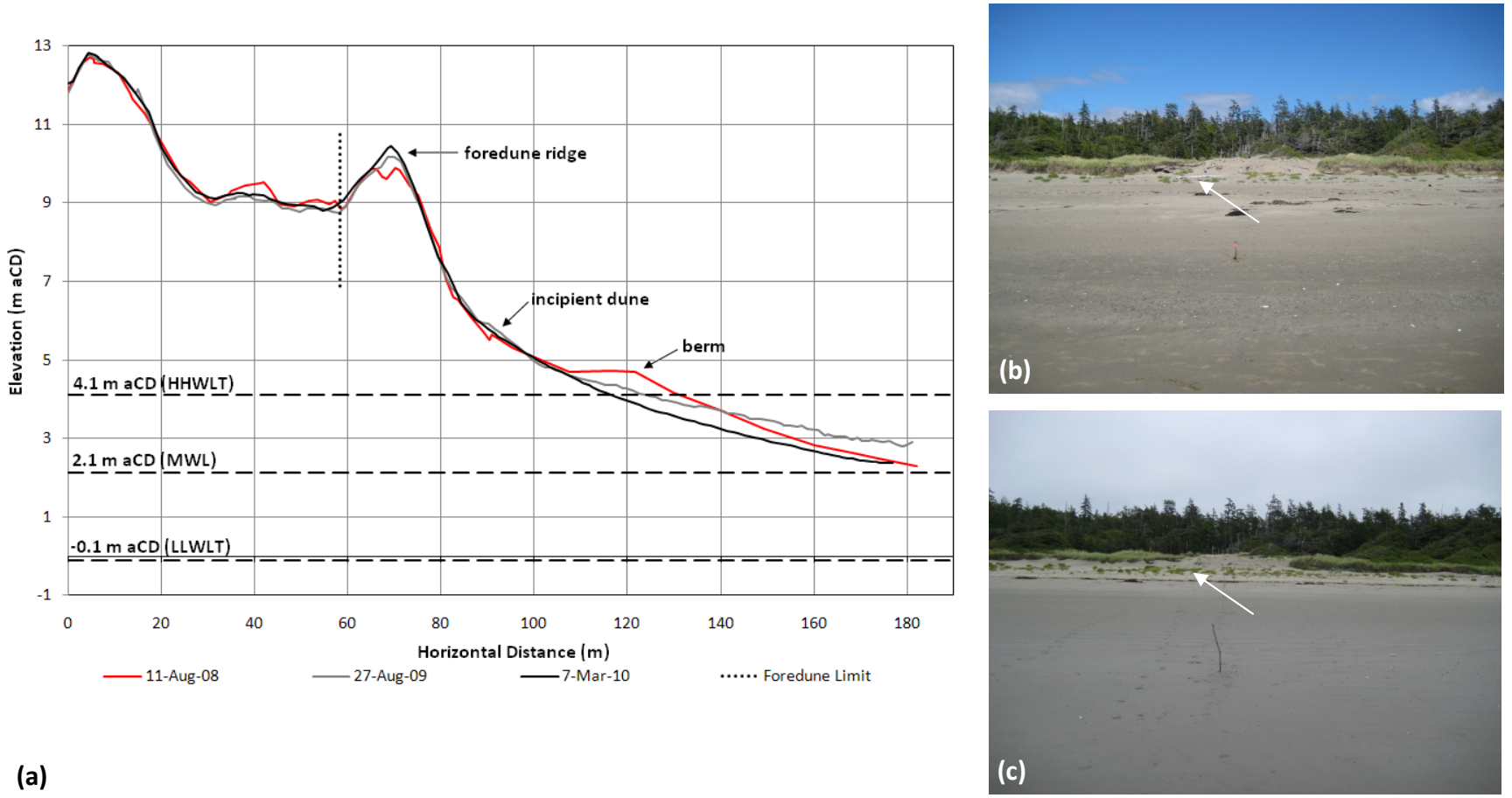

Figure 3.14. (a) Transect 1. Vertical exaggeration of the profile is 13.6 times. HHWLT indicates the highest high water large tide elevation, MWL indicates the mean water level elevation, and LLWLT indicates the lowest low water large tide elevation. (b) The 2008 vantage photograph from the waterline landward. Arrow indicates a scarped foredune. (c) The 2009 vantage photograph from the waterline landward. Arrow indicates infilled foredune.

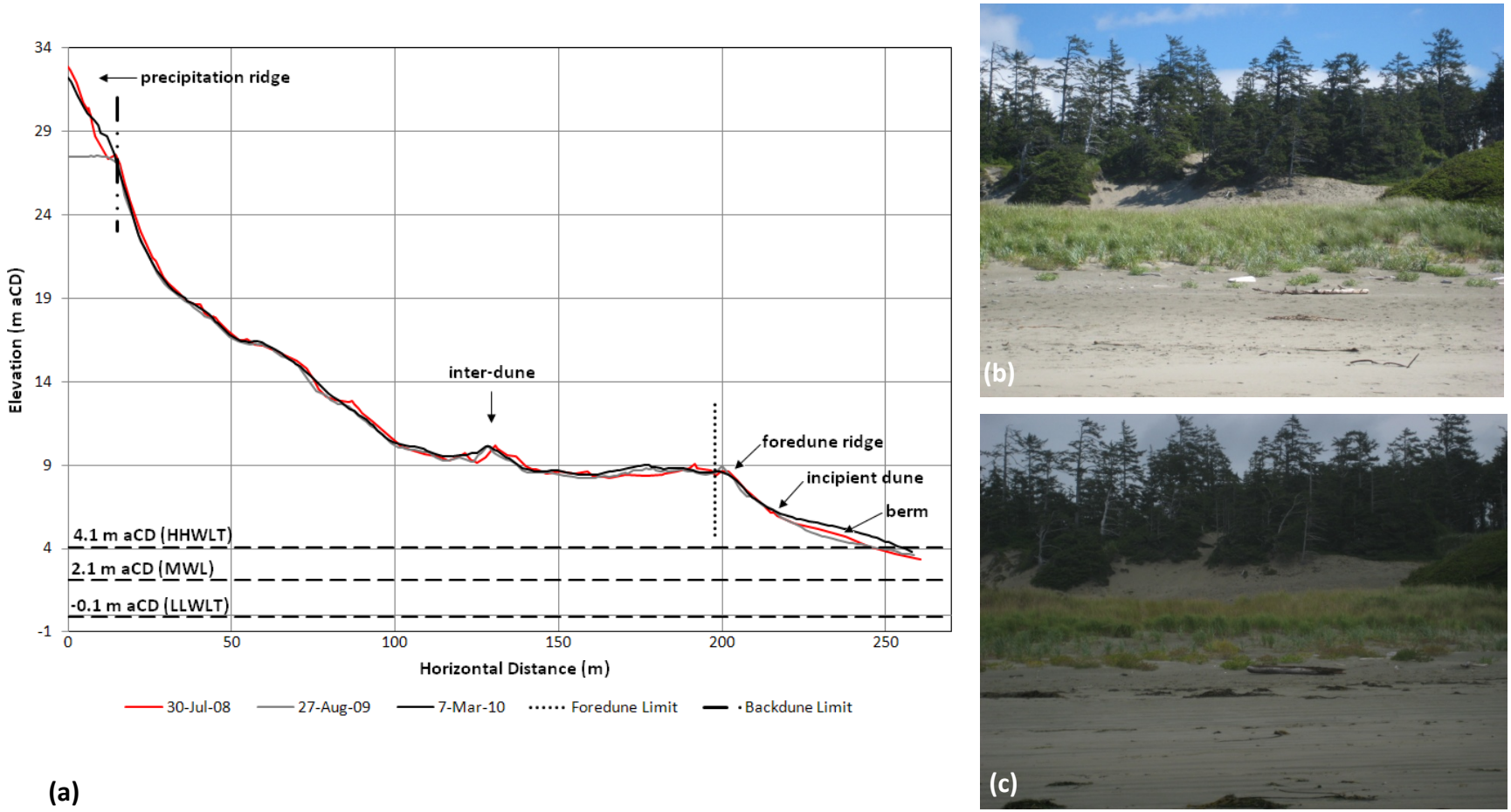

Figure 3.15. (a) Transect 2. Vertical exaggeration of the profile is 7.7 times. HHWLT indicates the highest high water large tide elevation, MWL indicates the mean water level elevation, and LLWLT indicates the lowest low water large tide elevation. (b) The 2008 vantage photograph from the waterline landward. (c) The 2009 vantage photograph from the waterline landward.

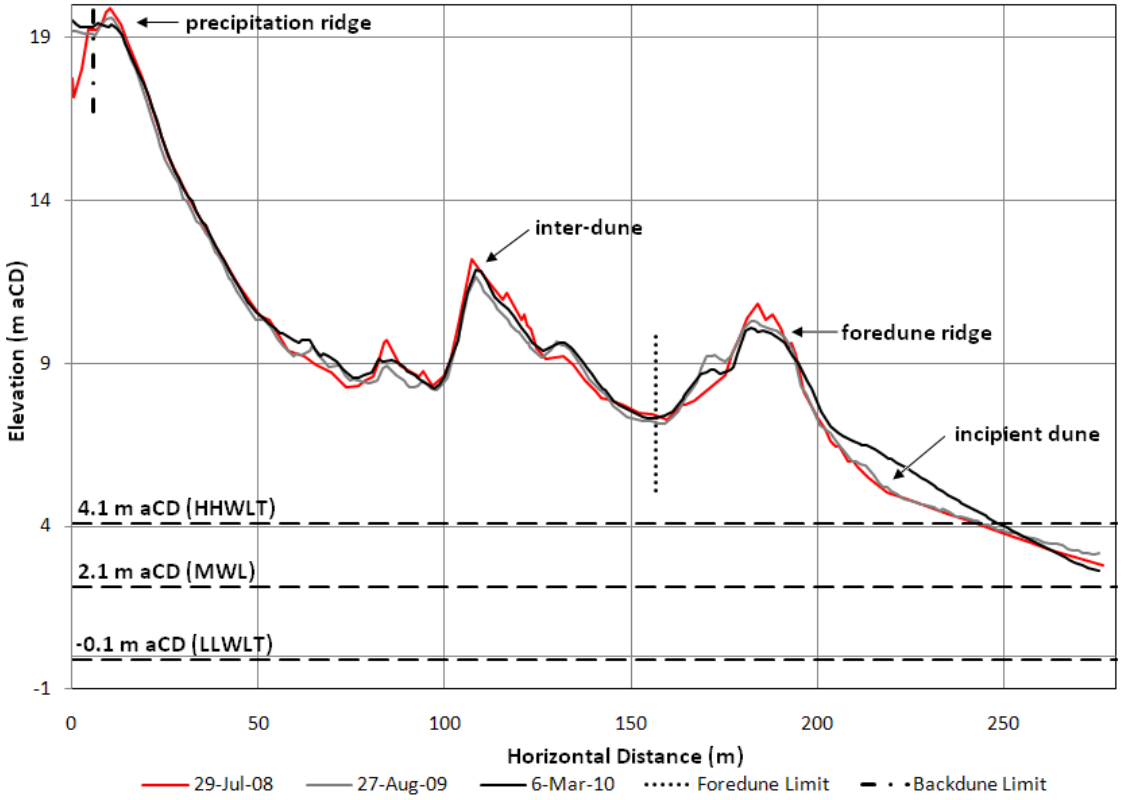

(a)

Figure 3.16. (a) Transect 3. Vertical exaggeration of the profile is 13.3 times. HHWLT indicates the highest high water large tide elevation, MWL indicates the mean water level elevation, and LLWLT indicates the lowest low water large tide elevation. (b) The 2008 vantage photograph from the waterline landward. (c) The 2009 vantage photograph from the waterline landward.

Volumetric change estimates for transect 1 (Table 3.5) indicate that it has generally experienced erosion from 2008 to 2010. Erosion was focused on the beach and foredune regions, whereas the backdune and inter-dune region changed little. Volumetric change on transect 2 (Table 3.6) from 2008 to 2010 was proportionally greater on the beach and foredune than on the inter-dune and backdune region. Closer analysis reveals that whereas volumetric change was proportionately greatest on the beach and foredune from 2008 to 2009, it was proportionately greatest from 2009 to 2010 in the backdune region. Volumetric change estimates for transect 3 (Table 3.7) show overall change on the beach and foredune was proportionately greater than change in the inter-dune and backdune region. However, change from 2008 to 2009 was greatest in the backdune region (erosion/deflation), and from 2009 to 2010 was greatest on the foredune and beach (accretion).

As the data are representative of different seasons (i.e., summer 2008 and 2009, winter 2010) and natural processes (e.g., onshore to offshore movement of sediment stores) have not yet had an opportunity to cycle in full in the final observation year, conclusions may be unrepresentative of the true conditions of sediment transport. Volumetric change between years 2008 to 2009 may be more representative of volumetric change on Wickaninnish Beach.

Table 3.5. Volumetric change of transect 1 from 2008 to 2010.

(a)

Volumetric Change (m^3) of Total Profile				
	2008	% Change (m^3m^{-3})	2009	% Change (m^3m^{-3})
2009	-2.05	-0.17	n/a	n/a
2010	-35.53	-2.92	-33.48	-2.76

(b)

Volumetric Change (m^3) of Foredune – Beach				
	2008	% Change (m^3m^{-3})	2009	% Change (m^3m^{-3})
2009	5.56	0.90	n/a	n/a
2010	-32.56	-5.26	-38.12	-6.11

(c)

Volumetric Change (m^3) of Foredune – Backdune				
	2008	% Change (m^3m^{-3})	2009	% Change (m^3m^{-3})
2009	-7.61	-1.27	n/a	n/a
2010	-2.97	-0.49	4.65	-0.79

Table 3.6. Volumetric change of transect 2 from 2008 to 2010.

(a)

Volumetric Change (m^3) of Total Profile				
	2008	% Change (m^3m^{-3})	2009	% Change (m^3m^{-3})
2009	-32.90	-1.26	n/a	n/a
2010	32.20	1.23	65.10	2.52

(b)

Volumetric Change (m^3) of Foredune – Beach				
	2008	% Change (m^3m^{-3})	2009	% Change (m^3m^{-3})
2009	-22.18	-6.27	n/a	n/a
2010	-1.70	-0.48	20.48	6.17

(c)

Volumetric Change (m^3) of Foredune – Backdune				
	2008	% Change (m^3m^{-3})	2009	% Change (m^3m^{-3})
2009	-10.72	-0.47	n/a	n/a
2010	33.90	1.50	44.62	1.98

Table 3.7. Volumetric change of transect 3 from 2008 to 2010.

(a)

Volumetric Change (m^3) of Total Profile				
	2008	% Change (m^3m^{-3})	2009	% Change (m^3m^{-3})
2009	-23.37	-0.98	n/a	n/a
2010	28.46	1.19	51.83	2.19

(b)

Volumetric Change (m^3) of Foredune – Beach				
	2008	% Change (m^3m^{-3})	2009	% Change (m^3m^{-3})
2009	0.29	0.04	n/a	n/a
2010	22.53	3.10	22.24	3.06

(c)

Volumetric Change (m^3) of Foredune – Backdune				
	2008	% Change (m^3m^{-3})	2009	% Change (m^3m^{-3})
2009	-17.76	-1.07	n/a	n/a
2010	5.93	0.36	23.69	1.44

3.4.6 Airphoto Analyses

Heathfield and Walker (in review) assessed changes in dune sand surface extent and shoreline positions at Wickaninnish, Long and Combers beaches in Wickaninnish Bay through the analysis of airphotos from 1973, 1996, and 2007. See Table 3.8 for a results summary.

Table 3.8. Rates of change in shoreline position and dune sand surface extent from 1973 to 2007 at Wickaninnish, Long and Combers beaches (Heathfield & Walker, in review).

	Mean Shoreline Position Change (m)				**Dune Sand Surface Extent (m^2)**				
Study Site		**1973 to 1996**	**1996 to 2007**	**Total Change**		**1973**	**1996**	**2007**	**Total % Change**
Wickaninnish Beach	Total Distance (m)	+2.24 ± 0.9	+5.02 ± 0.9	**+7.26 ± 0.9**	Total Area (m^2)	126,931 ± 0.81	91,013 ± 0.81	91,642 ± 0.81	**-27.8**
	Rate of Change (m a^{-1})	0.1	0.5	**0.2**	%Change	n/a	-28.3	+0.7	
Combers Beach	Total Distance (m)	+24.93 ± 0.9	+10.77 ± 0.9	**+35.70 ± 0.9**	Total Area (m^2)	n/a	n/a	n/a	**n/a**
	Rate of Change (m a^{-1})	1.1	1.0	**1.0**	%Change	n/a	n/a	n/a	
Long Beach	Total Distance (m)	+14.04 ± 0.9	-1.50 ± 0.9	**+12.45 ± 0.9**	Total Area (m^2)	n/a	n/a	n/a	**n/a**
	Rate of Change (m a^{-1})	0.6	-0.1	**0.4**	%Change	n/a	n/a	n/a	

The Wickaninnish dune complex has stabilized (loss of dune sand surface extent) over the period of 1973 to 2007 (Figure 3.18). Whereas the overall trend of stabilization accurately represents that seen from 1973 to 1996, specific analysis of the 1996 to 2007 airphotos actually reveals expansion of the dune sand surface. Heathfield and Walker (in review) attribute this to the growth of blowouts in the transgressive dune complex and expansion of the precipitation ridge into the forest at the SE extent of the dunefield (Figure 3.18). Much of the measured stabilization from 1973 to 2007 can be credited to invasion of beach grasses (*Ammophila* spp.) in the 1980s (B. Campbell, personal communication, 17 September, 2009). As seen in a 1970 airphoto (Figure 3.17), prior to the dominance of non-native species on the foredune, the foredune was more sparsely vegetated. As above, *Ammophila* spp. colonize the foredune more densely than native grasses thereby creating increased surface roughness. This disrupts aeolian flow over the foredune, resulting in the deposition of entrained sediments and interrupting

sand supply to the backdune (Weidemann & Pickart, 1996). Without sediment deposition and scour in the backdune, the setting becomes more conducive for non-specialized species and encroachment of forest communities, leading to a loss of dune sand surface extent. Stabilization is also encouraged under current climate change trends (see section 4.1.1), where increasing temperatures and precipitation favour vegetation growth versus system dynamism. However, while climate change trends favour productivity, increased nutrient leaching associated with increased precipitation may serve to delay stabilization and succession rates by limiting vegetation growth (Walker & Sydneysmith, 2008).

Figure 3.17. Aerial photograph of Wickaninnish Beach from 1 June 1970. Notice the foredunes are more sparsely vegetated as compared to the 2009 aerial photograph (Figure 2.17). Scale 1:15,840. BC airphoto BC7237-106, with permission.

While dune sand surface extent has decreased between 1973 and 2007, the shoreline has prograded. Shoreline progradation likely corresponds to regional tectonic uplift responsible

for a relative fall in sea level (Wolynec, 2004). Wickaninnish Beach appears to be capable of continuing with this trend of progradation given evidence of progradation in airphoto analysis (Heathfield & Walker, in review), obvious strong rebuilding potential shown in repeat vantage photography (Figure 3.14a and 3.14c), and potential sediment transport calculated for the beach.

The shoreline has also prograded just north of the Wickaninnish Interpretive Centre. This area of progradation coincides with a large woody debris (LWD) accumulation zone. Beyond the accumulation zone the shoreline is generally stable (Figure 3.19). Thus, this progradation may be due to accumulation of LWD.

As evident in sequential airphotos and from the analyses of Heathfield and Walker (in review), the mouth of Sandhill Creek at Combers Beach has extended parallel to the shoreline in a NW direction from 1973 to 2007 (Figure 3.21). This extension is responsible for continued backshore erosion and shoreline retreat, and resultant infrastructure damage is a concern for Parks Canada. To avoid loss of infrastructure, the continued seasonal closure of Combers Beach parking lot and the removal of the beach-access stairs is required. Erosion rates at this meander should continue to be monitored to assess the risk to further infrastructure, such as boardwalks, in the area. See section 2.8.1 for a discussion of the processes that contribute to this trend.

Figure 3.18. Comparative analysis of the sand surface extent and shoreline of the Wickaninnish dune system from 1973 to 2007 (Heathfield & Walker, in review, with permission).

Figure 3.19. Comparative analysis of the Wickaninnish shoreline from 1973 to 2007 (Heathfield & Walker, in review, with permission).

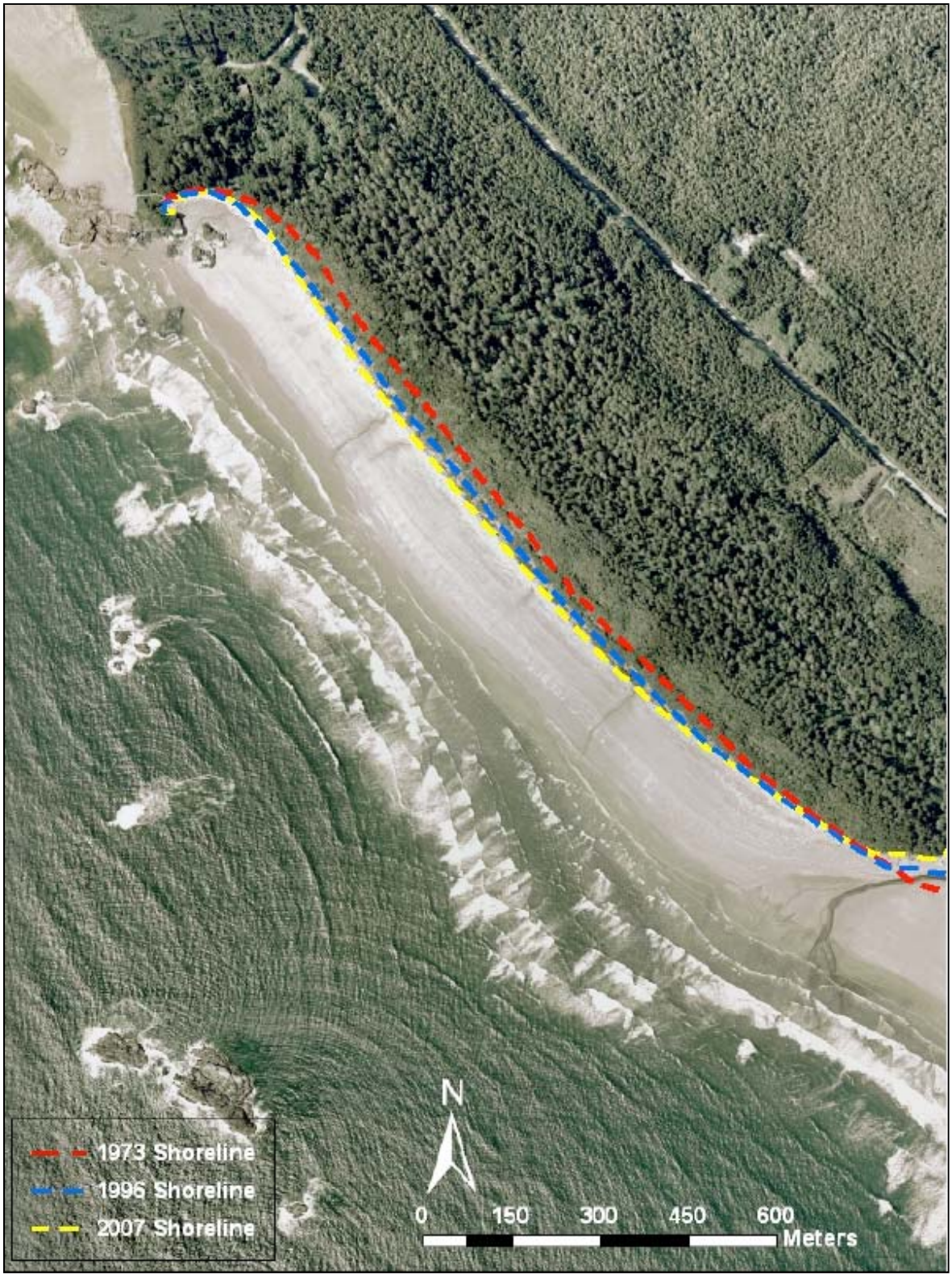

Figure 3.20. Analysis of shoreline change at Combers Beach from 1973 to 2007 (Heathfield & Walker, in review, with permission).

Figure 3.21. Analysis of shoreline change at Sandhill Creek 1973 to 2007 (Heathfield & Walker, in review, with permission).

While backshore erosion had occurred at the mouth of Sandhill Creek, the shore north of the creek (i.e., Combers Beach) has demonstrated rapid seaward progradation (35.7 m $\pm$ 0.9 m from 1973 to 2007, 1.0 m a^{-1}). This progradation may be attributed to a fall in relative sea level resulting from regional tectonic uplift (Wolynec, 2004), in conjunction with consistent onshore sediment supply, continued vegetation colonization, and, possibly, historical inputs of large woody debris (LWD) via escape logs from the coastal logging industry. Wave defraction and attenuation by the nearshore islets of Sea Lion Rocks may also reduce wave energy, allowing for continued shoreline progradation from deposition and/or alteration of nearshore sediment transport pathways. In addition, the creek may be contributing to progradation trends through the delivery of reworked backshore sediments. Both anecdotal evidence and Heathfield & Walker (in review) suggest that anthropogenic LWD inputs have decreased, perhaps due to improvement in logging transport technologies. LWD accumulations act as an 'accretion anchor' on the backshore, anchoring and storing sediments within the debris matrix. They also buffer the shoreline from wave attack. Furthermore, LWD is a nuclei for incipient dune formation, where shadow dunes are formed in the lee of the debris (Walker & Barrie, 2006). These attributes may have contributed to rapid shoreline progradation in recent history and, as a result of fewer LWD inputs, trends in progradation may slow.

3.5 Conclusion

As per the Masselink and Short (1993) classification, Wickaninnish Beach is a low tide bar/rip beach. This classification is generally fitting. Some bar morphology exists, with low amplitude bars on the summer shoreface and a moderately sized (250 m cross-shore width, 0.5 to 1 m height) nearshore bar around -6 m a CD. In addition, local knowledge, aerial photo evidence, and cuspate shoreface features suggest that rip cell circulation operates on Wickaninnish Beach. However, the McLaren Model (McLaren & Bowles, 1985) shows that a prevailing NW littoral current exists in the larger embayment. This finding explains the NW extension of the incipient foredune plain and the migration of the outlet of Sandhill Creek.

Rebuilding potential on the beach is high as evident from the RTP (3268.28 m^3 m^{-1} a^{-1}) and repeat vantage photography (Figures 3.14b and 3.14c). The potential sediment transport regime is bimodal, corresponding to the wind regime, with transport in summer months dominantly from the WNW and from the SE in winter. The RTD for the region is 356°. Whereas potential transport is greater from the SE during winter months, competent winds may decelerate due to topographic forcing and roughness effects created by Quisitis Point at the southern extent of Wickaninnish Bay. This theory is supported by the NW-SE alignment of the Wickaninnish dunes. However, north of the dunefield, morphological evidence (i.e., pattern of accretion in the lee of shadow dunes) indicates that the supratidal beach plain receives some of the SE component of the aeolian transport regime. Thus, the SE component plays a significant role in some areas and, might explain the continual NW extension of the incipient foredune complex.

Cross-shore transects show both erosion and accretion over the two years of *in situ* surveys. Thus, this reveals that over the shorter-term, erosion and accretion occur at concentrated locations across the beach and longer-term monitoring is required to reveal trends in the beach-dune system. Review of the aerial photo record reveals that, overall, Wickaninnish Beach is prograding (0.2 m a^{-1}) and the dunefield is stabilizing (27.8% reduction between 1973 to 2007). Much of the trend in stabilization may be attributed to the presence of *Ammophila* spp.*,* though it is recognized that climate change has also contributed to an environment more advantageous for vegetation growth (Whitfield & Taylor, 1998).

4.0 Erosive Water Level Regime and Correlations with Climatic Variability

4.1 Introduction

Recently in the northeastern Pacific and, more specifically, coastal British Columbia, there has been a demonstrated increase in the frequency and intensity of extreme events (Ruggiero *et al.*, 2001; Allan & Komar, 2006; Walker & Barrie, 2006; Cumming, 2007; Abeysirigunawardena & Walker, 2008; Walker & Sydneysmith, 2008). This increase may be linked to ocean-atmosphere phenomena including the El Niño-Southern Oscillation (ENSO), the Aleutian Low Pressure System, and the Pacific Decadal Oscillation (PDO) (Storlazzi *et al.*, 2000; Ruggiero *et al.*, 2001; Barrie & Conway, 2002; Allan & Komar, 2006; Walker & Barrie, 2006; Abeysirigunawardena & Walker, 2008); and may translate to higher winds (e.g., Graham & Diaz, 2001), temporarily elevated sea levels (e.g., Subbotina *et al.*, 2001; Barrie & Conway, 2002), higher significant wave heights and peak periods (e.g., Ruggiero *et al.*, 2001; Allan & Komar, 2006) which, in turn, create higher runup levels. Higher total water levels may contribute to increased coastal erosion, shoreline retreat and/or loss of beach-dune barrier systems, flooding, and ecosystem shifts, and higher wind levels may encourage system dynamism through increased aeolian erosion (e.g., blowout formation). These impacts have considerable implications for protected areas management approaches and infrastructure planning.

This chapter will examine the erosive water level regime on Wickaninnish Beach, identifying the recurrence interval of erosive events and annual to 100-year return levels. Subsequently, the relationship between variations in ocean-atmosphere phenomena in the study region (e.g., mean and maximum significant wave heights, modal peak wave period) and existing climate variability indices (e.g., PDO, Aleutian Low Pressure Index [ALPI]) will be investigated to explore the role of climate variability in the incidence and magnitude of extreme events that contribute to the erosive water level regime.

4.2 Literature Review

Total water levels are a function of the interaction between tidal elevation, surge, and wave runup (Ruggiero *et al.*, 2001). As above, a demonstrated link between extreme events and climate variability phenomena and climate change trends in the Northeastern Pacific exists (Storlazzi *et al.*, 2000; Ruggiero *et al.*, 2001; Barrie & Conway, 2002; Allan & Komar, 2006; Walker & Barrie, 2006; Abeysirigunawardena & Walker, 2008). Thus, this section will begin with review of climate variability phenomena and climate change trends in the Northeast Pacific and will be followed by a summary of research to date that addresses each component of the erosive water level regime in the Northeast Pacific.

4.2.1 Climate Variability Phenomena of the Northeastern Pacific Ocean

Variations in climate and sea level in the Northeastern Pacific Ocean are driven by known ocean-atmosphere phenomena including the El Niño Southern Oscillation (ENSO), the Aleutian Low Pressure System, and the Pacific Decadal Oscillation (PDO) (Gedalof & Smith, 2001; Ruggerio *et al.*, 2001; Barrie & Conway, 2002; Abeysirigunawardena & Walker, 2008). These phenomena are influenced by a number of common controlling factors, such as sea surface temperatures and sea level pressure, although all are distinct phenomena.

ENSO is caused by an alternating pattern of sea level pressure between the eastern and western equatorial Pacific. This phenomenon typically cycles between warm and cool phases over a period of three to seven years. During its warm phase (El Niño), easterly trade winds are slackened (and sometimes reversed) due to higher than average sea level pressures in the western equatorial Pacific, which causes warm surface waters to migrate eastward (Chelton & Enfield, 1986). This translates to reduced wind-driven upwelling along the Pacific Coast of the Americas and a resulting rise in coastal sea surface temperatures. Correspondingly, steric mean sea levels (i.e., those influenced by thermal expansion or contraction; Ryan & Noble, 2006) rise. La Niña is the cyclic counterpart to El Niño and is associated with basin wide cooling of the tropical Pacific. Although in the equatorial Pacific La Niña effects are generally opposite to those of El Niño, its global effects are more complex.

The Aleutian Low System is an annual winter weather pattern over the North Pacific Ocean influencing sea surface pressures and, correspondingly, controlling the strength of winter storms. Typically, it resides in the Gulf of Alaska, near the Aleutian Islands. The effects of the Aleutian Low System intensify late in the year, operating throughout the winter period, and weaken in the spring of the following year (Beamish *et al.*, 1999).

The PDO is a longer-term ocean-atmosphere phenomenon, oscillating over periods of 20 to 30 years. Unlike other ocean-atmosphere phenomena that oscillate at regular frequencies, the PDO experiences rapid shifts between its positive and negative phase (Gedalof & Smith, 2001). The cause of the PDO phenomena is, as yet, undetermined, but it is shown to be a controlling factor of sea surface temperatures in the North Pacific (Mantua *et al.*, 1997). Due to its influence over sea surface temperatures, the PDO can augment or suppress the strength of ENSO forcing at interdecadal frequencies (Gershunov & Barnett, 1998) (e.g., Mantua *et al.* (1999) show that the Aleutian Low is more intense during El Niño). The positive (negative) PDO phase corresponds with warm (cool) temperatures, low (high) precipitation, and reduced (enhanced) snowpack on the northwest coast of North America. During the positive phase of PDO, coastal waters are typically warmer, whereas in the central North Pacific Ocean sea surface temperatures are cooler than average (Mantua *et al.*, 1999).

4.2.2 Regional Climate Change Trends

Shorter-term variations in climate (i.e., climatic variability [CV]) are superimposed on longer-term trends (i.e., climate change [CC]). Over the last century of instrumental data, temperatures in coastal British Columbia have exhibited warming in all seasons, particularly over the last 30 years. The incidence of warm temperature extremes has increased with fewer extreme cold days and nights, and a longer frost-free period. Warming of 0.08 to 0.10°C per decade is recorded for Central Vancouver Island (Walker & Sydneysmith, 2008)[9] and, annually, the 0°C isotherm is shifting northward in BC (Bonsal & Prowse, 2003).

[9] Trends based on the 1900 to 2004 record. Seasonal trends may be greater than the annual average or of the opposite sign and may be concealed due to the use of annual averages.

On a broad scale, BC is experiencing more precipitation days, fewer consecutively dry days, and decreased mean daily precipitation (Vincent & Menkis, 2006). In other words, although there are more precipitation days, there is less precipitation on average on these days. More specifically, coastal BC is experiencing less snowfall overall (Mote, 2003), more locations with no snow on April 1^{rst}, and more winter rain (Whitfield & Taylor, 1998). On Vancouver Island total annual precipitation has increased by 2-3% per decade from 1961 to 1990 (Walker & Sydneysmith, 2008). In coastal BC, based on historical trends, continued increases are expected to be unequally distributed throughout the year, with increased winter streamflows and decreased late summer streamflows (Whitfield & Taylor, 1998; Whitfield *et al.*, 2002).

Due to climate change forcing, absolute sea level in the Northeast Pacific is rising at a rate of 1.7 $\pm$ 0.8 mm a^{-1} (Mazzotti *et al.,* 2008), where absolute sea level is a product of both eustatic and steric manipulations. However, relative sea level in the study area is falling as the rate of tectonic uplift exceeds the rate of absolute sea level rise (Wolynec, 2004; Mazzotti *et al.,* 2007; Mazzotti *et al.*, 2008). Table 4.1 summarizes the findings of regional uplift rates and trends in relative and absolute sea levels.

Table 4.1. Rates of tectonic uplift, relative sea level change, and absolute sea level change for Tofino, British Columbia derived from published research.

Study	Tectonic Uplift (mm a^{-1})	Relative Sea Level (mm a^{-1})	Absolute Sea Level (mm a^{-1})
Wigen & Stephenson, 1980[1]	2.50 $\pm$ 0.48	-1.25 $\pm$ 0.47	1.25
Wolynec, 2004[2]	2.92 $\pm$ 0.14	-1.67 $\pm$ 0.10	1.25
Mazzotti *et al.*, 2007[2]	2.7 $\pm$ 0.9	-1.7 $\pm$ 0.6	1.00
Mazzotti *et al.*, 2008[3]	2.6 $\pm$ 0.8	-0.9 $\pm$ 0.2	1.7 $\pm$ 0.8

[1] Relative sea level trends and uplift rates calculated from annual mean sea level data from tidal gauges. Absolute sea level values unpublished but derived from available data.

[2] Uplift rate calculated using continuous GPS data. Relative sea level trends calculated from monthly mean sea level data from tidal gauges. Absolute sea level values unpublished but derived from available data.

[3] Uplift rate calculated using continuous GPS data. Relative sea level trends calculated from monthly mean sea level data from tidal gauges and corrected for common ocean signals. Absolute sea level data are calculated using satellite altimetry methods.

There is also evidence that coastal storm intensities and surges have increased over the 20th century and may be driven, in part, by CV. Graham and Diaz (2001) show that storm intensities have amplified in the North Pacific since 1948, with an increasing frequency of extreme surface winds and related increases in extreme wave heights. On the north coast of British Columbia, the height of extreme water levels has increased since the positive PDO shift in 1972 (Abeysirigunawardena & Walker, 2008). Additionally, during El Niño events, sea levels on the west coast of North America are elevated above seasonal heights (Subbotina *et al.*, 2001; Barrie & Conway, 2002). Beyond CV forcing, elevated storm intensities may be fuelled by the greater available energy in warming ocean waters responding to climate change (Abeysirigunawardena & Walker, 2008). To date, no regional research exists that examines the impacts of CV on storm intensities and sea levels in the study area.

4.2.3 Contributions to Erosive Water Level Regimes in the Northeast Pacific

Total water level (TWL), which includes predicted tides, surge, and wave runup, is the predominant control of beach-dune erosion (Ruggerio *et al.*, 1997). Observed water level data obtained from tidal stations include predicted astronomical tide and surge components. The surge component results from regional thermal effects and geostrophic forcing, atmospheric pressure changes, and/or wind pile-up. Wave runup is the wave-induced increase of mean water levels on a beach and is a function of wave setup and swash components (Hughes & Turner, 1999; Ruggiero *et al.*, 2001)(see Figure 4.1). In essence, erosion of a beach-dune system occurs when TWL exceeds the elevation of the beach-dune junction. This requires both quantification of the vertical component of wave runup, R, and identification of extreme tides, E_T, and considers the joint probability that these components will combine to create erosive water levels, E_J.

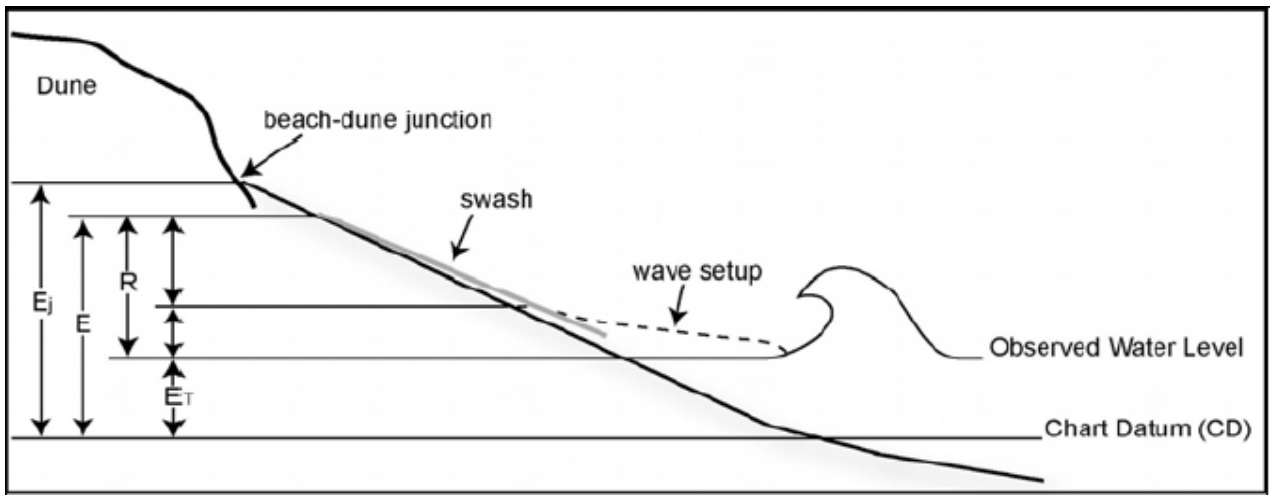

Figure 4.1. Components of erosional water levels on beaches. Chart Datum, *CD,* is the local reference datum, E_T is the elevation of the observed water levels, *R* is the overall wave runup as a function of wave setup and swash, *E* is total water level elevation, and E_J is the erosive water elevation. From Cumming (2007) Fig. 2.1, with permission (modified from Ruggiero *et al.,* 2001).

Ruggerio *et al.* (2001) present the following equation to calculate wave runup:

$$\frac{R_{\max}}{H_s} = C\xi \tag{22}$$

Where R_{max} is maximum vertical runup elevation (m aCD), H_s is the deep water significant wave height (four times the square root of the first moment of the wave spectrum, in metres), *C* is a dimensionless constant (dependent on substrate properties), and ξ is the surf similarity parameter or Iribarren number (Equation 6; Battjes, 1974). Based on their data and the findings of Holman (1986), Ruggiero *et al.* (2001) found that the following relationship explained runup variance on high energy, dissipative beaches in the Northeast Pacific:

$$R_{2\%} = 0.27(SH_s L_o)^{1/2} \tag{24}$$

Where $R_{2\%}$ is the beach elevation that only 2% of water level events exceed (i.e., the 2% exceedence value). Holman (1986) used the 2% exceedence value as a simpler alternative to choosing a representative extreme value frequency distribution. Ruggiero *et al.* (2001) suggest that the 2% exceedence value is a sufficient proxy for defining erosive events.

As total water levels result from a combination of ocean-atmosphere elements, they provide a combined proxy measure of CV phenomena. For instance, several recent studies

have identified strong relationships between total water levels and ENSO and PDO forcing on the West Coast of North America (Ruggerio *et al.*, 1997; Storlazzi & Griggs, 2000; Allan & Komar, 2002, 2006, Abeysirigunawardena & Walker, 2008, Abeysirigunawardena *et al.*, 2009). While CV phenomena, like ENSO and PDO, are recognized as dominant drivers in these trends, manifestations of ENSO forcing on the West Coast of North America are regionally variable and are not inherently related to all extreme conditions experienced by prevailing climatic elements. As above, the wind and wave regime influence total water levels and, accordingly, a review of the wind and wave regimes on the West Coast of North America are provided below.

4.2.3.1 Wind Regime

While the impacts of CV and CC on temperature and precipitation trends in BC have been investigated more rigorously (as reviewed in Walker & Sydneysmith, 2008), little research on the prevailing wind regimes has been conducted, particularly above 40°N. Wind studies have typically focused on the wind regime between 20° to 40°N, encompassing parts of Northern Mexico and extending northward to include California. For example, in the last 50 years, between 25° and 40°N the number of extreme wind events has increased 10-15%, the number of deep low pressure systems has increased 50%, and the magnitude of westerly winds has increased 5 to 10 m s^{-1} (Graham & Diaz, 2001). These trends contribute to an increasing incidence of extreme wave heights and, accordingly, an increase in storm intensities on the West Coast of North America. Although many studies attempt to draw linkages between the occurrence of extreme wind events and CV forcing, Graham and Diaz (2001) found no relation. They hypothesize the trends are a result of an increase in upper-tropospheric winds produced by warming in tropical sea surface temperatures (i.e., more closely linked with CC versus CV).

Whereas Graham and Diaz (2001) find an increase in wind speed along the coast from 1948 to 1996, a more local study by Tuller (2004) shows a decrease in wind speeds along Canada's West Coast. This work was conducted using a dataset from four climate stations (Cape St. James [34 year record], Comox Airport [42 year record], Vancouver International Airport [48 year record], and Victoria International Airport [42 year record]) with somewhat shorter periods of record as compared to those used by Graham and Diaz (2001). A decrease in annual

and seasonal mean wind speeds was identified at all stations except at the Comox Airport over the period of record. As well, a relation between the PDO and wind speed was found using the strength of shared variance, although no causative explanations were explored. Similarly, no relationship between wind speed and ENSO or the Aleutian Low Pressure System was explored. This study was based on a few stations which, in general, are located in environments considerably different than Wickaninnish Beach. Given that wind is very localized, influenced by topographic forcing and roughness effects, dependent on localized fetch conditions and coastline orientation, studies with a limited record length should only be used to draw conclusions on areas directly surrounding the climate station. Therefore, findings by Tuller (2004) may not be directly applicable to the study region.

The relationships between CV indices and extreme wind events on British Columbia's inner south coast (known as the Georgia Basin) are explored in more detail by Abeysirigunawardena *et al.* (2009). Using data from three climate stations (Vancouver International Airport [53 year record], Sand Heads [13 year record], and Saturna Island [13 year record]), this study shows that on BC's inner south coast La Niña event years are more closely associated with extreme wind speeds (particularly in fall and winter) as compared to El Niño years. This contrasts findings from the American West Coast where research in California has shown a higher incidence of extreme wind speeds in El Niño event years compared to La Niña or neutral years (Allan & Komar 2002). This is attributed to a southward shift in the jet stream that occurs during El Niño years delivering more extra-tropical storms to the Californian Coast. During La Niña and neutral years, the jet stream reverts to a split-flow form returning focus of the jet stream and the accompanying cyclonic systems to Canada's southern West Coast. This may explain the contrasting conclusions drawn by Abeysirigunawardena *et al.* (2009) whose study focuses on Canada's West Coast and Allan & Komar (2002) whose study focuses on the Californian Coast.

4.2.3.2 Wave Regime

Annual average, winter, and maximum deep-water significant wave heights in the Northeast Pacific have shown a progressive decadal increase over a 20 to 25 year period, where

increased wave heights may work to elevate local observed water levels via runup processes (Allan & Komar, 2000; Allan & Komar, 2006). In analysis of 10 wave buoys operated by the National Data Buoy Centre, Allan and Komar (2006) found a decadal significant wave height increase of 0.021 m a^{-1} in California, 0.028 m a^{-1} in Oregon, and 0.032 m a^{-1} in Washington for average winter wave heights over the period of record (period of record dependent on buoy, beginning in 1975 and extending to 1999). This increase in significant wave heights appears dependent on latitude, with higher latitudes experiencing a greater rate of wave height increase than lower latitudes (Allan & Komar, 2000). Extreme wave heights and wave periods are also increasing along the American West Coast, although, these trends do not exhibit a latitudinal dependence (Allan & Komar, 2006). Decadal trends in wave conditions are attributed to a combination of CV forcing (e.g., El Niño), and eustatic and steric sea level rise caused by CC which works to gradually reduce the elevation threshold for erosion at the beach-dune junction (Allan & Komar, 2002, 2006). Seymour (1998) found increased significant wave heights and peak periods during El Niño years in south to south-central California while, at more northern latitudes in Washington and Oregon, increased significant wave heights and peak periods increased during La Niña and/or neutral years. However, this study only used data from four buoys and it may be erroneous to draw inferences from so few stations.

4.3 Methods

4.3.1 Erosive Water Level Regime

As above, the two main components of total water levels are: (1) the observed water levels; and, (2) the vertical component of wave runup. Observed hourly tidal elevations were obtained from Canadian Hydrographic Service (CHS) for the Tofino tidal station (Fisheries and Oceans Canada [DFO] station 8615) corresponding to the 99-year period of record (1909 to 2008). This station provides the nearest, most representative water levels for the study region (A. Ballantyne, personal communication, August 25, 2008). Typically, the only post-processing of observed water levels corrects for the effect of the float/counter weight system on the tidal gauge. Generally, processed values are smaller than raw values and corrections are usually on

the order of a few centimetres. Required corrections are largest at low tides and smallest at high tides (A. Ballantyne, personal communication, August 25, 2008). A total of 236,379 erroneous water level records (e.g., 999.99 m aCD) were removed from the dataset. Missing values also occur throughout the dataset. Per Allan and Komar (2006), monthly and annual records with less than 80% continuous data were not included in subsequent analyses, leaving 77 years of available data with the following years removed: 1916, 1917, 1921 to 1939, 1942, 1944, 1946, 1948, 1953, 1984, 1987, and 1995.

The vertical component of wave runup, R, was calculated according to Equation 25. Deep water significant wave heights and periods from 1970 to 1998[10] were obtained from the MEDS buoy 103 (see Figure 1.1 and section 2.7). Deep water wavelengths were calculated using Equation 24. MEDS 103 measured wave data once every three hours from 1970 to 1986, then measurement frequency was increased to hourly from 1987 to 1998, at which point it was decommissioned. The La Perouse Bank buoy (C46206; see Figure 1.1) is further offshore and still operational, although it has a shorter period of record (1988 to present) and therefore, is not used in this analysis. Quality control fields in the wave dataset provided by MEDS were used to remove potentially erroneous data. All quality three (Q3) flagged data (element appears doubtful) and quality four (Q4) flagged data (element appears erroneous) were removed from the dataset and monthly records with less than 80% continuous data were not included in analyses.

An average beach slope of 0.02m m^{-1} was determined using transect 1, which was the only cross-shore profile to capture the entire intertidal zone. Where water level and runup values were combined to calculate total water levels, water level had to be coarsened to complement the period (1970 to 1998) as wave attribute data were recorded at a three hour frequency (versus hourly frequency of water level measurements). Only water levels measured at corresponding times with wave attribute measurement were used and all other water levels were disregarded.

[10] Available online from http://www.meds-sdmm.dfo-mpo.gc.ca/isdm-gdsi/waves-vagues/search-recherche/list-liste/data-donnees-eng.asp?medsid=MEDS103

Erosive water level events were defined as those equal to, or greater than, the elevation of the beach-dune junction, where the beach-dune junction was defined by the average elevation of the incipient dunes (i.e., average of the lower and upper elevation of the incipient dune field for all three transects). As incipient dunes are formed around both annual and perennial vegetation (see Figures 2.8a, 2.8b, and 2.11b) the elevation of the beach-dune junction is always shifting. In this research, the threshold value was determined using the 2008 summer profiles, during a period when incipient dunes were well-developed. Thus, for the purposes of future comparison, the elevation of the beach-dune junction should be determined during a similar period (i.e., end of summer) when the incipient dunes have had equal opportunity to form. A threshold value of 5.5 m aCD was determined from the average beach-dune junction elevation on all four cross-shore monitoring profiles on Wickaninnish Beach (Figures 3.14 to 3.16). The frequency of erosive events was estimated using return levels and recurrence intervals for four water level scenarios: (1) observed water levels alone for 1909 to 2008; (2) observed water levels plus corresponding wave runup values based on observed wave conditions for 1970 to 1998 (period of analysis restricted to length of wave record); (3) observed water levels plus estimated runup values for 1909 to 2008 (based on monthly and annual average wave conditions from 1970 to 1998); and, (4) observed water levels and estimated runup values based on monthly and annual maximum observed wave conditions from 1970 to 1998 (period of analysis extended to length of water level record, 1909 to 2008). Monthly and annual runup values were calculated to enable correlation with monthly and annual CV indices.

Return levels were calculated for all four water level scenarios using the Extreme Values Toolkit[11], an open source R-based statistics package (Gilleland *et al.*¸ 2003). Annual maximum water levels were fit to a Generalized Extreme Value (GEV) distribution using a block maxima approach. This analysis yielded 1, 5, 10, 25, 50, and 100-year return levels as elevations above chart datum. With datasets of greater than 50 records, a strong GEV model fit can be reached and inferences can be made for return levels of three to four times the length of the observation period (Abeysirigunawardena & Walker, 2008). Consequently, water level scenarios

[11] Available online from http://www.isse.ucar.edu/extremevalues/extk/html

one, three and four will yield a better fit to the GEV model as they have 77 maximum annual water level elevations, whereas water level scenario two only has 28 maximum annual water level elevations. Maximum annual water levels were identified and ranked in order to calculate recurrence intervals (R_{INT}, *in years*) of erosive events using the following equation:

$$R_{INT} = \frac{1+n}{m} \tag{25}$$

Where *n* is the total number of observations (years of record) and *m* is the magnitude ranking (water level elevations) of these observations. From this, the probability (*P*) of an erosive event of a specified magnitude (m) can be determined as follows:

$$P_m = R^{-1} \bullet 100 \tag{26}$$

Where P_m is expressed as a % value of probable occurrence in any given year. This analysis does not account for within year variability, where some years may experience more than one erosive water level event. Total recurrence interval (R_t) was also calculated as a simple ratio according to the following equation:

$$R_t = \frac{N}{n} \tag{27}$$

Where *N* is the number of years of record and *n* is the total number of erosive events within that period. This produces a long-term average recurrence interval in years, but does not account for the variability in occurrence of extreme events (i.e., some years may experience many erosive events and other years none).

4.3.2 Climatic Variability Phenomena and the Regional Water Level Regime

The strength of shared variance between relevant climate variability indices and oceanographic elements (e.g., significant wave height, peak wave period, observed water levels, and calculated total water levels) was determined through correlation analysis. Data on oceanographic elements were coarsened to create monthly and annual average and maximum values. Correlation was performed between monthly data and monthly MEI, NOI, and PDO index values and between annual data and the annual ALPI index. The Multivariate ENSO Index

(MEI)[12] is designed to express the effects of ENSO in the tropics (Wolter & Timlin, 1993) whereas the Northern Oscillation Index (NOI)[13] is designed to express the effects of ENSO in the Pacific Northeast (Schwing *et al.*, 2002). MEI is a weighted average of a number of tropical Pacific ocean-atmosphere variables including sea surface temperature, east-west and north-south components of surface winds, sea level pressure, and percent cloud cover (Wolter & Timlin, 1993). Negative MEI values are representative of the La Niña phase of ENSO, whereas positive values are representative of the El Niño phase. NOI is a measure of sea level pressure anomalies between the climatologically mean position of the North Pacific High (UTM Zone 9, 408793.45 m E, 3873522.51 m N), and Darwin, Australia (UTM Zone 52, 609597.68 m E, 8894415.31 m S; Schwing *et al.*, 2002). Unlike MEI, negative NOI values indicate the El Niño phase of ENSO, whereas positive NOI values indicate the La Niña phase. A number of other indices exist that describe the extra-tropical effects of ENSO (e.g., the North Pacific Index) but NOI was chosen for this analysis as it is argued to better capture these effects (Schwing *et al.*, 2002). The PDO Index[14] is derived using the leading principal component of monthly sea surface temperature variability in the North Pacific (poleward of 20°N; Mantua *et al.,* 1997). Positive PDO Index values correspond with warm phases whereas negative PDO Index values correspond with cool phases. Lastly, the Aleutian Low Pressure Index (ALPI)[15] is a measure of the relative strength of the winter Aleutian Low System and corresponds to the mean area (km^2) with a sea level pressure less than or equal to 100.5 kPa as compared to the 1950 to 1997 mean (Beamish & Bouillon, 1993). Positive ALPI values indicate a strong Aleutian Low whereas negative ALPI values indicate a weak Aleutian Low.

Pearson's Product Moment Coefficient (r) was used to determine the strength of the relationships between the CV indices and oceanographic elements. Environmental data typically are positively skewed and violate the regression assumption that the variables are normally distributed. Additionally, autocorrelation within the residuals and multicollinearity

[12] Available online from http://www.cdc.noaa.gov/ClimateIndices/List/index.html
[13] Available online from http://www.pfeg.noaa.gov/products/PFEL/modeled/indices/NOIx/noix.html
[14] Available online from http://jisao.washington.edu/pdo/PDO.latest

[15] Available online from http:// www.pac.dfo-mpo.gc.ca/sci/sa-mfpd/climate/clm_indx_alpi.htm

between MEI and NOI (both measures of ENSO) is likely. For these reasons, multiple regression analysis was not conducted.

4.4 Results & Discussion

4.4.1 Erosive Water Level Regime

4.4.1.1 Return Levels

As water levels are one of the principal controls of beach-dune erosion, estimation of return levels aims to provide insight to the geomorphic evolution of the Wickaninnish beach-dune system and to inform park management actions. The 1, 5, 10, 25, 50, and 100-year return levels were calculated for water level scenarios 1 through 4 (see section 4.3.1 and Table 4.2). These four scenarios will be referred to throughout as scenarios 1 through 4, respectively.

Table 4.2. Return level for the four water level scenarios: (1) observed water levels alone for 1909 to 2008; (2) observed water levels plus corresponding wave runup values based on observed wave conditions for 1970 to 1998; (3) observed water levels plus estimated runup values for 1909 to 2008; and, (4) observed water levels and simulated runup values based on monthly and annual maximum observed wave conditions for 1970 to 1998. Confidence limits are taken from the largest confidence bounds.

Return Interval (years)	**1**	**5**	**10**	**25**	**50**	**100**
Scenario 1						
Return Level (m aCD)	4.22	4.42	4.50	4.58	4.64	4.68
95% Confidence Limit (m)	± 0.01	± 0.05	± 0.07	± 0.10	± 0.13	± 0.17
95% Lower Bound (m aCD)	n/a	4.37	4.45	4.53	4.57	4.61
95% Upper Bound (m aCD)	n/a	4.47	4.56	4.69	4.77	4.85
Scenario 2						
Return Level (m aCD)	5.59	6.19	6.36	6.50	6.57	6.62
95% Confidence Limit (m)	±0.11	±0.23	±0.20	±0.22	±0.23	±0.25
95% Lower Bound (m aCD)	n/a	5.95	6.18	6.36	6.40	6.46
95% Upper Bound (m aCD)	n/a	6.37	6.56	6.73	6.81	6.88
Scenario 3						
Return Level (m aCD)	5.14	5.37	5.45	5.53	5.58	5.63
95% Confidence Limit (m)	0.02	0.05	0.07	0.10	0.13	0.16
95% Lower Bound (m aCD)	n/a	5.32	5.40	5.48	5.52	5.56
95% Upper Bound (m aCD)	n/a	5.42	5.52	5.64	5.71	5.78
Scenario 4						
Return Level (m aCD)	6.97	7.28	7.38	7.46	7.51	7.54
95% Confidence Limit (m)	0.03	0.06	0.06	0.07	0.08	0.08
95% Lower Bound (m aCD)	n/a	7.22	7.32	7.41	7.46	7.50
95% Upper Bound (m aCD)	n/a	7.34	7.44	7.53	7.59	7.63

The beach-dune junction elevation on Wickaninnish Beach is approximately 5.5 m aCD as identified from cross-shore beach profiles (see Figures 3.14 to 3.16). In scenario 1, water levels never reach this elevation for recurrence intervals from 1 to 100 years. This scenario, however, is the least plausible as it does not account for the effects of wave runup and erosive events that have occurred throughout the period of record as shown in airphotos, cross-shore profiles, and through anecdotal evidence. In scenario 2, water levels exceed the elevation of the beach-dune junction by 4 cm (i.e., TWL_1 = 5.59 m aCD) at least once a year. In scenario 3, return levels reach the beach-dune junction elevation threshold between 25 and 50 years (i.e., TWL_{25} = 5.53 m aCD and TWL_{50} = 5.58 m aCD) and, in scenario 4, water levels exceed this elevation significantly at least once every year (i.e., TWL_1=6.97 m aCD).

Of all scenarios, scenario 2 is arguably the most representative of true total water levels on Wickaninnish Beach as it accounts for both components of total water level (i.e., observed water levels and wave runup) and is based on direct observations of both (not averages as used in scenarios 3 and 4). Unfortunately, scenario 2 has the shortest period of record (1970 to 1998), compared to the other three scenarios, and, as evident by its confidence intervals, has a higher level of uncertainty associated with its return level predictions.

Even with this uncertainty, both anecdotal and observational accounts fit best with this scenario (e.g., foredune scarping and removal of incipient occurred in both years of this study). The estimated erosion threshold represents the average elevation of incipient dune formation. These features are typically ephemeral features (Hesp, 2002) and are often removed at annual to inter-annual frequencies. Therefore, water level scenario 2 aptly displays this removal. Additionally, more extreme erosive events that are responsible for foredune erosion are also described by this water level scenario but occur over longer intervals than the smaller-scale events responsible for incipient dune erosion. Figure 4.3 illustrates return levels of scenario 2 overlain on cross-sectional profiles on Wickaninnish Beach. Simulated water level scenarios (scenarios 3 and 4) appear to underestimate and overestimate total water levels, respectively.

The runup model ($R_{2\%}$) is suitable for Wickaninnish Beach as it was developed for similar high energy, dissipative beaches in the Northeast Pacific. However, to improve confidence in total water levels in future, a runup equation could be developed specific to Wickaninnish Beach per the methods of Ruggerio *et al.* (2001) (i.e., video observation techniques).

4.4.1.2 Recurrence Intervals and Probabilities of Erosive Water Level Events

The recurrence intervals defining erosive events that exceed the beach-dune junction elevation threshold of 5.5 m aCD were determined for each scenario using Equation 26 (Table 4.3). Under scenario 1, water levels never reach the erosion threshold whereas with scenario 2 erosive water levels occur with a recurrence of 1.53 years, or with a probability of 65% in any given year. In scenario 3, erosive water levels occur with a recurrence of 13 years, or with a probability of 8% in any given year and with scenario 4, water levels reach erosive levels every year.

Table 4.3. Recurrence intervals and probabilities of erosive events on Wickaninnish Beach for four water level scenarios: (1) observed water levels alone for 1909 to 2008; (2) observed water levels plus corresponding wave runup values based on observed wave conditions for 1970 to 1998; (3) observed water levels plus estimated runup values for 1909 to 2008; and, (4) observed water levels and simulated runup values based on monthly and annual maximum observed wave conditions for 1970 to 1998.

Water Level Scenario	Recurrence Interval (years)	Probability of Occurrence (% chance in any year)
1	0	0
2	1.53	65
3	13	8
4	1	100

As above, scenario 2 seems most representative of water level events on Wickaninnish Beach given observational and anecdotal evidence of frequent minor erosive events occurring inter-annually, annually to biannually in the region. Scenario 1 and 4 appear to drastically underestimate and overestimate water levels, respectively, while water level scenario 3 seems to slightly underestimate the frequency of erosive events. Figure 4.3 illustrates erosive water levels overlain on cross-shore profiles derived from scenario 2 for the period 1970 to 1998.

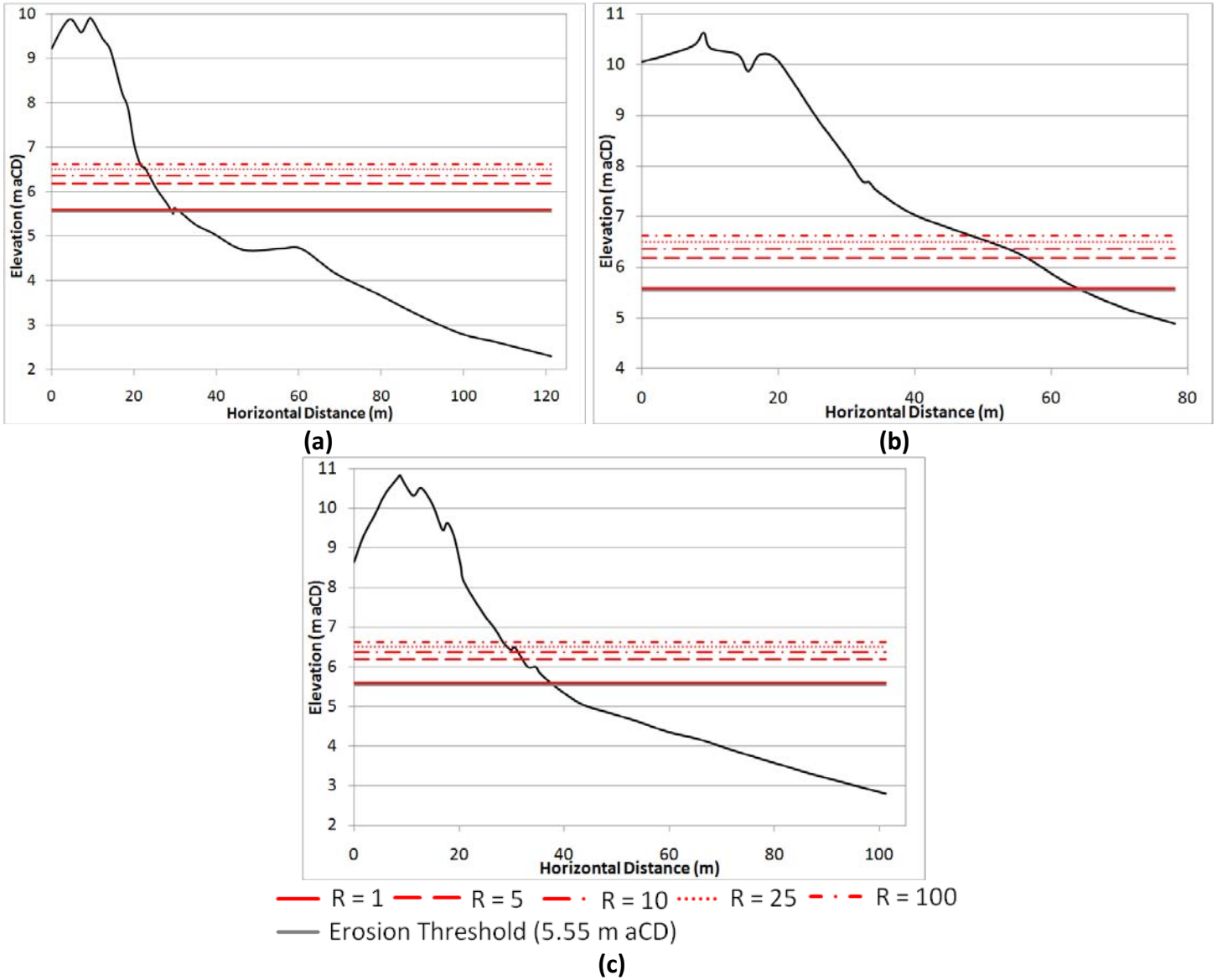

Figure 4.2. Return water levels, according to scenario 2, overlain on cross-sectional profiles. (a) Transect 1; (b) Transect 2; and, (c) Transect 3.

The total recurrence interval, R_t, (Equation 28) for scenario 2 suggests that erosive water levels are reached, on average, 3.53 times annually (99 threshold exceedences over the 28-year record). Unfortunately, none of the methods used are able to accurately capture the variability of erosive events, where some years experience no erosive events and others experience many erosive events. The variability of extreme events is attributed to the complexities of interactions (constructive or destructive) between controlling regimes, in addition to the influence of CV and CC forcing on these regimes. Resultantly, under this uncertainty, the occurrence of erosive events is difficult to predict.

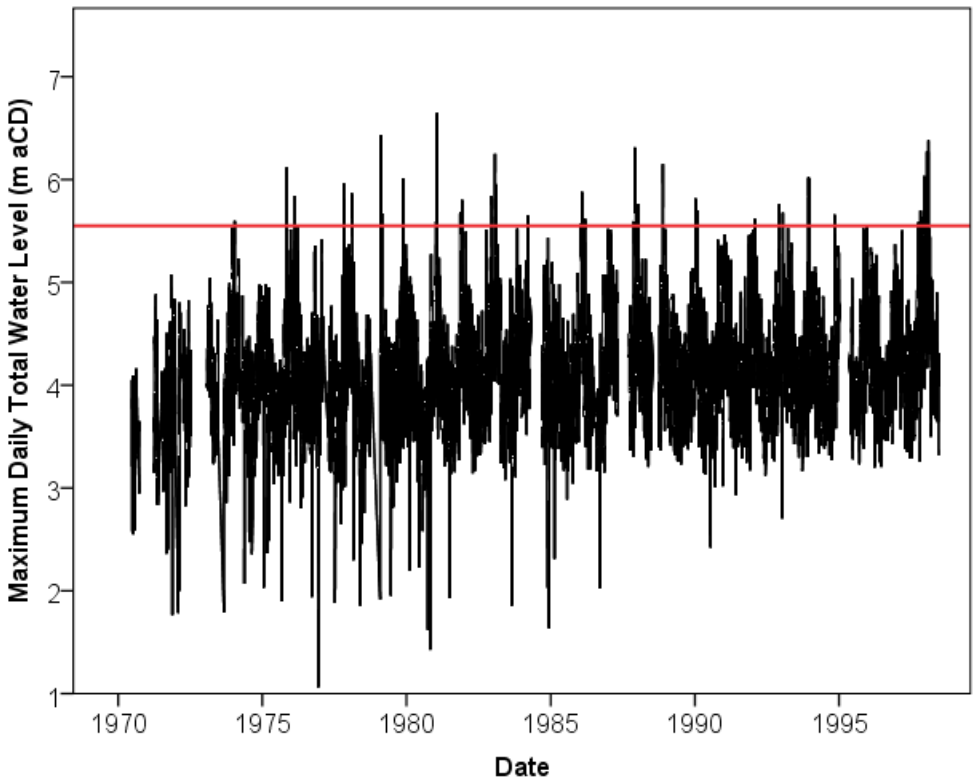

Figure 4.3. Daily maximum water levels according to scenario 2 (i.e., observed water levels plus corresponding wave runup values based on observed wave conditions for 1970 to 1998) over period of record. The red line indicates the threshold elevation for erosion of the beach-dune junction. During this 28-year period, 99 events breached this erosional threshold. Note there are a number of gaps in the record.

Figure 4.4 shows maximum water levels from 1970 to 1998 according to scenario 2. It appears that there is a component of seasonality in the maximum water level regime where

maximum water levels are reached more frequently in the winter season. This is expected as average significant wave height and peak periods are greater in the winter season (see section 2.7). In addition, not only are the tidal heights at a maximum in the winter season when the Earth is closer in its rotation with the sun and moon, but storms are more frequent in correspondence with the Aleutian Low Pressure System.

4.4.2 Climate Variability and Regional Wave and Water Level Conditions

The strength of shared variance was explored between climate variability indices (monthly PDO, NOI, MEI, and annual ALPI) and a number of oceanographic elements, aggregated monthly and annually (maximum and mean significant wave height, maximum and mean peak wave periods, maximum and mean water levels under scenario 1 and scenario 2). While a preference for scenario 2 has already been stated, scenario 1 is also explored as it expresses the original, underived component of total water levels. Water levels alone, without consideration of wave runup, still maintain a central role in the occurrence of beach-dune erosion as the severity of extreme events is highly dependent on the tidal stage it is coincident with. Per Cumming (2007), *r* values less than 0.3 show poor correlation, *r* values greater than 0.3 but less than 0.6 show moderately strong correlation, and *r* values greater than 0.6 show strong correlation.

Shared variance between significant wave heights and climate variability indices are shown in Table 4.4. The only climate variability index significantly correlated ($p < 0.05$) to mean significant wave height was ALPI. According to the parameters above, the correlation between mean significant wave height and ALPI is moderately strong. No climate variability indices are significantly correlated to maximum significant wave heights.

Table 4.4. Strength of shared variance between mean (H_o) and maximum (H_{omax}) significant wave heights and climate variability indices. Bold text indicates that the relationship is significant at the 95% level ($p < 0.05$). Wave height record is from MEDS buoy 103 (UTM Zone 10, 299588.68 m E, 5429953.93 m N) for the period June 1970 to 1998. *r* represents Pearson's product-moment coefficient and $\propto$ indicates the significance level.

Significant Wave Height (m)	PDO		NOI		MEI		ALPI	
	r	$\propto$	r	$\propto$	r	$\propto$	r	$\propto$
Mean	- 0.058	0.150	- 0.085	0.063	- 0.017	0.383	**0.374**	**0.023**
Maximum	- 0.046	0.204	- 0.066	0.119	- 0.003	0.482	0.103	0.297

All monthly climate variability indices exhibit a statistically significant ($p < 0.01$) shared variance with mean (T) and maximum (T_{max}) peak wave periods (Table 4.5). All correlations are poor, though significant. The strongest correlation is shared between MEI and T_{max}. Negative and positive *r* values between NOI and MEI, respectively, and peak wave period is indicative of a relationship to the El Niño phase of ENSO.

Table 4.5. Strength of shared variance between mean (T) and maximum (T_{max}) peak wave periods and climate variability indices. Bold text indicates that the relationship is significant at the 99% level ($p < 0.01$). Wave height record is from MEDS buoy 103 (UTM Zone 10, 299588.68 m E, 5429953.93 m N) for the period June 1970 to 1998. *r* represents Pearson's product-moment coefficient and $\propto$ indicates the significance level.

Peak Wave Period (s)	PDO		NOI		MEI		ALPI	
	r	$\propto$	r	$\propto$	r	$\propto$	r	$\propto$
Mean	**0.179**	**0.001**	**-0.231**	**0.000**	**0.198**	**0.000**	0.187	0.166
Maximum	**0.263**	**0.000**	**-0.217**	**0.000**	**0.288**	**0.000**	0.202	0.146

Under scenario 1, mean water levels have a significant correlation ($p < 0.05$) with PDO, NOI, and MEI (Table 4.6). NOI is the only index to share a moderately strong correlation (negative) with mean water levels. All other indices with a significant correlation with both mean and maximum water levels are poorly correlated. Maximum water levels are significantly correlated ($p < 0.05$) to NOI and MEI. Again, negative and positive *r* values of NOI and MEI, respectively, are indicative of a correlation with the El Niño phase of ENSO. Both mean and maximum water levels have a stronger correlation and equal or stronger significance with NOI as compared to MEI. This is expected as MEI is a global index whereas NOI is regionally specific.

Table 4.6. Strength of shared variance between scenario 1 and climate variability indices. Bold text indicates that the relationship is significant at the 95% level ($p < 0.05$). Water level data are from the Tofino tidal station (station 8615) for the period 1909 to 2008. *r* represents Pearson's product-moment coefficient and $\propto$ indicates the significance level.

	PDO		NOI		MEI		ALPI	
Water Level (m aCD)	**r**	**$\propto$**	**r**	**$\propto$**	**r**	**$\propto$**	**r**	**$\propto$**
Mean	**0.083**	**0.015**	**- 0.346**	**0.000**	**0.162**	**0.000**	0.090	0.233
Maximum	0.037	0.140	**- 0.185**	**0.000**	**0.088**	**0.011**	0.182	0.069

Under scenario 2, mean water levels are significantly correlated ($p < 0.05$) to both NOI (moderately strong correlation) and MEI (poor correlation) (Table 4.7). The maximum water levels are significantly correlated ($p < 0.05$) to NOI (poor correlation), MEI (poor correlation), and ALPI (moderately strong correlation). Again, NOI and MEI *r* values signify a positive relationship with the El Niño phase of ENSO. Both mean and maximum water levels have a stronger correlation and significance with NOI as compared to MEI. As above, this is expected as MEI is a global index whereas NOI is regionally specific.

Table 4.7. Strength of shared variance between scenario 2 and climate variability indices. Bold text indicates that the relationship is significant at the 95% level ($p < 0.05$). Water level data from the Tofino tidal station (station 8615) and wave data from the MEDS 103 buoy for the period 1970 to 1998. *r* represents Pearson's product-moment coefficient and $\propto$ indicates the significance level.

	PDO		NOI		MEI		ALPI	
Water Level (m aCD)	**r**	**$\propto$**	**r**	**$\propto$**	**r**	**$\propto$**	**r**	**$\propto$**
Mean	0.032	0.291	**- 0.338**	**0.000**	**0.120**	**0.018**	0.432	0.010
Maximum	0.045	0.219	**- 0.264**	**0.000**	**0.153**	**0.004**	**0.347**	**0.033**

These correlations generally reveal poor to moderately strong relationships between ENSO indices (NOI and MEI) and all oceanographic elements, except mean and maximum significant wave heights. In all cases, except maximum peak wave periods, the relationship is stronger with the NOI. This makes sense as NOI aims to express the extra-tropical effects of ENSO in the Northeast Pacific, whereas MEI is a measure of the tropical expression of ENSO. In all significant cases, NOI expresses negative *r* values and MEI expresses positive *r* values, showing that the oceanographic elements are responsive to the El Niño phase of ENSO. Oceanographic elements are responsive to a number of controlling regimes, including the wind

regime. Though studies on Canada's West Coast suggest La Niña event years are responsible for most extreme wind speed reoccurrences (see section 4.2.3.1; Abeysirigunawardena *et al.*, 2009) this signal was not found in this study within the oceanographic elements. To expand on this research in future, wind data from the Tofino Airport meteorological station could be regressed to identify trends in wind speed and direction that may be linked to climate change forcing, and correlated with CV indices to investigate the influence of climate variability forcing. The relationship between extreme wind speeds, directional mode, and La Niña may not be maintained within the study area as winds are very local in their character.

PDO is poorly, but significantly, correlated with both mean and maximum peak wave periods and mean observed water levels. Tuller (2004) found a relationship between wind speeds and the PDO index, and it is therefore unsurprising that a relationship between the PDO and wave periods exists as they are, among other things, a function of wind speeds. However, as above, the relationship between regional winds and PDO remains to be explored in the study area and the findings of Tuller (2004) may not be applicable to Wickaninnish Beach. ALPI has a moderately strong relationship with mean significant wave heights and total water levels. Correlations with total water levels may be an artifact of correlations with significant wave heights as they are a variable in calculated total water levels. Given the Aleutian Low Pressure System controls the strength of winter storms, it is understandable that it correlates well with mean significant wave heights. It is interesting that the ALPI is not significantly correlated to maximum significant wave heights, however. Maximum significant wave heights occur more frequently in winter months (see Chapter 2) and it seems logical that they then might be influenced by forcing from the Aleutian Low Pressure System as the phenomenon is principally a winter phenomenon. Perhaps the Aleutian Low Pressure System is less responsible for extreme events and is associated more closely with more moderate winter storm events.

4.4.3 Beach-Dune Response to Sea Level Change

While relative sea levels are falling in the region (see section 4.2.2), climate variability forcing can temporarily and frequently elevate mean observed water levels. These elevated water levels play an important role in the erosive water level regime at Wickaninnish Beach. For

example, during El Niño events, sea levels in coastal British Columbia typically rise about 10 to 20 cm above seasonal heights and remain above normal for several months (Crawford *et al.*, 1999). Storm surge and wave runup, superimposed on temporarily elevated mean water levels, may interact to increase the severity of extreme events, particularly if timed with high tides.

Although extreme values analysis (section 4.4.1) reveals that erosive events occur frequently, though they may be minor, shoreline trends are predominantly responsive to relative sea level regression in the region and the shoreline is currently prograding at a rate of 0.2 m a^{-1} (see Chapter 3). These erosive events may serve to encourage the creation of foredune blowouts (e.g., through dieback of stabilizing vegetation and the formation of scarps), revealing a greater available bare sand surface for aeolian transport (Hesp, 2002). The creation of foredune blowouts is part of natural foredune morphology, dynamics and evolution (Hesp, 2002). As dynamism is desired in coastal dune systems and there is not a significant amount of infrastructure at risk in the study area, the occurrence of erosive events is not viewed negatively.

Though speculative, the following statements examine the potential response of the Wickaninnish Bay beach-dune system to sea level regression with superimposed, higher-frequency erosive events. In an attempt to realize equilibrium with the incident wave base (-79.70 m aCD based on average wave conditions), erosion of the nearshore may occur as the water level shallows due to sea level regression. Eroded nearshore sediments may contribute positively to the beach-dune sediment budget, supplying materials for the formation of beach berms and foredune ridges. Whereas long-term shoreline progradation with continued onshore sand supply and competent winds should lead to the seaward expansion of the present dune system, the effectiveness of *Ammophila* ssp. at foredune stabilization (see section 2.6.2) combined with current climate change trends (i.e., increasing temperatures and precipitation) may inhibit natural system dynamism and continue to encourage stabilization trends within the dune system (see section 3.4.6) and seaward expansion may not necessarily translate to system expansion.

4.5 Conclusion

Estimated return levels and recurrence intervals vary greatly with different water level scenarios. According to both anecdotal and observational evidence, a water level utilizing both observed water levels and corresponding calculated runup values appears to be the most representative of true conditions on Wickaninnish Beach. Under this scenario, the probability of an erosive event (i.e., events where water levels exceed 5.5 m aCD) is 65% in any given year. The annual return level is 5.59 m aCD, suggesting erosive events occur at least once per annum and the ratio of erosive water levels (frequency of erosive water levels over period of record) is 3.53 times per year. However, this does not account for the variability in the occurrence of erosive water levels where some years may experience many erosive water levels and other years none.

ENSO forcing has the greatest shared variance with oceanographic elements. In particular, the El Niño phase of ENSO was responsible for all significant shared variance between MEI and NOI indices and oceanographic elements. PDO was shown to have a significant shared variance with peak wave periods and ALPI showed a significant shared variance with total water levels and significant wave heights. ALPI was the only climate variability index to show shared variances with wave heights. These findings suggest that climate variability phenomena have a relationship with the oceanographic regime at the study area and, correspondingly, may direct some aspects of site morphodynamics.

Shoreline progradation trends will likely continue under current water level scenarios. The frequency of erosive events will contribute to the maintenance of natural foredune dynamism given that dynamism is not hindered by the efficiency of non-native species at recolonization nor the favourable stabilization conditions created by climate change. Under regressing sea levels the wave base (-79.70 m aCD based on average wave conditions) will likely erode the nearshore, striving to reach equilibrium, and eroded sediments may contribute to the continued development of beach berms and foredunes.

A number of areas are still left to explore regarding the controlling regimes on Wickaninnish Beach. Simple linear regression of total water levels (observed water levels and corresponding calculated runup values) should be undertaken to gain insight into total water

levels trends. Simple linear regression of significant wave heights and peak wave periods over the period of record would reveal increasing or decreasing trends in the incident wave regime. Extreme wind speeds and directional modes should be evaluated for the region using extreme values analysis. Climate variability indices should later be included as covariates in this analysis to determine if extreme wind speeds and their directional modes are influenced by climate variability forcing (as per Abeysirigunawardena *et al.*, 2009). Lastly, simple linear regression of wind speeds should be explored to identify increasing or decreasing trends.

5.0 Conclusions

5.1 Summary and Conclusions

This research improves the current understanding of the morphodynamics of high-energy, wave dominated, mesotidal beaches in British Columbia and explores potential impacts of climatic variability and change. These results also help inform protected areas management approaches in Pacific Rim National Park Reserve. The specific objectives of this research were to: (i) describe site morphology; (ii) characterize site morphodynamic processes and regimes; (iii) assess the potential for onshore aeolian sediment transport; (iv) examine the erosion potential of the beach-dune system and develop a modern recurrence interval of erosive events; and, (v) explore correlations between regional climate variability signals and the total water level regime to investigate the possible relationships between climate variability and beach-dune erosion. A summary of key findings of this research are presented below.

5.1.1 Beach-Dune Morphodynamics

The incident wind regime on Wickaninnish Beach is bimodal with a WNW summer component resulting from clockwise circulation around the North Pacific High Pressure System, (centred in the eastern North Pacific Ocean) and a SE component in the winter corresponding to anticlockwise rotation around the Aleutian Low Pressure System (centred in the Gulf of Alaska). Similar to the regional wind regime, the potential aeolian sediment transport regime is bimodal. Although potential sand transport is greater from the SE, the NW to SE alignment of the transgressive dunes at Wickaninnish Beach suggests that dune morphodynamics are more controlled by the WNW (summer) component of the wind regime. These winds may be altered due to topographic steering effects to produce the resultant NW to SE morphologies. Dune alignment likely responds to the WNW (summer) winds due to the SW aspect of Wickaninnish Bay and the resultant obstruction of incident SE (winter) winds caused by Quisitis Point in the south. However, the NW extension of the foredune complex fronting Sandhill Creek to the NW of the transgressive dunes may be responsive to both wind modes, where the annual resultant

transport direction (RTD) is about 356°. While the RTD is northerly, dominant transport modes are WNW and SE and should, when considered individually, produce a NW/SE alignment of morphological features. As the SE (winter) winds are of greater magnitude, it is assumed that their contribution to resultant morphology is greater when unobstructed and may, in part, encourage the NW extension of the foredune complex. This NW extension is also a result of the collective interaction with other processes including a net NW littoral transport direction and stabilization caused by increasing *Ammophila* populations that acts to reinforce the foredune complex.

Wickaninnish Beach has a strong aeolian rebuilding potential with a total transport potential of 9984.31 m^3 m^{-1} a^{-1}, a resultant transport potential of 3268.28 m^3 m^{-1} a^{-1}, and an onshore, northerly (356°) RTD (see section 3.4.3). Consequently, erosive events, although common, may not significantly affect the maintenance of the Wickaninnish beach-dune systems. Rather, erosive events likely contribute to system dynamism, a key element in the maintenance of habitat for specialized pioneer dune species. If rebuilding potential was low, erosive events would be more destructive, causing shoreline retreat and habitat loss for specialized dune species. This finding suggests that erosive events on Wickaninnish Beach are beneficial to the beach-dune system, and that no direct management intervention is required to support the system. However, the erosion of the outer meander bank at the mouth of Sandhill Creek is a problem for park infrastructure. To avoid loss of infrastructure, the continued seasonal closure of Combers Beach parking lot and the removal of the beach-access stairs is required. Erosion rates at this meander should continue to be monitored to assess the risk to further infrastructure, such as boardwalks, in the area.

Rip cell circulation on Wickaninnish Beach is present as noted through local knowledge, aerial photograph evidence, and morphodynamic beach classification (i.e., low tide bar/rip beach). However, a longshore littoral transport cell also operates as revealed by the McLaren model (section 3.4.2; McLaren & Bowles, 1985) and as suggested by the embayment scaling parameter (per Short & Masselink, 1999). Nearshore sand transport has a net longshore trend to the NW. As above, this likely contributes to the NW extension of the foredune complex

fronting Sandhill Creek. More detailed quantification of nearshore sediment transport pathways is needed to provide insight to sediment sources and sinks on Wickaninnish Beach.

Assuming a consistently available sediment supply and a continued relative sea level regression in the area (-0.9 $\pm$ 0.2 mm a^{-1}), current rates of shoreline progradation at Wickaninnish Beach (+0.2 m a^{-1}) should persist. Although progradation should lead to an expansion of the transgressive dune system, the system is presently trending towards stabilization (Heathfield & Walker, in review), causing a loss of active sand surface area that supports specialized species. Stabilization may be due to both the presence of *Ammophila* spp. that have reduced sand supply from the beach to the transgressive dunes and to climatic trends of increased temperature and precipitation, which contribute to accelerated vegetation growth and higher sand moisture contents that elevate aeolian transport thresholds.

While shoreline progradation is occurring over the longer-term (Heathfield & Walker, in review), cross-shore monitoring profiles show that this is a dynamic process. Over the shorter-term, both shoreline erosion and accretion occur, with erosion resulting from high water levels and extreme wind events, and accretion occurring due to the strong aeolian sand transport potential within the beach-dune system. Thus, as noted above, erosive events affecting the beach-dune system should not be a major concern to park management. However, stabilization of the dune system is a management concern as it has led to the loss of valuable habitat that provides for early successional and specialized dune species. Ongoing dune restoration efforts align with the need to not only to remove non-native species (i.e., *Ammophila* spp.) but also to re-establish dynamic habitats favourable to early-successional, specialized dune species, many of which are species at risk (e.g., *Lathyrus littoralis, Abronia umbellata*). Dune restoration efforts are presently planned for a five-year term. However, a longer-term plan should be developed, as most effective restoration efforts require persistence.

5.1.2 Erosive Water Level Regime

Although four total water level (TWL) scenarios were simulated, the scenario based on observed water levels and corresponding calculated runup values (28-year record, 1970 to 1998) was most reliable. Three approaches were assumed in the analysis of the frequency of

erosive water levels including probabilities, return levels, and simple ratios. According to the regional water level regime and an identified erosion threshold elevation (5.5 m aCD), the probability of an erosive event on Wickaninnish Beach is 1/1.53 or 65%. Data fit to a generalized extreme value distribution gave an annual return level of 5.59 m aCD, suggesting erosive events occur annually. Lastly, analysis of the simple ratio of erosive events over time reveals that erosive water levels are reached 3.53 times per year. None of the approaches to analysis of erosive water levels account for variability, where some years may experience many erosive events and other years experience none. These findings are significant for other high-energy, wave dominated, mesotidal beaches in British Columbia, particularly if they are lacking a consistent sediment supply, or are removed from regions of tectonic uplift. Dependent on shoreline geology, areas lacking tectonic influence or areas where tectonic uplift occurs at a rate slower than absolute sea level rise (+ 1.7 $\pm$ 0.8 mm a^{-1}; Mazzotti *et al.*, 2008) may experience increased erosion due to rising global sea levels. Furthermore, areas of tectonic subsidence will experience accelerated rates of sea level rise which may, correspondingly, translate to more shoreline erosion. It is expected that other sedimentary, high-energy, wave dominated, mesotidal shorelines in British Columbia will experience annual erosive high water events, and will likely retreat if they lack the buffering capacity provided by relative sea level fall or a strong rebuilding potential, comparable to that of Wickaninnish Beach.

5.1.3 Climate Variability and Regional Wave and Water Level Conditions

Climate variability phenomena are known to influence climate and sea levels in the Northeastern Pacific (Gedalof & Smith, 2001; Ruggerio *et al.*, 2001; Barrie & Conway, 2002; Abeysirigunawardena & Walker, 2008). Therefore, using climate variability indices, the strength of shared variance was explored between several oceanographic elements and the El Niño Southern Oscillation, the Aleutian Low Pressure System, and the Pacific Decadal Oscillation. The positive El Niño component of the El Niño Southern Oscillation (ENSO) shared the greatest variance with incident oceanographic elements. Of particular interest, El Niño was shown to be significantly correlated with maximum wave period (NOI r = -0.217; MEI r = 0.288) and maximum water levels (NOI r = -0.185; MEI r = 0.088). These elements both serve to elevate

total water levels and, while a causal relationship cannot be drawn, these findings suggest that El Niño events may contribute to the occurrence of erosion events at Wickaninnish Beach. These findings are in agreement with a number of other studies along the West Coast of North America (e.g., Ruggerio *et al.*, 1997; Storlazzi & Griggs, 2000; Allan & Komar, 2002, 2006, Abeysirigunawardena & Walker, 2008). More in-depth statistical exploration (e.g., Cumulative Sum Analysis, Superposed Epoch Analysis), coupled with direct observation and monitoring of beach profile responses, are required to validate the relationship between El Niño forcing and the frequency of erosive water level events on Wickaninnish Beach.

5.2 Future Research Considerations

This research on beach-dune morphodynamics and climate variability impacts on Wickaninnish Beach has left a number of areas in need of study, including:

- Surveying of nearshore bathymetry to enable better understanding of bar morphology and the nature of the surf zone;
- Expansion of littoral transport studies (e.g., with tracer dyes) to determine transport direction and, potentially, sediment sources (e.g., is there a current that rounds Quisitis Point from Florencia Bay delivering sediments to Wickaninnish Beach);
- *In situ* sediment transport experiments to provide insight to the actual transport regime and to quantify the impacts of *Ammophila* spp. on the competency of the aeolian transport regime and capacity for transport to the backdune;
- Continuation of the cross-shore monitoring program (using *stakeout* methods to re-establish the profile) to develop a longer-term understanding of beach-dune trends (e.g., erosion, accretion);
- A repeat airborne LiDAR mission (or other, more economical, approach to volumetric data collection that provides 15 cm horizontal and vertical accuracies and 1 m spatial resolution) five years after initial restoration to enable detailed volumetric change analysis within the larger transgressive and foredune systems;

- Application of simple linear regression to water levels, wind speeds, and wave heights and period to investigate if directional trends exist (i.e., increasing or decreasing);
- Further statistical analysis of the erosive water level regime and climate variability indices;
- Correlation of wind directional modes and climate variability indices to explore potential relationships; and,
- Investigation of the seasonality of erosion and rebuilding events and contributing processes to improve understanding of the variability in regional ocean-atmosphere regimes.

References

Aagaard, T., Davidson-Arnott, R., Greenwood, B. & Nielsen, J. (2004). Sediment supply from shoreface to dunes: linking sediment transport measurements and long-term morphological evolution. *Geomorphology*, 60, 205-224.

Abeysirigunawardena, D.S. & Walker, I.J. (2008). Sea level responses to climate variability and change in Northern British Columbia. *Atmosphere-Ocean*, 46 (3), 277-296.

Abeysirigunawardena, D.S., Gilleland, E., Bronaugh, D. & Wong, P. (2009). Extreme wind regime responses to climate variability and change in the inner South Coast of British Columbia, Canada. *Atmosphere-Ocean*, 47 (1), 1480-9214.

Allan, J.C. & Komar, P.D. (2000). Are ocean wave heights increasing in the eastern North Pacific? *EOS, Transaction of the American Geophysical Union*, 47, 561-567.

Allan, J.C. & Komar, P.D. (2002). Extreme storms on the Pacific northwest coast during the 1997-8 El Niño and 1998-9 La Niña. *Journal of Coastal Research*, 18, 175-193.

Allan, J.C. & Komar, P.D. (2006). Climate controls on US West Coast erosion processes. *Journal of Coastal Research*, 22(3), 511-539.

Alley, N.F. & Chatwin, S.C. (1979). Late Pleistocene history and geomorphology, southwestern Vancouver Island, British Columbia. *Canadian Journal of Earth Sciences*, 16 (9), 1645-1657.

Arens, S.M. (1996). Patterns of sand transport on vegetated dunes. *Geomorphology*, 17, 339-350.

Arens, S.M., Slings, Q. & de Vries, C.N. (2004). Mobility of a remobilised parabolic dune in Kennermerland, The Netherlands. *Geomorphology*, 59, 175-188.

Bagnold, R.A. (1941). *The physics of blown sand and desert dunes*. London, England: Methuen Publishing Ltd.

Barrie, J.V. & Conway, K. (2002). Rapid sea level changes and coastal evolution on the Pacific margin of Canada. *Journal of Sedimentary Geology,* 150, 171-183.

Barrows, C.W. (1996). An ecological model for the protection of a dune ecosystem. *Conservation Biology*, 10 (3), 888-891.

Battjes, J.A. (1974). Surf similarity. *American Society of Civil Engineers: Proceedings of the 14th International Conference on Coastal Engineering,* Copenhagen, Denmark (pp. 466-480).

Bauer, B.O. & Davidson-Arnott, R.G.D. (2002). A general framework for modeling sediment supply to coastal dunes including wind angle, beach geometry, and fetch effects. *Geomorphology*, 49, 89-108.

Bauer, B.O., Davidson-Arnott, R.G.D., Hesp, P.A., Namikas, S.L., Ollerhead, J. & Walker, I.J. (2009). Aeolian sediment transport on a beach: Surface moisture, wind fetch, and mean transport. *Geomorphology*, 105 (1-2), 106-116.

Beamish, R.J. & Bouillon, D.R. (1993). Pacific salmon production trends in relation to climate. *Canadian Journal of Fisheries and Aquatic Sciences,* 50, 1002-1016.

Beamish, R.J., Noakes, D.J., McFarlane, G.A., Klyashtorin, L., Ivanoc, V.V. & Kurashov, V. (1999). The regime concept and natural trends in the production of Pacific salmon. *Canadian Journal of Fisheries and Aquatic Sciences,* 56, 516-526.

BC Conservation Data Centre (2010). *BC Species and Ecosystems Explorer*. Retrieved 27 April 2010 from http://a100.gov.bc.ca/pub/eswp/.

Blott, S. & Pye, K. (2001). GRADISTAT: A grain size distribution and statistics package for the analysis of unconsolidated sediments. *Earth Surface Processes and Landforms,* 26, 1237-1248. Retrieved 27 March, 2009 from http://www.kpal.co.uk/gradistat_abstract.htm

Bonsal, B.R. & Prowse, T.D. (2003). Trends and variability in spring and autumn 0°C isotherm dates over Canada. *Climate Change,* 57, 341-358.

Brandon, M.T. (1989). Deformational styles in a sequence of olistostromal mélanges, Pacific Rim Complex, western Vancouver Island, Canada. *Geological Society of American Bulletin*, 101, 1520-1542.

Bremner, J.M. (1970). *The geology of Wreck Bay, Vancouver Island*. Unpublished master's thesis. University of British Columbia, Vancouver, Canada.

Bruun, P. (1954). *Coastal erosion and the development of beach profiles* (Beach Erosion Board Technical Memorandum No. 44). Washington DC, United States: US Army Corps of Engineers.

Chelton, D.B. & Enfield, D.B. (1986). Ocean signals in tide gauge records. *Journal of Geophysical Research,* 91(B9), 9081-9098.

Clague, J.J. & Bornhold, B.D. (1980). Morphology and littoral processes of the Pacific Coast of Canada. In S.B. McCann (Ed.) *The Coastline of Canada Conference* (pp. 339-380). Halifax, Canada: Geological Survey of Canada.

Clague, J.J. & Bobrowsky, P.T. (1994). Evidence for a large earthquake and tsunami 100-400 years ago on Western Vancouver Island, British Columbia. *Quaternary Research*, 41, 176-184.

Clague, J.J. & James, T.S. (2002). History and isostatic effects of the last ice sheet in southern British Columbia. *Quaternary Science Reviews*, 21, 71-87.

Cornaglia, P. (1977). On beaches (W.N. Felder, Trans.). In J.S. Fisher & R. Dolan (Eds.), *Beach Processes and Coastal Hydrodynamics. Vol. 39 Benchmark Papers in Geology* (pp. 11-26). Stroudsburg, United States: Dowden, Hutchinson & Ross, Inc. (Original work published 1889).

Cowell, P.J., Hanslow, D.J. & Meleo, J.F. (1999). The shoreface. In A.D. Short (Ed.), *Handbook of Beach and Shoreface Morphodynamics* (pp. 39-71). West Sussex, England: John Wiley & Sons, Inc.

Craig, M.S. (2000). Aeolian sand transport at the Lanphere dunes, northern California. *Earth Surface Processes and Landforms*, 25, 239-253.

Crawford, W., Cherniawsky, J., Foreman, M. & Chandler, P. (1999). *El Niño sea level signal along the West Coast of Canada* (North Pacific Marine Science Organization (PICES), Scientific Report No. 10). Retrieved 8 June, 2010 from http://www.pices.int/publications/scientific_reports/

Cumming, R.M. (2007). *Beach-dune morphodynamics and climatic variability in Gwaii Haanas National Park Reserve and Haida Heritage Site, British Columbia, Canada*. Unpublished master's thesis. University of Victoria, Victoria, Canada.

Dean, R.G. (1976). Equilibrium beach profiles and response to storms. In *Proceedings of the 15th Conference on Coastal Engineering*, Honolulu, United States.

Dean, R.G. (1977). Equilibrium beach profiles: U.S. Atlantic and Gulf Coasts (Ocean Engineering Technical Report No. 12). Newark, United States: Department of Civil Engineering, University of Delaware.

Dean, R.G. (1991). Equilibrium beach profiles: Characteristics and applications. *Journal of Coastal Research*, 7(1), 53-84.

Eamer, J.B.R. & Walker, I.J. (2010). Quantifying sand storage capacity of large woody debris on beaches using LiDAR. *Geomorphology*, 118 (1-2), 33-47.

Eid, B., Calnan, C., Henschel, M. & McGrath, B. (1993). Wind and wave climate atlas: Volume IV the West Coast of Canada. Montreal, Quebec, Canada: Transport Canada. Retrieved 12 May 2010 from http://www.meds-sdmm.dfo-mpo.gc.ca/alphapro/wave/TDCAtlas/tdcatlaswc.htm

Ferguson, R.I. & Church, M. (2004). A simple universal equation for grain settling velocity. *Journal of Sedimentary Research,* 74 (6), 933-937.

Fryberger, S.G. & Dean, G. (1979). Dune forms and wind regime. In E.D. McKee, (Ed.), *A Study of Global Sand Seas* (pp. 137-169). Washington DC, United States: USGS Professional Paper 1052.

Gao, S. & Collins, M. (1991). A critique of the "McLaren Method" for defining sediment transport paths – discussion. *Journal of Sedimentary Petrology,* 61 (1), 143-146.

Gedalof, Z. & Smith, D.J. (2001). Interdecadal climate variability and regime-scale shifts in Pacific North America. *Geophysical Research Letters,* 28 (8), 1515-1518.

Gershunov, A. & Barnett, T.P. (1998). Interdecadal modulation of ENSO teleconnections. *Bulletin of the American Meteorological Society*, 79 (12), 2715-2725.

Gilleland, E., Katz, R., & Young, G. (2003). Extremes toolkit: Weather and climate applications of extreme values statistics. Retrieved 3 February 2010 from http://www.isse.ucar.edu/extremevalues/evtk.html

Graham, N.E. & Diaz, H.F. (2001). Evidence for intensification of North Pacific winter cyclones since 1948. *Bulletin of the American Meteorological Society,* 82 (9), 1869 – 1893.

Guza, R.T. & Inman, D.L. (1975). Edge waves and beach cusps. *Journal of Geophysical Research*, 80 (21), 2997-3012.

Harper, J.R. (1980). Seasonal changes to beach morphology along the British Columbia coast. *Proceedings of the 1980 Canadian Coastal Conference*. Burlington, Canada: National Research Council.

Harper, J.R. & Sawyer, B. (1983). *Coastal analysis of the Long Beach segment and Broken Group Islands, Pacific Rim National Park* (Report No. 12-4). Victoria, Canada: Woodward-Clyde Consultants.

Heathfield, D. & Walker, I.J. (in review). *Coastal dune stabilization and large woody debris at Long Beach and Wickaninnish Bay, Pacific Rim National Park, British Columbia*. Manuscript submitted to *The Canadian Geographer* for review.

Hesp, P.A. (1983). Morphodynamics of incipient foredunes in New South Wales, Australia. In M.E. Brookfield and T.S. Ahlbrandt (Eds.), *Eolian Sediments and Processes* (pp. 325-342). Amsterdam, The Netherlands: Elsevier.

Hesp, P.A. (1989). A review of biological and geomorphological processes involved in the initiation and development of incipient foredunes. In C.H. Gimingham, W. Tirchie, B.B. Willets & A.J. Willis (Eds.), *Coastal Sand Dunes*: *Proceedings of the royal society of Edinburgh* (pp. 181-201). Edinburgh, Scotland: The Royal Society of Edinburgh.

Hesp, P.A. (1991). *Ecological processes and plant adaptations on coastal dunes.* Journal of Arid Environments, 21, 165-191.

Hesp, P.A. (1992). Foredunes and blowouts: Initiation, geomorphology and dynamics. *Geomorphology,* 245-268.

Hesp, P.A. (1999). The beach, backshore and beyond. In A.D. Short (Ed.), *Handbook of Beach and Shoreface Morphodynamics* (pp. 119-144). West Sussex, England: John Wiley & Sons, Inc.

Hesp, P.A. (2002). Foredunes and blowouts: Initiation, geomorphology and dynamics. *Geomorphology*, 48, 245-268.

Heyligers, P. (1985). The impact of introduced plants on foredune formation in south-eastern Australia. *Proceedings of the Ecological Society of Australia,* 14, 23-41.

Hillen, R. & Roelse, P. (1995). Dynamic preservation of the coastline in the Netherlands. *Journal of Coastal Conservation*, 1 (1), 17-28.

Hilton, M., Duncan, M. & Jus, A. (2005). Processes of *Ammophila arenaria* (marram grass) invasion and indigenous species displacement, Stewart Island, New Zealand. *Journal of Coastal Research*, 21 (1), 175-185.

Holland, S.S. (1976). *Landforms of British Columbia: A physiographic outline* (Bulletin 48). Victoria, Canada: British Columbia Department of Mines and Petroleum.

Holman, R.A. (1986). Extreme values statistics for wave run-up on a natural beach. *Coastal Engineering,* 9, 527-544.

Hubbard, W.A. (1969). *The grasses of British Columbia*: *Handbook no. 9*. Victoria, Canada: A. Sutton.

Hugenholtz, C.H., Wolfe, S.A., Walker, I.J. & Moorman, B.J. (2009). Spatial and temporal patterns of Aeolian sediment transport on an inland parabolic dune, Bigstick Sand Hills Saskatchewan, Canada. *Geomorphology,* 105, 158-170.

Hugenholtz, C.H., Bender, D. & Wolfe, S.A. (in press). Declining sand dune activity in the southern Canadian prairies: Historical context, controls and ecosystem implications. *Aeolian Research.*

Hughes, M. & Turner, I. (1999). The beachface. In A.D. Short (Ed.), *Handbook of Beach and Shoreface Morphodynamics* (pp. 119-144). West Sussex, England: John Wiley & Sons, Inc.

Hyndman, R.D., Rogers, G.C., Dragert, H., Wang, K., Clague, J.J., Adams, J. & Bobrowsky, P.T. (1996). Giant earthquakes beneath Canada's West Coast. *Geoscience Canada*, 23, 63-72.

International Towing Tank Conference (1999). *ITTC recommended procedures 7.5-02-01-03: testing and extrapolation methods, general density and viscosity of water*. Retrieved 16 June, 2010 from http://ittc.sname.org/2002_recomm_proc/7.5-02-01-03.pdf

Kawamura, R. (1964). Study of sand movement by wind (Hydraulic Engineer Laboratory Report No. HEL-2-8). Berkeley, United States: University of California. (Original work published 1951).

Konlechner, T.M. & Hilton, M.J. (2009). The potential for marine dispersal of *Ammophila arenaria* (Marram Grass) rhizome in New Zealand. *Journal of Coastal Research*, SI 56, 434-437.

Köppen, W. (1923). *Die climate der Erde.* Berlin: Walter de Gruyter.

Kocurek, G. & Lancaster, N. (1999). Aeolian system sediment state: Theory and Mojave Dester Kelso dune field example. *Sedimentology*, 46, 505-515.

Lang, A.H. & Muller, J.E. (1975). *The geology of Long Beach Segment Pacific Rim National Park and its approaches.* Ottawa, Canada: Geological Survey of Canada.

Lang, O.S. (2003). *The veil of chaos: living with weather along the British Columbia Coast.* Vancouver, Canada: Environment Canada.

Larson, M. (1991). Equilibrium profile of a beach with varying grain size. *American Society of Civil Engineers: Proceedings of Coastal Sediments '91*, Seattle, United States (pp. 905-919).

Lettau, K. & Lettau, H.H. (1978). Experimental and micrometerological field studies on dune migration. In K. Lettau and H.H. Lettau (Eds.), *Exploring the World's Driest Climate* (pp.110-147). Madison, United States: Institute for Environmental Studies, University of Madison-Wisconsin.

Mantua, N.J., Hare, S.R., Zhang, Y., Wallace, J.M. & Francis, R.C. (1997). A Pacific interdecadal climate oscillation with impacts on salmon production. *Bulletin of the American Meteorological Society,* 78 (6), 1069-1079.

Masselink, G. & Short, A.D. (1993). The effect of tide range on beach morphodynamics and morphology: A conceptual beach model. *Journal of Coastal Research,* 9 (3), 785-800.

Masselink, G. & Turner, I. (1999). The effect of tides on beach morphodynamics. In A.D. Short (Ed.), *Handbook of Beach and Shoreface Morphodynamics* (pp. 204-229). West Sussex, England: John Wiley & Sons, Inc.

Masselink, G. & Hughes, M.G. (2003). *Introduction to coastal processes and geomorphology*. New York, United States: Oxford University Press.

Mazzotti, S., Dragert, H., Henton, J., Schmidt, M., Hyndman, R., James, T., Lu, Y. & Craymer, M. (2003). Current tectonics of northern Cascadia from a decade of GPS measurements. *Journal of Geophysical Research*, 108 (B12), 2554.

Mazzotti, S., Lambert, A., Courtier, N., Nykolaishen, L. & Dragert, H. (2007). Crustal uplift and sea level rise in northern Cascadian from GPS, absolute gravity, and tide gauge data. *Geophysical Research Letters,* 34 (15), L15306.

Mazzotti, S., Jones, C. & Thomson, R.E. (2008). Relative and absolute sea level rise in western Canada and northwestern United States from a combined tide gauge-GPS analysis. *Journal of Geophysical Research*, 113, C11019.

McLaren, P. (1981). An interpretation of trends in grain size measures. *Journal of Sedimentary Petrology*, 15 (2), 611-624.

McLaren, P. & Bowles, D. (1985). The effects of sediment transport on grain-size distributions. *Journal of Sedimentary Petrology*, 55 (4), 457-470.

Mitasova, H., Overton, M.F., Recalde, J.J., Bernstein, D.J. & Freeman, C.W. (2009). Raster-based analysis of coastal terrain dynamics from multitemporal LiDAR data. *Journal of Coastal Research*, 25 (2), 507-514.

Mote, P.W. (2003). Twentieth-century fluctuation and trends in temperature, precipitation, and mountain snowpack in the Georgia Basin – Puget Sound region. *Canadian Water Resources Journal,* 28 (4), 567-585.

Oke, T.R. (1978). *Boundary layer climates.* New York, United States: Methuen & Co.

Page, N. (2001). *Ammophila breviligulata* (*Poaceae*) new to British Columbia. *Botanical Electronic News*, 276, doi: 1188-603X.

Page, N. (2003). *Community and regional scale patterns of native and exotic plant species in sand beaches of Vancouver Island, British Columbia.* Unpublished master's thesis. University of British Columbia, Vancouver, Canada.

Parizeau, H.D., Davies, L.R. Wills, W.K., Ettershank, R.H., Young, R.B., Stewardson, A., Johnson, J.D., McQuarrie, H.N. & Wiebe, V. (1931). Field sheet III-L: Bonilla Point to Leonard Island [Bathymetric map]. Sidney, Canada: Canadian Hydrographic Service.

Parks Canada Agency (2005). Monitoring and reporting ecological integrity in Canada's National Parks: Volume 1 guiding principles. Hull, Canada: Government of Canada.

Ranwell, D.S. (1972). *Ecology of salt marshes and sand dunes.* London, England: Chapman and Hill Ltd.

Ritter, D.F., Kochel, R.C. & Miller, J.R. (2002). *Process Geomorphology* (4th ed.). New York, United States: McGraw-Hill Science.

Ruggiero, P., Kaminsky, G.M., Komar, P.D. & McDougal, W.G. (1997). Extreme Waves and Coastal Erosion in the Pacific Northwest. Proceedings of the 3rd International Symposium, Waves '97*: Ocean Wave Measurement and Analysis.* Virginia Beach, United States: American Society of Civil Engineers.

Ruggiero, P., Komar, P.D., McDougal W.G., Marra, J.J. & Beach, R.A. (2001). Wave runup, extreme water levels and the erosion of properties backing beaches. *Journal of Coastal Research*, 17 (2), 407-419.

Ryan, H.F. & Noble, M.A. (2006). Alongshore wind forcing of coastal sea level as a function of frequency. *Journal of Physical Oceanography*, 36, 2173-2184.

Sarre, R.D. (1987). Aeolian sand transport. *Progress in Physical Geography,* 11, 157-182.

Schwing, F.B., Murphree, T. & Green, P.M. (2002). The Northern Oscillation Index (NOI): A new climate index for the northeast Pacific. *Progress in Oceanography*, 53 (2-4), 115-139.

Seymour, R.J. (1998). Effects of El Niño on the west coast wave climate. *Shore Beach*, 66, 3-6.

Sherman, D.J., Jackson, D.W.T., Namikas, S.L. & Wang, J. (1998) Wind-blown sand on beaches: an evaluation of models. *Geomorphology,* 22, 113-133.

Short, A.D. (1982). Wave, beach and dune interactions in Southeastern Australia. *Marine Geology*, 48, 259-284.

Short, A.D. (1999). Beaches. In A.D. Short (Ed.), *Handbook of Beach and Shoreface Morphodynamics* (pp. 3-20). West Sussex, England: John Wiley & Sons, Inc.

Short, A.D. & Masselink, G. (1999). Embayed and structurally controlled beaches. In A.D. Short (Ed.), *Handbook of Beach and Shoreface Morphodynamics* (pp. 230-250). West Sussex, England: John Wiley & Sons, Inc.

Spiegl, M.R. (1961). *Theory and problems of statistics Schaum's outline series*. New York, United States: McGraw Hill.

Storlazzi, C.D. & Griggs, G.B. (2000). Influence of El Niño-Southern Oscillation (ENSO) events on the evolution of central California's shoreline. *Geological Society of America Bulletin*, 112, 236-249.

Storlazzi, C.D., Willis, C.M. & Griggs, G.B. (2000). Comparative impacts of the 1982 – 83 and 1997 – 98 El Niño winters on the central California coast. *Journal of Coastal Research,* 16 (4), 1022-1036.

Subbotina, M.M., Thomson, R.E. & Rabinovich, A.B. (2001). Spectral characteristics of sea level variability along the west coast of North America during the 1982-83 and 1997-98 El Niño events. *Progress in Oceanography,* 49, 353-372.

Swales, A. (2002). Geostatistical estimation of short-term changes in beach morphology and sand budget. *Journal of Coastal Research*, 18 (2), 338-351.

Thomson, R.E. (1981). *Oceanography of the British Columbia coast* (Canadian Special Publication of Fisheries and Aquatic Sciences 56). Ottawa, Canada: Minister of Supply and Services Canada.

Tuller, S. (2004). Measured wind speed trends on the West Coast of Canada. *International Journal of Climatology*, 24, 1359-1374.

Valentine, K.W.G. (1971). *Soils of the Tofino-Ucluelet Lowland of British Columbia* (Report No. 11). Ottawa, Canada: Department of Agriculture.

Van der Meulen, F. & van der Maarel, E. (1989). Coastal defence alternatives and nature development perspectives. In F. van der Meulen, P.D. Jungerius & J.H. Visser (Eds.), *Perspectives in coastal dune management* (pp. 183 – 195). The Hague, The Netherlands: SPB Academic Publishing.

Van Hook, S.S. (1983). *A study of European beachgrass, Ammophila arenaria (L.) Link: Controls methods and a management plan for the Lanphere-Christensen Dunes Preserve*. Arcata, United States: The Nature Conservancy.

Vincent, L.A. & Menkis, É. (2006). Changes in daily and extreme temperature and precipitation indices for Canada over the twentieth century. *Atmosphere-Ocean*, 44 (2), 177-193.

Walker, I.J. & Barrie, J.V. (2006). Geomorphology and sea-level rise on one of Canada's most sensitive coasts: Northeast Graham Island, British Columbia. *Journal of Coastal Research*, SI 39, 220-226.

Walker, I.J., Hesp, P.A., Davidson-Arnott, R.G.D. & Ollerhead, J. (2006). Topographic steering of alongshore airflow over a vegetated foredune: Greenwich Dunes, Prince Edward Island, Canada. *Journal of Coastal Research*, 22, 1278-1291.

Walker, I.J. & Sydneysmith, R. (2008). British Columbia. In D.S. Lemmen, F. Warren, E. Bush, and J. Lacroix (Eds.), *From Impacts to Adaptation: Canada in a Changing Climate 2007* (pp.329-386). Ottawa, Canada: Government of Canada.

Walker, I.J., Hesp, P.A., Davidson-Arnott, R.G.D., Bauer, B.O., Namikas, S.L. & Ollerhead, J. (2009). Responses of three-dimensional flow variations in the angle of incident wind and profile form of dunes: Greenwich Dunes, Prince Edward Island, Canada. *Geomorphology*, 105 (1-2), 127-138.

Whitfield, P.H. & Taylor, E. (1998). Apparent recent changes in hydrology and climate of coastal British Columbia. In Y. Alila (Ed.), *Proceedings of 51rst Annual Canadian Water Resources Conference: Mountains to Sea: Human Interaction with the Hydrologic Cycle.* Cambridge, Canada: Canadian Water Resources Association.

Whitfield, P.H., Reynolds, C.J. & Cannon, A.J. (2002). Modelling streamflows in present and future climates – Examples from Georgia Basin, British Columbia. *Canadian Water Resources Journal,* 27 (4), 427-456.

Wiedemann, A.M. & Pickart, A. (1996). The *Ammophila* problem on the Northwest Coast of North America. *Landscape and Urban Planning*, 34, 287-299.

Wigen, S.O. & Stephenson, F.E. (1980). Mean sea level on the Canadian West Coast. In *Proceedings of 2nd International Symposium on Problems Related to the Redefinition of North American Vertical Geodetic Networks (NAD)*. Ottawa, Canada: Canadian Institute of Surveying and Mapping.

Wolter, K. & Timlin, M.S. (1993). Monitoring ENSO in COADS with a seasonally adjusted principle component index. In *Proceedings of the 17th Climate Diagnostics Workshop* (pp. 52-57). Norman, United States: University of Oklahoma.

Wolynec, L. (2004). *Improving model constraints for vertical deformation across the northern Cascadia margin*. Unpublished master's thesis. University of Victoria, Victoria, Canada.

Wright, S. & Short, A.D. (1983). Morphodynamics of beaches and surf zones in Australia. In P. Komar (Ed.), *CRC Handbook of Coastal Processes and Erosion*, (pp. 35-64). Boca Raton, United States: CRC Press.

Yorath, C. (2005). *The geology of Southern Vancouver Island*. Madeira Park, Canada: Harbour Publishing.

Ziv, A., Cochard, A. & Schmittbuhl, J. (2005). Does elastic rebound theory apply to seismic faults. In A. Carpinteri (Ed.), *Proceedings of the 11th International Conference on Fracture.* Torino, Italy: Innovative Learning and Training on Fracture.

Appendices

Appendix A

Sediment moment statistics for Wickaninnish Beach.

Sample	Easting (UTM, Zone 10)	Northing (UTM, Zone 10)	Positional Accuracy (±m)	Mean (ϕ)	Mode D50† (ϕ)
0	304296	5432189	1.9	2.671	2.605
1	304444	5432666	5.1	2.604	2.605
2	304338	5433150	1.9	2.633	2.605
3	304057	5433572	2.1	2.583	2.605
4	303761	5433973	1.9	1.887	1.616
5	303483	5434370	2	2.337	2.605
6	303209	5434803	2.5	1.648	1.616
7	302900	5435159	3.4	2.547	2.605
8	302591	5435468	2.7	2.535	2.605
9	302015	5435803	2.8	2.546	2.605
10	301618	5436208	2.5	2.618	2.605
11	301323	5436578	3.6	2.606	2.605
12	301214	5436689	3.1	2.664	2.605
13	300949	5436987	3.1	2.615	2.605
14	300669	5437306	2.3	2.658	2.605
15	300303	5437663	2.2	2.639	2.605
16	299930	5438017	2.3	2.629	2.605
17	299557	5438327	2.7	2.608	2.605
18	299158	5438597	3.5	2.581	2.605
19	298724	5438821	2.7	2.614	2.605
20	298277	5439028	3.1	2.694	2.605
21	297787	5439118	2.2	2.676	2.605
22	297252	5439101	4.2	2.699	2.605
23	296704	5438747	2.6	2.725	2.868

† D50 indicates median grain size.

Appendix B

Provided below are data for the period 2008 to 2010 required to reproduce Wickaninnish cross-shore transects 1 through 3.

Transect 1 2008 Data[†]			
Northing (UTM, Zone 10)	**Easting (UTM, Zone 10)**	**Horizontal Distance (m)**	**Elevation (m aCD)**
5433300.76	304415.62	0.00	11.94
5433300.76	304415.58	0.03	11.82
5433300.27	304414.83	0.93	12.09
5433299.04	304412.95	3.18	12.57
5433298.12	304411.78	4.66	12.72
5433297.71	304411.10	5.45	12.66
5433297.67	304411.07	5.50	12.58
5433296.65	304409.48	7.38	12.54
5433294.83	304406.68	10.73	12.33
5433293.47	304404.46	13.33	11.78
5433293.09	304404.08	13.85	11.66
5433291.43	304402.09	16.43	11.29
5433290.47	304400.83	18.01	10.94
5433286.98	304395.89	24.05	9.69
5433285.79	304393.92	26.36	9.54
5433283.51	304390.38	30.57	9.04
5433281.28	304387.05	34.57	9.23
5433281.04	304386.78	34.94	9.31
5433279.44	304384.12	38.03	9.45
5433277.99	304381.51	41.00	9.50
5433277.25	304380.69	42.10	9.52
5433276.48	304379.74	43.32	9.34
5433275.31	304378.07	45.36	8.96
5433273.66	304375.33	48.55	8.91
5433271.85	304372.90	51.58	9.04
5433270.59	304371.30	53.61	9.10
5433269.21	304369.27	56.06	8.97
5433268.92	304368.16	57.15	9.04
5433268.06	304367.23	58.40	8.87
5433267.47	304366.50	59.34	8.89
5433266.65	304365.10	60.95	9.23
5433265.61	304362.93	63.33	9.66
5433264.54	304361.60	65.04	9.87
5433263.90	304360.71	66.13	9.85
5433263.52	304359.50	67.35	9.68

5433263.00	304358.67	68.33	9.60
5433262.00	304357.18	70.13	9.91
5433261.43	304356.38	71.11	9.83
5433260.20	304354.54	73.32	9.45
5433259.24	304352.91	75.21	9.19
5433257.46	304350.85	77.91	8.27
5433256.35	304349.68	79.49	7.88
5433255.56	304348.44	80.97	7.07
5433254.84	304346.96	82.60	6.59
5433254.35	304346.08	83.60	6.53
5433252.96	304343.73	86.33	6.08
5433251.54	304341.49	88.98	5.73
5433250.56	304340.41	90.43	5.51
5433250.35	304339.99	90.89	5.63
5433247.97	304336.25	95.32	5.30
5433246.87	304334.49	97.40	5.19
5433245.24	304332.20	100.21	5.06
5433241.28	304326.07	107.50	4.69
5433236.42	304318.34	116.63	4.72
5433233.57	304314.07	121.76	4.71
5433229.13	304307.27	129.88	4.16
5433223.89	304299.43	139.31	3.74
5433218.37	304291.04	149.36	3.26
5433212.39	304282.13	160.08	2.81
5433207.88	304275.04	168.49	2.63
5433205.21	304270.35	173.88	2.50
5433200.31	304263.69	182.13	2.30

† Transect surveyed August 11, 2008. Water line tagged at 15:34 at UTM Zone 10, 5433200.31 m N, 304263.69 m E, 2.30 m aCD.

Transect 1 2009 Data†			
Northing (UTM, Zone 10)	**Easting (UTM, Zone 10)**	**Horizontal Distance (m)**	**Elevation (m aCD)**
5433300.90	304415.27	0.00	11.79
5433300.90	304414.27	1.00	12.07
5433299.90	304414.27	1.41	12.15
5433299.90	304414.27	1.41	12.15
5433297.90	304412.27	4.24	12.81
5433297.90	304411.27	5.00	12.74
5433296.90	304410.27	6.40	12.63
5433296.90	304410.27	6.40	12.63
5433295.90	304408.27	8.60	12.59

5433294.90	304407.27	10.00	12.35
5433293.90	304405.27	12.21	12.17
5433293.90	304404.27	13.04	11.98
5433292.90	304403.27	14.42	11.80
5433291.90	304403.27	15.00	11.90
5433290.90	304401.27	17.20	11.18
5433289.90	304400.27	18.60	10.77
5433288.90	304399.27	20.00	10.37
5433287.90	304398.27	21.40	9.98
5433287.90	304397.27	22.20	9.84
5433285.90	304395.27	25.00	9.40
5433284.90	304393.27	27.20	9.18
5433284.90	304392.27	28.02	9.12
5433283.90	304391.27	29.41	9.03
5433282.90	304389.27	31.62	8.95
5433281.90	304388.27	33.02	9.04
5433281.90	304387.27	33.84	9.07
5433279.90	304386.27	35.81	9.12
5433280.90	304386.27	35.23	9.12
5433279.90	304385.27	36.62	9.16
5433278.90	304383.27	38.83	9.16
5433277.90	304382.27	40.22	9.09
5433276.90	304380.27	42.44	9.07
5433276.90	304379.27	43.27	9.10
5433275.90	304378.27	44.65	8.99
5433274.90	304377.27	46.04	8.86
5433273.90	304376.27	47.43	8.87
5433272.90	304374.27	49.65	8.79
5433271.90	304373.27	51.04	8.85
5433270.90	304372.27	52.43	8.87
5433269.90	304370.27	54.64	8.86
5433268.90	304369.27	56.04	8.80
5433268.90	304368.27	56.86	8.78
5433267.90	304367.27	58.25	8.75
5433266.90	304366.27	59.64	8.96
5433266.90	304365.27	60.46	9.08
5433265.90	304364.27	61.85	9.41
5433265.90	304363.27	62.68	9.50
5433264.90	304362.27	64.07	9.66
5433263.90	304360.27	66.29	9.85
5433263.90	304359.27	67.12	9.91
5433262.90	304358.27	68.51	10.17
5433261.90	304357.27	69.89	10.17

5433260.90	304356.27	71.28	10.05
5433260.90	304355.27	72.11	9.86
5433259.90	304353.27	74.33	9.16
5433257.90	304352.27	76.28	8.74
5433257.90	304351.27	77.10	8.43
5433256.90	304350.27	78.49	7.96
5433255.90	304348.27	80.71	7.19
5433254.90	304347.27	82.10	6.84
5433253.90	304346.27	83.49	6.68
5433253.90	304345.27	84.31	6.61
5433252.90	304344.27	85.70	6.38
5433251.90	304342.27	87.92	6.00
5433251.90	304341.27	88.75	5.95
5433250.90	304340.27	90.14	5.92
5433249.90	304339.27	91.53	5.80
5433249.90	304339.27	91.53	5.80
5433248.90	304338.27	92.91	5.67
5433248.90	304337.27	93.74	5.59
5433246.90	304335.27	96.52	5.33
5433245.90	304333.27	98.74	5.10
5433245.90	304332.27	99.57	5.00
5433244.90	304331.27	100.96	4.90
5433243.90	304330.27	102.34	4.80
5433242.90	304329.27	103.73	4.80
5433242.90	304328.27	104.56	4.78
5433241.90	304327.27	105.95	4.69
5433240.90	304326.27	107.34	4.61
5433240.90	304325.27	108.17	4.57
5433239.90	304324.27	109.55	4.52
5433238.90	304323.27	110.94	4.51
5433238.90	304322.27	111.77	4.48
5433237.90	304321.27	113.16	4.46
5433237.90	304320.27	113.99	4.41
5433236.90	304319.27	115.38	4.38
5433235.90	304317.27	117.60	4.36
5433234.90	304316.27	118.98	4.29
5433234.90	304315.27	119.82	4.27
5433233.90	304314.27	121.20	4.23
5433232.90	304313.27	122.59	4.15
5433231.90	304312.27	123.98	4.11
5433231.90	304311.27	124.81	4.08
5433230.90	304310.27	126.19	4.06
5433229.90	304309.27	127.58	3.97

5433229.90	304308.27	128.41	3.96
5433228.90	304306.27	130.63	3.92
5433227.90	304305.27	132.02	3.86
5433226.90	304304.27	133.41	3.83
5433226.90	304303.27	134.24	3.81
5433225.90	304302.27	135.62	3.83
5433224.90	304301.27	137.01	3.80
5433224.90	304300.27	137.84	3.77
5433222.90	304298.27	140.62	3.70
5433222.90	304297.27	141.45	3.62
5433221.90	304296.27	142.84	3.64
5433220.90	304295.27	144.22	3.61
5433220.90	304294.27	145.06	3.58
5433219.90	304293.27	146.44	3.50
5433218.90	304292.27	147.83	3.49
5433218.90	304291.27	148.66	3.50
5433217.90	304290.27	150.05	3.48
5433216.90	304289.27	151.43	3.43
5433215.90	304288.27	152.82	3.38
5433215.90	304287.27	153.65	3.34
5433214.90	304286.27	155.04	3.32
5433213.90	304285.27	156.43	3.31
5433213.90	304284.27	157.26	3.34
5433212.90	304283.27	158.64	3.23
5433211.90	304281.27	160.86	3.22
5433210.90	304280.27	162.25	3.07
5433210.90	304279.27	163.08	3.11
5433209.90	304278.27	164.47	3.04
5433208.90	304277.27	165.86	3.04
5433208.90	304276.27	166.69	3.05
5433207.90	304275.27	168.07	2.96
5433206.90	304274.27	169.46	3.01
5433206.90	304273.27	170.29	2.93
5433205.90	304272.27	171.68	2.94
5433205.90	304271.27	172.51	2.96
5433204.90	304269.27	174.73	2.90
5433203.90	304268.27	176.12	2.94
5433202.90	304267.27	177.50	2.86
5433201.90	304266.27	178.89	2.80
5433201.90	304265.27	179.72	2.82
5433200.90	304264.27	181.11	2.92

[†]Extracted in PCI Geomatica from LiDAR flown August 27, 2009.

Transect 1 2010 Data[†]			
Northing (UTM, Zone 10)	Easting (UTM, Zone 10)	Horizontal Distance (m)	Elevation (m aCD)
5433300.53	304415.45	0.00	12.03
5433300.53	304414.45	1.00	12.11
5433300.53	304414.45	1.00	12.11
5433299.53	304413.45	2.24	12.42
5433298.53	304411.45	4.47	12.81
5433297.53	304410.45	5.83	12.76
5433296.53	304410.45	6.40	12.72
5433297.53	304410.45	5.83	12.76
5433295.53	304408.45	8.60	12.48
5433295.53	304407.45	9.43	12.43
5433294.53	304405.45	11.66	12.22
5433293.53	304404.45	13.04	12.03
5433292.53	304403.45	14.42	11.78
5433292.53	304403.45	14.42	11.78
5433290.53	304401.45	17.20	11.32
5433289.53	304399.45	19.42	10.63
5433289.53	304398.45	20.25	10.39
5433288.53	304397.45	21.63	10.11
5433287.53	304396.45	23.02	9.86
5433286.53	304394.45	25.24	9.57
5433285.53	304392.45	27.46	9.29
5433284.53	304391.45	28.84	9.21
5433283.53	304390.45	30.23	9.14
5433282.53	304389.45	31.62	9.12
5433282.53	304388.45	32.45	9.14
5433281.53	304387.45	33.84	9.18
5433280.53	304386.45	35.23	9.22
5433280.53	304385.45	36.06	9.26
5433279.53	304384.45	37.44	9.24
5433278.53	304383.45	38.83	9.21
5433278.53	304382.45	39.66	9.22
5433277.53	304380.45	41.88	9.18
5433276.53	304379.45	43.27	9.12
5433275.53	304378.45	44.65	9.06
5433274.53	304377.45	46.04	9.00
5433274.53	304376.45	46.87	8.98
5433272.53	304374.45	49.65	8.93
5433272.53	304373.45	50.48	8.93
5433271.53	304371.45	52.70	8.90
5433269.53	304370.45	54.64	8.82

5433269.53	304369.45	55.47	8.84
5433268.53	304368.45	56.86	8.88
5433267.53	304367.45	58.25	9.00
5433267.53	304366.45	59.08	9.09
5433266.53	304365.45	60.46	9.29
5433266.53	304364.45	61.29	9.41
5433265.53	304363.45	62.68	9.62
5433264.53	304361.45	64.90	9.84
5433263.53	304360.45	66.29	10.03
5433263.53	304359.45	67.12	10.16
5433262.53	304358.45	68.51	10.41
5433262.53	304357.45	69.34	10.44
5433261.53	304356.45	70.72	10.30
5433260.53	304355.45	72.11	10.01
5433259.53	304353.45	74.33	9.35
5433258.53	304351.45	76.55	8.57
5433257.53	304350.45	77.94	8.10
5433256.53	304349.45	79.32	7.63
5433255.53	304348.45	80.71	7.35
5433255.53	304347.45	81.54	7.21
5433254.53	304346.45	82.93	6.84
5433253.53	304345.45	84.31	6.46
5433253.53	304344.45	85.15	6.32
5433252.53	304342.45	87.37	6.03
5433251.53	304341.45	88.75	5.91
5433250.53	304340.45	90.14	5.80
5433250.53	304339.45	90.97	5.73
5433249.53	304339.45	91.53	5.69
5433249.53	304338.45	92.36	5.60
5433248.53	304337.45	93.74	5.50
5433247.53	304335.45	95.96	5.33
5433246.53	304333.45	98.18	5.18
5433245.53	304332.45	99.57	5.07
5433244.53	304331.45	100.96	4.98
5433243.53	304330.45	102.34	4.89
5433243.53	304329.45	103.17	4.84
5433242.53	304328.45	104.56	4.75
5433241.53	304327.45	105.95	4.68
5433241.53	304326.45	106.78	4.63
5433240.53	304325.45	108.17	4.56
5433239.53	304324.45	109.55	4.48
5433239.53	304323.45	110.39	4.43
5433238.53	304322.45	111.77	4.35

5433238.53	304321.45	112.61	4.29
5433237.53	304320.45	113.99	4.22
5433236.53	304319.45	115.38	4.16
5433235.53	304317.45	117.60	4.06
5433235.53	304316.45	118.43	4.02
5433234.53	304315.45	119.82	3.97
5433233.53	304314.45	121.20	3.91
5433232.53	304313.45	122.59	3.86
5433232.53	304312.45	123.42	3.82
5433231.53	304311.45	124.81	3.76
5433230.53	304310.45	126.19	3.70
5433230.53	304309.45	127.03	3.67
5433229.53	304308.45	128.41	3.62
5433228.53	304306.45	130.63	3.55
5433227.53	304305.45	132.02	3.50
5433227.53	304304.45	132.85	3.47
5433226.53	304303.45	134.24	3.43
5433225.53	304302.45	135.62	3.39
5433225.53	304301.45	136.46	3.36
5433224.53	304300.45	137.84	3.31
5433223.53	304298.45	140.06	3.24
5433222.53	304297.45	141.45	3.19
5433221.53	304296.45	142.84	3.15
5433221.53	304295.45	143.67	3.12
5433220.53	304294.45	145.06	3.08
5433219.53	304293.45	146.44	3.06
5433219.53	304292.45	147.28	3.03
5433218.53	304291.45	148.66	2.99
5433217.53	304290.45	150.05	2.95
5433217.53	304289.45	150.88	2.92
5433216.53	304288.45	152.27	2.88
5433215.53	304287.45	153.65	2.85
5433214.53	304286.45	155.04	2.81
5433214.53	304285.45	155.87	2.78
5433213.53	304284.45	157.26	2.75
5433212.53	304283.45	158.64	2.72
5433211.53	304281.45	160.86	2.66
5433211.53	304280.45	161.70	2.63
5433210.53	304279.45	163.08	2.60
5433210.53	304278.45	163.92	2.58
5433209.53	304277.45	165.30	2.55
5433209.53	304276.45	166.14	2.53
5433208.53	304275.45	167.52	2.50

5433208.53	304274.45	168.36	2.48
5433208.53	304273.45	169.20	2.46
5433208.53	304272.45	170.04	2.44
5433208.53	304271.45	170.88	2.43
5433208.53	304269.45	172.57	2.42
5433208.53	304268.45	173.42	2.41
5433208.53	304267.45	174.26	2.39
5433208.53	304266.45	175.11	2.39
5433208.53	304265.45	175.97	2.38
5433208.53	304264.45	176.82	2.37

[†]Extracted in PCI Geomatica from a full topographic survey conducted March 7, 2010.

Transect 2 2008 Data			
Northing (UTM, Zone 10)	**Easting (UTM, Zone 10)**	**Horizontal Distance (m)**	**Elevation (m aCD)**
5433750.85	304252.53	0.00	32.88
5433750.70	304251.93	0.58	32.68
5433749.51	304250.37	2.53	31.88
5433748.35	304248.49	4.74	30.70
5433747.42	304247.32	6.23	30.22
5433747.42	304247.36	6.27	30.39
5433747.26	304247.11	6.57	30.14
5433747.07	304246.68	7.03	29.97
5433746.88	304246.60	7.21	29.53
5433746.05	304245.73	8.39	28.71
5433743.89	304242.47	12.31	27.33
5433742.04	304241.01	14.57	27.62
5433741.75	304239.76	15.75	27.03
5433741.16	304238.20	17.37	26.00
5433740.43	304236.68	19.03	24.88
5433738.89	304233.89	22.20	23.02
5433736.63	304231.18	25.72	21.45
5433735.75	304230.56	26.73	21.25
5433734.23	304228.62	29.19	20.25
5433733.41	304227.46	30.61	19.93
5433731.07	304224.69	34.23	19.30
5433730.13	304223.34	35.87	18.86
5433728.76	304220.82	38.71	18.62
5433727.84	304219.48	40.34	18.63
5433727.11	304218.35	41.69	18.13
5433726.23	304216.61	43.62	17.81
5433725.62	304216.16	44.33	17.93

5433725.30	304215.86	44.76	17.85
5433725.05	304215.50	45.21	17.88
5433724.44	304214.82	46.11	17.59
5433723.05	304212.76	48.60	17.09
5433720.73	304209.77	52.37	16.47
5433720.02	304208.66	53.69	16.47
5433719.37	304207.88	54.71	16.57
5433718.11	304205.74	57.18	16.21
5433716.47	304203.69	59.80	16.18
5433713.43	304199.45	65.02	15.73
5433710.65	304195.39	69.94	15.23
5433709.31	304192.61	72.98	14.77
5433708.20	304190.67	75.20	14.07
5433707.22	304189.64	76.61	13.55
5433705.83	304187.91	78.83	13.13
5433704.07	304185.90	81.48	12.93
5433701.37	304182.31	85.97	12.75
5433700.82	304181.67	86.81	12.84
5433700.24	304181.01	87.68	12.65
5433699.49	304180.23	88.76	12.37
5433698.76	304179.54	89.74	12.11
5433696.98	304176.51	93.24	11.63
5433693.95	304172.07	98.62	10.71
5433692.77	304170.61	100.49	10.35
5433692.11	304169.60	101.70	10.14
5433690.30	304167.21	104.69	9.89
5433687.64	304163.72	109.08	9.64
5433685.56	304160.81	112.66	9.52
5433684.36	304159.18	114.68	9.40
5433683.26	304157.79	116.46	9.26
5433681.44	304155.12	119.68	9.51
5433680.57	304153.49	121.51	9.75
5433679.60	304151.90	123.37	9.26
5433679.27	304151.37	124.00	9.25
5433678.68	304150.49	125.06	9.11
5433677.23	304148.16	127.79	9.45
5433675.23	304146.04	130.68	10.18
5433674.78	304145.48	131.39	9.98
5433673.23	304143.22	134.14	9.58
5433671.83	304140.72	136.99	9.54
5433670.80	304139.44	138.63	9.19
5433669.87	304138.53	139.91	8.93
5433668.48	304136.90	142.04	8.73

5433667.85	304135.86	143.25	8.73
5433666.99	304134.25	145.06	8.63
5433666.32	304133.26	146.27	8.51
5433663.91	304129.85	150.44	8.60
5433661.21	304126.46	154.77	8.47
5433659.16	304123.06	158.72	8.60
5433658.02	304121.38	160.75	8.29
5433655.26	304119.33	164.03	8.29
5433654.46	304117.95	165.61	8.24
5433652.07	304113.78	170.39	8.39
5433648.03	304108.76	176.82	8.37
5433645.48	304104.73	181.58	8.43
5433645.06	304103.98	182.44	8.52
5433642.92	304101.01	186.10	8.65
5433640.47	304097.87	190.09	8.85
5433639.65	304096.71	191.50	9.09
5433639.12	304095.88	192.49	8.79
5433637.06	304092.39	196.52	8.66
5433636.38	304091.05	198.01	8.33
5433635.30	304089.86	199.60	8.65
5433633.70	304088.17	201.91	8.60
5433631.95	304086.06	204.64	8.11
5433630.68	304084.00	207.06	7.61
5433629.57	304082.27	209.11	7.21
5433629.55	304082.28	209.11	7.22
5433627.56	304079.49	212.54	6.60
5433626.10	304077.81	214.75	6.16
5433625.59	304076.95	215.75	6.14
5433625.05	304075.96	216.88	5.98
5433622.02	304071.79	222.03	5.52
5433617.48	304065.80	229.54	5.15
5433612.96	304059.02	237.69	4.74
5433608.57	304053.32	244.87	4.15
5433603.79	304046.85	252.92	3.67
5433599.79	304040.37	260.52	3.36

[†]Transect surveyed July 30, 2008. Water line tagged at 12:12 at UTM Zone 10, 5433599.79 m N, 304040.37 m E, 3.36 m aCD.

Transect 2 2009 Data[†]			
Northing (UTM, Zone 10)	Easting (UTM, Zone 10)	Horizontal Distance (m)	Elevation (m aCD)
5433750.92	304251.17	0.00	27.46
5433749.92	304251.17	1.00	27.48
5433748.92	304249.17	2.83	27.48
5433747.92	304247.17	5.00	27.47
5433746.92	304246.17	6.40	27.48
5433746.92	304246.17	6.40	27.48
5433746.92	304246.17	6.40	27.48
5433745.92	304246.17	7.07	27.52
5433745.92	304245.17	7.81	27.51
5433744.92	304245.17	8.49	27.55
5433744.92	304244.17	9.22	27.53
5433743.92	304243.17	10.63	27.50
5433742.92	304242.17	12.04	27.45
5433741.92	304240.17	14.21	27.21
5433740.92	304239.17	15.62	26.94
5433740.92	304237.17	17.20	25.18
5433739.92	304236.17	18.60	24.49
5433738.92	304235.17	20.00	23.81
5433737.92	304233.17	22.20	22.43
5433736.92	304232.17	23.60	21.99
5433735.92	304230.17	25.81	21.03
5433734.92	304229.17	27.20	20.51
5433733.92	304227.17	29.41	19.87
5433732.92	304226.17	30.81	19.63
5433731.92	304225.17	32.20	19.43
5433729.92	304224.17	34.21	19.10
5433729.92	304222.17	35.81	18.81
5433728.92	304221.17	37.20	18.72
5433727.92	304220.17	38.60	18.46
5433726.92	304218.17	40.80	18.12
5433726.92	304217.17	41.62	17.90
5433724.92	304216.17	43.60	17.82
5433724.92	304215.17	44.41	17.63
5433724.92	304215.17	44.41	17.63
5433723.92	304214.17	45.80	17.40
5433723.92	304214.17	45.80	17.40
5433722.92	304213.17	47.20	17.16
5433721.92	304212.17	48.60	16.81
5433721.92	304211.17	49.41	16.66
5433719.92	304209.17	52.20	16.42

5433718.92	304207.17	54.41	16.30
5433718.92	304207.17	54.41	16.30
5433717.92	304206.17	55.80	16.22
5433716.92	304205.17	57.20	16.30
5433716.92	304204.17	58.01	16.24
5433715.92	304203.17	59.41	16.23
5433714.92	304202.17	60.80	16.10
5433713.92	304201.17	62.20	16.03
5433713.92	304200.17	63.01	15.84
5433712.92	304198.17	65.22	15.53
5433711.92	304197.17	66.61	15.45
5433710.92	304196.17	68.01	15.30
5433710.92	304195.17	68.82	15.19
5433709.92	304194.17	70.21	15.02
5433709.92	304193.17	71.03	14.79
5433708.92	304191.17	73.24	14.15
5433706.92	304189.17	76.03	13.46
5433705.92	304188.17	77.42	13.29
5433704.92	304187.17	78.82	13.17
5433703.92	304186.17	80.21	12.91
5433702.92	304185.17	81.61	12.78
5433702.92	304184.17	82.42	12.66
5433701.92	304183.17	83.82	12.63
5433700.92	304181.17	86.02	12.51
5433699.92	304180.17	87.42	12.21
5433698.92	304180.17	88.01	12.11
5433698.92	304179.17	88.81	11.93
5433697.92	304178.17	90.21	11.71
5433697.92	304177.17	91.02	11.58
5433696.92	304176.17	92.42	11.37
5433695.92	304175.17	93.81	11.24
5433695.92	304174.17	94.63	11.12
5433694.92	304173.17	96.02	10.84
5433693.92	304172.17	97.42	10.54
5433692.92	304171.17	98.81	10.33
5433691.92	304169.17	101.02	10.07
5433690.92	304168.17	102.42	10.07
5433690.92	304167.17	103.23	10.02
5433689.92	304166.17	104.62	9.94
5433688.92	304165.17	106.02	9.90
5433687.92	304164.17	107.42	9.89
5433686.92	304163.17	108.81	9.81
5433685.92	304162.17	110.21	9.76

5433684.92	304160.17	112.41	9.45
5433683.92	304158.17	114.62	9.29
5433682.92	304157.17	116.02	9.25
5433681.92	304156.17	117.41	9.31
5433680.92	304154.17	119.62	9.49
5433679.92	304152.17	121.83	9.33
5433678.92	304151.17	123.22	9.22
5433678.92	304150.17	124.04	9.23
5433677.92	304149.17	125.43	9.57
5433677.92	304148.17	126.25	9.72
5433675.92	304147.17	128.22	10.19
5433674.92	304146.17	129.62	9.88
5433674.92	304145.17	130.43	9.74
5433673.92	304144.17	131.83	9.52
5433672.92	304143.17	133.22	9.40
5433672.92	304142.17	134.03	9.36
5433671.92	304141.17	135.43	9.28
5433670.92	304140.17	136.82	9.05
5433669.92	304138.17	139.03	8.67
5433668.92	304137.17	140.43	8.58
5433667.92	304136.17	141.82	8.56
5433666.92	304135.17	143.22	8.57
5433665.92	304133.17	145.43	8.54
5433665.92	304132.17	146.24	8.53
5433664.92	304131.17	147.63	8.54
5433663.92	304130.17	149.03	8.52
5433662.92	304129.17	150.43	8.43
5433661.92	304128.17	151.82	8.39
5433661.92	304127.17	152.63	8.38
5433660.92	304125.17	154.84	8.31
5433659.92	304124.17	156.24	8.26
5433658.92	304123.17	157.63	8.24
5433658.92	304122.17	158.45	8.24
5433656.92	304120.17	161.24	8.21
5433655.92	304120.17	161.82	8.28
5433654.92	304118.17	164.03	8.33
5433653.92	304117.17	165.42	8.31
5433652.92	304116.17	166.82	8.37
5433652.92	304115.17	167.63	8.37
5433651.92	304114.17	169.03	8.50
5433650.92	304113.17	170.42	8.54
5433650.92	304112.17	171.23	8.52
5433649.92	304111.17	172.63	8.67

5433648.92	304110.17	174.03	8.68
5433647.92	304109.17	175.42	8.68
5433646.92	304108.17	176.82	8.79
5433646.92	304107.17	177.63	8.74
5433645.92	304106.17	179.03	8.79
5433645.92	304105.17	179.84	8.68
5433644.92	304104.17	181.23	8.63
5433643.92	304103.17	182.63	8.70
5433643.92	304102.17	183.44	8.64
5433641.92	304100.17	186.23	8.71
5433640.92	304099.17	187.63	8.74
5433640.92	304098.17	188.44	8.71
5433639.92	304097.17	189.83	8.65
5433638.92	304096.17	191.23	8.60
5433638.92	304095.17	192.04	8.56
5433637.92	304094.17	193.44	8.52
5433636.92	304093.17	194.83	8.45
5433636.92	304091.17	196.46	8.47
5433635.92	304090.17	197.85	8.57
5433633.92	304089.17	199.83	8.95
5433632.92	304087.17	202.04	8.50
5433631.92	304086.17	203.44	8.18
5433630.92	304085.17	204.83	7.72
5433630.92	304084.17	205.64	7.52
5433629.92	304083.17	207.04	7.24
5433628.92	304083.17	207.62	7.12
5433628.92	304081.17	209.25	7.14
5433627.92	304080.17	210.64	6.85
5433626.92	304078.17	212.85	6.57
5433625.92	304077.17	214.25	6.46
5433624.92	304076.17	215.64	6.32
5433623.92	304075.17	217.04	6.04
5433623.92	304074.17	217.85	5.89
5433622.92	304073.17	219.24	5.73
5433621.92	304072.17	220.64	5.62
5433620.92	304071.17	222.04	5.52
5433620.92	304070.17	222.85	5.46
5433619.92	304069.17	224.24	5.28
5433618.92	304068.17	225.64	5.11
5433617.92	304067.17	227.04	4.96
5433616.92	304065.17	229.24	4.88
5433615.92	304064.17	230.64	4.75
5433615.92	304063.17	231.45	4.71

5433614.92	304062.17	232.85	4.64
5433613.92	304061.17	234.24	4.58
5433613.92	304060.17	235.05	4.54
5433611.92	304058.17	237.84	4.41
5433610.92	304057.17	239.24	4.32
5433610.92	304056.17	240.05	4.32
5433609.92	304055.17	241.45	4.29
5433608.92	304054.17	242.84	4.23
5433607.92	304052.17	245.05	4.11
5433606.92	304051.17	246.45	4.09
5433605.92	304050.17	247.84	4.02
5433605.92	304049.17	248.65	3.99
5433604.92	304048.17	250.05	3.95
5433603.92	304047.17	251.45	3.93
5433602.92	304046.17	252.84	3.87
5433602.92	304045.17	253.65	3.80
5433601.92	304044.17	255.05	3.70
5433600.92	304043.17	256.44	3.69
5433600.92	304042.17	257.26	3.70
5433599.92	304041.17	258.65	3.64

† Extracted in PCI Geomatica from LiDAR flown August 27, 2009.

Transect 2 2010 Data†			
Northing (UTM, Zone 10)	**Easting (UTM, Zone 10)**	**Horizontal Distance (m)**	**Elevation (m aCD)**
5433750.53	304251.10	0.00	32.22
5433749.53	304251.10	1.00	31.98
5433748.53	304249.10	2.83	31.09
5433747.53	304247.10	5.00	30.39
5433747.53	304246.10	5.83	30.10
5433746.53	304246.10	6.40	29.99
5433746.53	304246.10	6.40	29.99
5433746.53	304246.10	6.40	29.99
5433745.53	304245.10	7.81	29.68
5433745.53	304245.10	7.81	29.68
5433744.53	304244.10	9.22	29.35
5433744.53	304243.10	10.00	28.91
5433742.53	304242.10	12.04	28.70
5433741.53	304240.10	14.21	27.60
5433741.53	304239.10	15.00	27.00
5433740.53	304237.10	17.20	25.58

5433739.53	304236.10	18.60	24.81
5433739.53	304235.10	19.42	24.10
5433738.53	304233.10	21.63	22.78
5433737.53	304232.10	23.02	22.18
5433735.53	304230.10	25.81	21.11
5433734.53	304229.10	27.20	20.68
5433733.53	304228.10	28.60	20.31
5433732.53	304226.10	30.81	19.71
5433731.53	304225.10	32.20	19.48
5433730.53	304224.10	33.60	19.29
5433729.53	304222.10	35.81	19.00
5433729.53	304221.10	36.62	18.82
5433728.53	304220.10	38.01	18.68
5433727.53	304218.10	40.22	18.41
5433726.53	304217.10	41.62	18.22
5433725.53	304216.10	43.01	18.03
5433724.53	304215.10	44.41	17.79
5433724.53	304215.10	44.41	17.79
5433724.53	304214.10	45.22	17.56
5433723.53	304214.10	45.80	17.51
5433723.53	304213.10	46.62	17.31
5433722.53	304212.10	48.01	17.06
5433721.53	304211.10	49.41	16.84
5433720.53	304209.10	51.61	16.56
5433719.53	304208.10	53.01	16.44
5433718.53	304207.10	54.41	16.41
5433718.53	304206.10	55.22	16.38
5433717.53	304205.10	56.61	16.42
5433716.53	304204.10	58.01	16.40
5433715.53	304203.10	59.41	16.34
5433715.53	304202.10	60.22	16.23
5433714.53	304201.10	61.61	16.10
5433713.53	304200.10	63.01	15.97
5433712.53	304198.10	65.22	15.70
5433712.53	304197.10	66.03	15.57
5433711.53	304196.10	67.42	15.38
5433710.53	304195.10	68.82	15.21
5433710.53	304194.10	69.63	15.07
5433709.53	304193.10	71.03	14.91
5433708.53	304192.10	72.42	14.68
5433707.53	304190.10	74.63	14.29
5433706.53	304189.10	76.03	14.02
5433704.53	304187.10	78.82	13.41

5433704.53	304186.10	79.63	13.28
5433703.53	304185.10	81.02	13.10
5433702.53	304184.10	82.42	12.93
5433701.53	304183.10	83.82	12.73
5433700.53	304181.10	86.02	12.42
5433699.53	304181.10	86.61	12.34
5433699.53	304180.10	87.42	12.24
5433698.53	304179.10	88.81	12.03
5433698.53	304178.10	89.63	11.95
5433697.53	304177.10	91.02	11.76
5433696.53	304176.10	92.42	11.51
5433696.53	304175.10	93.23	11.40
5433695.53	304174.10	94.63	11.12
5433694.53	304173.10	96.02	10.85
5433694.53	304172.10	96.83	10.72
5433693.53	304171.10	98.23	10.52
5433692.53	304170.10	99.62	10.40
5433691.53	304168.10	101.83	10.22
5433690.53	304167.10	103.23	10.17
5433689.53	304166.10	104.62	10.13
5433688.53	304165.10	106.02	10.09
5433687.53	304164.10	107.42	10.05
5433686.53	304163.10	108.81	9.98
5433686.53	304162.10	109.62	9.84
5433684.53	304160.10	112.41	9.64
5433683.53	304158.10	114.62	9.56
5433682.53	304157.10	116.02	9.52
5433681.53	304156.10	117.41	9.55
5433680.53	304154.10	119.62	9.57
5433679.53	304152.10	121.83	9.61
5433678.53	304151.10	123.22	9.71
5433678.53	304150.10	124.04	9.71
5433678.53	304149.10	124.85	9.74
5433677.53	304148.10	126.25	9.94
5433676.53	304147.10	127.64	10.11
5433675.53	304146.10	129.03	10.09
5433674.53	304145.10	130.43	9.94
5433674.53	304144.10	131.24	9.85
5433673.53	304143.10	132.64	9.67
5433672.53	304142.10	134.03	9.49
5433672.53	304141.10	134.85	9.38
5433671.53	304140.10	136.24	9.18
5433669.53	304138.10	139.03	8.82

5433668.53	304137.10	140.43	8.75
5433667.53	304136.10	141.82	8.69
5433667.53	304135.10	142.64	8.65
5433666.53	304133.10	144.84	8.60
5433665.53	304132.10	146.24	8.63
5433664.53	304131.10	147.63	8.66
5433664.53	304130.10	148.45	8.68
5433663.53	304129.10	149.84	8.67
5433662.53	304128.10	151.24	8.61
5433661.53	304127.10	152.63	8.55
5433660.53	304125.10	154.84	8.47
5433659.53	304124.10	156.24	8.46
5433659.53	304123.10	157.05	8.46
5433658.53	304122.10	158.45	8.44
5433656.53	304121.10	160.42	8.40
5433655.53	304120.10	161.82	8.43
5433654.53	304118.10	164.03	8.53
5433653.53	304117.10	165.42	8.60
5433653.53	304116.10	166.23	8.63
5433652.53	304115.10	167.63	8.69
5433652.53	304114.10	168.44	8.71
5433651.53	304113.10	169.84	8.76
5433650.53	304112.10	171.23	8.82
5433649.53	304111.10	172.63	8.88
5433648.53	304110.10	174.03	8.94
5433648.53	304109.10	174.84	8.93
5433647.53	304108.10	176.23	9.00
5433646.53	304107.10	177.63	8.99
5433646.53	304106.10	178.44	8.90
5433645.53	304105.10	179.84	8.86
5433644.53	304104.10	181.23	8.83
5433644.53	304103.10	182.04	8.77
5433643.53	304102.10	183.44	8.79
5433642.53	304100.10	185.65	8.79
5433641.53	304099.10	187.04	8.80
5433640.53	304098.10	188.44	8.80
5433639.53	304097.10	189.83	8.77
5433638.53	304096.10	191.23	8.72
5433638.53	304095.10	192.04	8.65
5433637.53	304094.10	193.44	8.55
5433637.53	304093.10	194.25	8.53
5433636.53	304091.10	196.46	8.56
5433635.53	304090.10	197.85	8.61

5433634.53	304089.10	199.25	8.62
5433632.53	304087.10	202.04	8.42
5433632.53	304086.10	202.85	8.30
5433631.53	304085.10	204.25	8.08
5433630.53	304084.10	205.64	7.82
5433630.53	304083.10	206.46	7.65
5433628.53	304083.10	207.62	7.37
5433628.53	304081.10	209.25	7.08
5433628.53	304080.10	210.06	6.96
5433626.53	304078.10	212.85	6.59
5433625.53	304077.10	214.25	6.43
5433625.53	304076.10	215.06	6.35
5433624.53	304075.10	216.45	6.22
5433623.53	304074.10	217.85	6.11
5433622.53	304073.10	219.24	6.00
5433622.53	304072.10	220.06	5.95
5433621.53	304071.10	221.45	5.86
5433620.53	304070.10	222.85	5.79
5433619.53	304069.10	224.24	5.73
5433618.53	304068.10	225.64	5.67
5433618.53	304067.10	226.45	5.66
5433616.53	304065.10	229.24	5.54
5433616.53	304064.10	230.05	5.51
5433615.53	304063.10	231.45	5.45
5433614.53	304062.10	232.85	5.40
5433614.53	304061.10	233.66	5.37
5433613.53	304060.10	235.05	5.30
5433612.53	304058.10	237.26	5.20
5433611.53	304057.10	238.66	5.15
5433610.53	304056.10	240.05	5.07
5433609.53	304055.10	241.45	4.99
5433609.53	304054.10	242.26	4.93
5433607.53	304052.10	245.05	4.77
5433607.53	304051.10	245.86	4.71
5433606.53	304050.10	247.26	4.63
5433605.53	304049.10	248.65	4.52
5433604.53	304048.10	250.05	4.42
5433604.53	304047.10	250.86	4.36
5433603.53	304046.10	252.26	4.27
5433602.53	304045.10	253.65	4.16
5433601.53	304044.10	255.05	4.05
5433601.53	304043.10	255.86	3.99
5433600.53	304042.10	257.26	3.88

5433600.53	304041.10	258.07	3.82

[†]Extracted in PCI Geomatica from a full topographic survey conducted March 7, 2010.

Transect 3 2008 Data[†]			
Northing (UTM, Zone 10)	**Easting (UTM, Zone 10)**	**Horizontal Distance (m)**	**Elevation (m aCD)**
5433881.28	304149.05	0.00	17.75
5433880.91	304148.64	0.55	17.17
5433879.55	304147.15	2.54	18.03
5433877.93	304145.94	4.47	19.29
5433877.35	304145.27	5.34	19.23
5433876.67	304144.22	6.59	19.23
5433875.82	304142.89	8.17	19.45
5433875.19	304142.10	9.18	19.77
5433874.36	304141.42	10.21	19.89
5433872.54	304139.23	13.05	19.40
5433871.63	304137.75	14.79	18.97
5433869.37	304134.11	19.06	17.75
5433869.36	304134.11	19.07	17.76
5433865.44	304128.66	25.78	15.36
5433862.57	304124.62	30.74	14.20
5433859.02	304119.20	37.21	12.92
5433854.80	304113.07	44.65	11.43
5433851.81	304108.16	50.40	10.44
5433850.23	304106.03	53.04	10.33
5433847.07	304102.11	58.06	9.40
5433844.70	304098.56	62.33	9.24
5433843.07	304095.91	65.44	8.96
5433840.92	304092.26	69.67	8.72
5433838.56	304088.88	73.78	8.28
5433837.06	304086.16	76.88	8.32
5433835.96	304084.78	78.64	8.46
5433834.67	304083.01	80.82	8.62
5433833.81	304082.13	82.04	8.93
5433832.86	304080.82	83.66	9.63
5433832.34	304080.11	84.54	9.71
5433830.23	304077.31	88.03	8.92
5433829.19	304071.99	93.01	8.58
5433828.31	304071.16	94.19	8.78
5433827.49	304070.26	95.40	8.55
5433826.39	304069.26	96.85	8.30

5433824.51	304067.18	99.63	8.59
5433823.34	304065.70	101.51	9.07
5433821.77	304064.05	103.76	10.18
5433819.66	304061.15	107.34	12.21
5433818.15	304058.98	109.99	11.74
5433815.04	304054.11	115.76	10.94
5433814.45	304053.50	116.60	11.18
5433812.23	304050.07	120.68	10.35
5433811.78	304049.64	121.29	10.49
5433811.58	304048.87	122.05	10.16
5433810.87	304047.85	123.28	10.06
5433810.28	304046.44	124.78	9.45
5433808.87	304044.49	127.19	9.15
5433807.61	304042.89	129.22	9.18
5433806.15	304040.72	131.83	9.23
5433804.73	304038.58	134.40	8.99
5433804.23	304037.74	135.37	8.83
5433802.87	304035.72	137.81	8.46
5433801.36	304033.39	140.59	8.16
5433800.68	304032.24	141.92	7.95
5433799.76	304030.48	143.89	7.90
5433797.51	304027.48	147.64	7.72
5433794.76	304024.01	152.06	7.47
5433792.80	304020.96	155.68	7.45
5433791.10	304017.40	159.57	7.26
5433789.12	304013.80	163.67	7.75
5433787.97	304013.87	164.25	7.74
5433786.18	304011.83	166.95	7.86
5433781.50	304005.08	175.16	8.65
5433779.42	304004.38	176.92	9.29
5433777.69	304002.84	179.17	9.85
5433776.19	304001.54	181.10	10.37
5433776.13	303998.16	183.91	10.84
5433776.14	303998.18	183.94	10.83
5433774.85	303996.18	186.32	10.33
5433773.97	303994.81	187.94	10.51
5433772.74	303993.07	190.07	10.11
5433771.83	303991.64	191.76	9.51
5433771.55	303991.28	192.22	9.45
5433771.13	303990.68	192.95	9.63
5433770.49	303989.63	194.18	9.30
5433769.84	303988.54	195.44	8.58
5433769.47	303987.96	196.13	8.14

5433767.29	303985.03	199.78	7.34
5433766.09	303983.20	201.97	6.97
5433765.06	303981.84	203.68	6.60
5433764.41	303980.58	205.08	6.43
5433763.98	303980.01	205.79	6.49
5433762.46	303978.16	208.18	6.01
5433761.60	303976.84	209.76	6.00
5433761.12	303976.14	210.61	5.84
5433759.37	303973.59	213.70	5.48
5433756.60	303969.54	218.60	5.05
5433753.40	303965.17	224.02	4.83
5433750.30	303960.79	229.38	4.61
5433747.19	303956.12	234.99	4.36
5433743.78	303951.61	240.64	4.18
5433740.52	303946.68	246.55	3.93
5433736.79	303941.92	252.59	3.68
5433734.24	303938.31	257.01	3.51
5433731.37	303934.33	261.91	3.31
5433721.46	303923.52	276.44	2.80

[†]Transect surveyed July 29, 2008. Water line tagged at 14:00 at UTM Zone 10, 5433721.46 m N, 303923.52 m E, 2.80 m aCD.

Transect 3 2009 Data[†]

Northing (UTM, Zone 10)	Easting (UTM, Zone 10)	Horizontal Distance (m)	Elevation (m aCD)
5433880.92	304149.17	0.00	19.20
5433879.92	304148.17	1.41	19.19
5433879.92	304147.17	2.24	19.14
5433878.92	304146.17	3.61	19.13
5433876.92	304145.17	5.66	19.14
5433876.92	304144.17	6.40	19.10
5433875.92	304143.17	7.81	19.36
5433874.92	304142.17	9.22	19.60
5433873.92	304141.17	10.63	19.61
5433873.92	304140.17	11.40	19.53
5433872.92	304139.17	12.81	19.24
5433871.92	304138.17	14.21	18.93
5433870.92	304137.17	15.62	18.38
5433869.92	304136.17	17.03	18.04
5433869.92	304135.17	17.80	17.79
5433867.92	304133.17	20.62	16.82

5433868.92	304133.17	20.00	17.05
5433867.92	304132.17	21.40	16.53
5433866.92	304131.17	22.80	16.01
5433866.92	304130.17	23.60	15.70
5433865.92	304129.17	25.00	15.24
5433864.92	304127.17	27.20	14.78
5433863.92	304126.17	28.60	14.51
5433862.92	304125.17	30.00	14.07
5433862.92	304124.17	30.81	13.97
5433861.92	304123.17	32.20	13.67
5433860.92	304122.17	33.60	13.37
5433860.92	304121.17	34.41	13.30
5433859.92	304120.17	35.81	13.00
5433858.92	304119.17	37.20	12.81
5433857.92	304118.17	38.60	12.43
5433857.92	304117.17	39.41	12.32
5433856.92	304116.17	40.80	12.03
5433855.92	304115.17	42.20	11.63
5433855.92	304114.17	43.01	11.52
5433854.92	304113.17	44.41	11.21
5433853.92	304112.17	45.80	10.96
5433853.92	304111.17	46.62	10.84
5433852.92	304110.17	48.01	10.58
5433851.92	304109.17	49.41	10.34
5433850.92	304107.17	51.61	10.33
5433849.92	304106.17	53.01	10.16
5433849.92	304105.17	53.82	10.05
5433848.92	304104.17	55.22	9.78
5433847.92	304103.17	56.61	9.57
5433845.92	304101.17	59.41	9.23
5433845.92	304100.17	60.22	9.28
5433844.92	304099.17	61.61	9.28
5433843.92	304097.17	63.82	9.40
5433843.92	304096.17	64.64	9.55
5433842.92	304095.17	66.03	9.27
5433841.92	304094.17	67.42	9.10
5433840.92	304093.17	68.82	8.89
5433839.92	304091.17	71.03	8.91
5433839.92	304090.17	71.85	8.93
5433838.92	304089.17	73.24	8.66
5433837.92	304088.17	74.63	8.49
5433837.92	304087.17	75.45	8.50
5433835.92	304085.17	78.24	8.45

5433834.92	304084.17	79.63	8.39
5433833.92	304082.17	81.84	8.48
5433832.92	304081.17	83.23	8.85
5433831.92	304080.17	84.63	8.94
5433831.92	304079.17	85.45	8.83
5433830.92	304078.17	86.84	8.65
5433829.92	304076.17	89.05	8.46
5433829.92	304075.17	89.87	8.35
5433829.92	304074.17	90.70	8.28
5433829.92	304073.17	91.53	8.28
5433828.92	304072.17	92.91	8.33
5433827.92	304071.17	94.30	8.49
5433826.92	304070.17	95.69	8.30
5433826.92	304069.17	96.52	8.21
5433825.92	304068.17	97.91	8.20
5433824.92	304067.17	99.30	8.34
5433823.92	304066.17	100.69	8.58
5433821.92	304065.17	102.65	9.35
5433820.92	304063.17	104.86	10.36
5433819.92	304062.17	106.25	11.14
5433818.92	304060.17	108.47	11.68
5433817.92	304059.17	109.86	11.41
5433817.92	304058.17	110.68	11.20
5433816.92	304057.17	112.07	11.04
5433815.92	304056.17	113.46	10.83
5433815.92	304055.17	114.28	10.68
5433813.92	304053.17	117.07	10.33
5433813.92	304052.17	117.89	10.16
5433812.92	304051.17	119.28	10.00
5433812.92	304050.17	120.10	9.96
5433810.92	304049.17	122.07	9.65
5433811.92	304048.17	122.32	9.66
5433810.92	304048.17	122.89	9.50
5433810.92	304047.17	123.71	9.43
5433809.92	304045.17	125.92	9.19
5433807.92	304043.17	128.71	9.44
5433806.92	304042.17	130.10	9.67
5433805.92	304041.17	131.49	9.57
5433805.92	304040.17	132.31	9.55
5433804.92	304039.17	133.70	9.43
5433803.92	304037.17	135.92	9.06
5433803.92	304037.17	135.92	9.06
5433802.92	304036.17	137.31	8.82

5433801.92	304035.17	138.70	8.52
5433801.92	304034.17	139.52	8.45
5433800.92	304032.17	141.74	8.18
5433799.92	304031.17	143.13	8.06
5433798.92	304029.17	145.34	7.68
5433797.92	304028.17	146.73	7.55
5433796.92	304026.17	148.95	7.38
5433795.92	304025.17	150.34	7.30
5433794.92	304024.17	151.73	7.29
5433793.92	304023.17	153.12	7.24
5433793.92	304022.17	153.94	7.25
5433792.92	304021.17	155.33	7.24
5433791.92	304020.17	156.72	7.18
5433791.92	304019.17	157.55	7.14
5433790.92	304018.17	158.94	7.15
5433789.92	304016.17	161.15	7.34
5433788.92	304015.17	162.54	7.54
5433788.92	304014.17	163.37	7.68
5433788.92	304014.17	163.37	7.68
5433787.92	304013.17	164.76	7.98
5433786.92	304012.17	166.15	8.18
5433785.92	304011.17	167.54	8.45
5433784.92	304010.17	168.93	8.83
5433783.92	304009.17	170.32	9.23
5433782.92	304008.17	171.71	9.20
5433782.92	304007.17	172.53	9.28
5433781.92	304006.17	173.93	9.12
5433780.92	304005.17	175.32	9.07
5433779.92	304004.17	176.71	9.21
5433777.92	304003.17	178.68	9.65
5433776.92	304002.17	180.07	10.06
5433775.92	304000.17	182.28	10.28
5433775.92	303999.17	183.10	10.31
5433775.92	303998.17	183.92	10.24
5433775.92	303997.17	184.74	10.20
5433775.92	303997.17	184.74	10.20
5433773.92	303995.17	187.52	10.04
5433772.92	303994.17	188.92	9.99
5433771.92	303992.17	191.13	9.82
5433770.92	303990.17	193.34	9.44
5433770.92	303990.17	193.34	9.44
5433770.92	303990.17	193.34	9.44
5433769.92	303988.17	195.56	8.33

5433768.92	303987.17	196.95	8.06
5433768.92	303987.17	196.95	8.06
5433767.92	303986.17	198.34	7.68
5433766.92	303984.17	200.55	7.10
5433764.92	303982.17	203.33	6.84
5433764.92	303981.17	204.16	6.72
5433763.92	303979.17	206.37	6.39
5433762.92	303979.17	206.94	6.37
5433761.92	303977.17	209.15	5.98
5433760.92	303976.17	210.54	5.99
5433760.92	303975.17	211.37	5.93
5433759.92	303974.17	212.76	5.87
5433758.92	303972.17	214.97	5.57
5433757.92	303971.17	216.36	5.34
5433756.92	303970.17	217.75	5.22
5433756.92	303969.17	218.58	5.20
5433755.92	303968.17	219.97	5.08
5433754.92	303967.17	221.36	4.98
5433753.92	303966.17	222.75	4.87
5433753.92	303965.17	223.57	4.82
5433752.92	303964.17	224.96	4.77
5433751.92	303963.17	226.36	4.74
5433750.92	303962.17	227.75	4.66
5433750.92	303961.17	228.57	4.65
5433749.92	303960.17	229.96	4.63
5433748.92	303959.17	231.35	4.56
5433747.92	303958.17	232.74	4.45
5433747.92	303957.17	233.57	4.53
5433746.92	303955.17	235.78	4.41
5433745.92	303954.17	237.17	4.28
5433744.92	303953.17	238.56	4.28
5433743.92	303952.17	239.95	4.25
5433742.92	303950.17	242.17	4.16
5433742.92	303949.17	242.99	4.15
5433741.92	303948.17	244.38	4.05
5433740.92	303947.17	245.77	4.04
5433739.92	303946.17	247.16	3.98
5433738.92	303945.17	248.56	3.89
5433737.92	303944.17	249.95	3.86
5433736.92	303943.17	251.34	3.80
5433735.92	303941.17	253.55	3.81
5433734.92	303940.17	254.95	3.67
5433734.92	303939.17	255.77	3.66

5433733.92	303937.17	257.98	3.65
5433732.92	303936.17	259.37	3.58
5433731.92	303935.17	260.76	3.50
5433730.92	303933.17	262.98	3.47
5433729.92	303932.17	264.37	3.46
5433728.92	303931.17	265.76	3.41
5433727.92	303930.17	267.15	3.32
5433726.92	303929.17	268.54	3.27
5433725.92	303928.17	269.94	3.24
5433724.92	303927.17	271.33	3.19
5433723.92	303926.17	272.72	3.16
5433722.92	303925.17	274.12	3.15
5433721.92	303924.17	275.51	3.17

[†]Extracted in PCI Geomatica from LiDAR flown August 27, 2009.

Transect 3 2010 Data[†]			
Northing UTM, Zone 10)	**Easting (UTM, Zone 10)**	**Horizontal Distance (m)**	**Elevation (m aCD)**
5433881.31	304149.40	0.00	19.54
5433880.31	304148.40	1.41	19.39
5433880.31	304147.40	2.24	19.33
5433878.31	304146.40	4.24	19.34
5433877.31	304145.40	5.66	19.34
5433876.31	304144.40	7.07	19.45
5433876.31	304143.40	7.81	19.41
5433875.31	304141.40	10.00	19.33
5433874.31	304141.40	10.63	19.41
5433873.31	304140.40	12.04	19.28
5433872.31	304139.40	13.45	19.08
5433872.31	304138.40	14.21	18.84
5433871.31	304136.40	16.40	18.28
5433870.31	304135.40	17.80	17.94
5433869.31	304134.40	19.21	17.58
5433868.31	304133.40	20.62	17.19
5433868.31	304133.40	20.62	17.19
5433868.31	304132.40	21.40	16.90
5433867.31	304131.40	22.80	16.42
5433866.31	304130.40	24.21	15.96
5433865.31	304129.40	25.61	15.52
5433864.31	304127.40	27.80	14.89
5433864.31	304126.40	28.60	14.71
5433863.31	304125.40	30.00	14.39

5433862.31	304124.40	31.40	14.10
5433862.31	304123.40	32.20	13.97
5433861.31	304122.40	33.60	13.67
5433860.31	304121.40	35.00	13.36
5433860.31	304120.40	35.81	13.24
5433859.31	304119.40	37.20	12.93
5433858.31	304118.40	38.60	12.64
5433857.31	304117.40	40.00	12.33
5433857.31	304116.40	40.80	12.19
5433856.31	304115.40	42.20	11.87
5433855.31	304114.40	43.60	11.57
5433855.31	304113.40	44.41	11.44
5433854.31	304112.40	45.80	11.17
5433853.31	304111.40	47.20	10.90
5433853.31	304110.40	48.01	10.80
5433852.31	304109.40	49.41	10.57
5433851.31	304107.40	51.61	10.38
5433850.31	304106.40	53.01	10.21
5433849.31	304105.40	54.41	10.08
5433848.31	304104.40	55.80	9.93
5433848.31	304103.40	56.61	9.93
5433846.31	304101.40	59.41	9.74
5433845.31	304100.40	60.80	9.64
5433845.31	304099.40	61.61	9.72
5433844.31	304097.40	63.82	9.71
5433843.31	304096.40	65.22	9.42
5433842.31	304095.40	66.61	9.24
5433842.31	304094.40	67.42	9.30
5433841.31	304093.40	68.82	9.22
5433840.31	304091.40	71.03	9.07
5433839.31	304090.40	72.42	8.85
5433839.31	304089.40	73.24	8.77
5433838.31	304087.40	75.45	8.54
5433837.31	304086.40	76.84	8.55
5433836.31	304085.40	78.24	8.63
5433835.31	304083.40	80.45	8.73
5433833.31	304082.40	82.42	9.14
5433833.31	304081.40	83.23	9.07
5433832.31	304079.40	85.45	9.10
5433831.31	304079.40	86.02	9.09
5433831.31	304078.40	86.84	9.05
5433830.31	304076.40	89.05	8.89
5433830.31	304075.40	89.87	8.79

5433829.31	304074.40	91.26	8.67
5433829.31	304073.40	92.09	8.62
5433829.31	304072.40	92.91	8.56
5433828.31	304071.40	94.30	8.43
5433827.31	304070.40	95.69	8.33
5433826.31	304069.40	97.08	8.25
5433825.31	304068.40	98.47	8.35
5433824.31	304067.40	99.86	8.62
5433823.31	304066.40	101.26	8.97
5433822.31	304064.40	103.47	9.73
5433821.31	304063.40	104.86	10.49
5433820.31	304062.40	106.25	11.21
5433819.31	304060.40	108.47	11.86
5433818.31	304059.40	109.86	11.83
5433817.31	304058.40	111.25	11.56
5433817.31	304057.40	112.07	11.38
5433816.31	304056.40	113.46	11.05
5433815.31	304055.40	114.86	10.86
5433814.31	304053.40	117.07	10.66
5433813.31	304052.40	118.46	10.48
5433813.31	304051.40	119.28	10.33
5433812.31	304050.40	120.67	10.09
5433811.31	304049.40	122.07	9.87
5433811.31	304048.40	122.89	9.77
5433811.31	304047.40	123.71	9.64
5433810.31	304046.40	125.10	9.51
5433809.31	304045.40	126.49	9.40
5433808.31	304043.40	128.71	9.50
5433807.31	304041.40	130.92	9.63
5433806.31	304040.40	132.31	9.63
5433805.31	304039.40	133.70	9.53
5433805.31	304038.40	134.53	9.44
5433804.31	304037.40	135.92	9.21
5433803.31	304036.40	137.31	8.99
5433803.31	304035.40	138.13	8.90
5433802.31	304034.40	139.52	8.67
5433801.31	304033.40	140.91	8.44
5433800.31	304032.40	142.30	8.22
5433800.31	304031.40	143.13	8.17
5433799.31	304029.40	145.34	7.87
5433798.31	304028.40	146.73	7.72
5433796.31	304026.40	149.51	7.55
5433796.31	304025.40	150.34	7.51

5433795.31	304024.40	151.73	7.42
5433794.31	304023.40	153.12	7.37
5433793.31	304022.40	154.51	7.33
5433793.31	304021.40	155.33	7.32
5433792.31	304020.40	156.72	7.34
5433792.31	304019.40	157.55	7.36
5433791.31	304018.40	158.94	7.39
5433790.31	304016.40	161.15	7.54
5433789.31	304015.40	162.54	7.72
5433788.31	304014.40	163.93	7.95
5433789.31	304013.40	164.20	7.97
5433788.31	304013.40	164.76	8.11
5433787.31	304012.40	166.15	8.30
5433785.31	304010.40	168.93	8.67
5433784.31	304009.40	170.32	8.74
5433784.31	304008.40	171.14	8.81
5433783.31	304007.40	172.53	8.79
5433782.31	304006.40	173.93	8.69
5433782.31	304005.40	174.75	8.72
5433780.31	304004.40	176.71	8.79
5433779.31	304004.40	177.28	8.91
5433778.31	304003.40	178.68	9.32
5433776.31	304002.40	180.65	10.02
5433776.31	304000.40	182.28	10.10
5433776.31	303999.40	183.10	10.03
5433776.31	303998.40	183.92	9.99
5433775.31	303997.40	185.31	10.02
5433775.31	303997.40	185.31	10.02
5433774.31	303995.40	187.52	9.94
5433773.31	303993.40	189.74	9.77
5433772.31	303992.40	191.13	9.62
5433771.31	303990.40	193.34	9.24
5433771.31	303990.40	193.34	9.24
5433770.31	303989.40	194.73	9.00
5433770.31	303988.40	195.56	8.83
5433769.31	303987.40	196.95	8.53
5433768.31	303987.40	197.52	8.42
5433768.31	303986.40	198.34	8.23
5433766.31	303984.40	201.12	7.53
5433765.31	303982.40	203.33	7.08
5433764.31	303980.40	205.55	6.87
5433763.31	303979.40	206.94	6.77
5433763.31	303979.40	206.94	6.77

5433761.31	303977.40	209.72	6.61
5433761.31	303975.40	211.37	6.53
5433760.31	303975.40	211.94	6.50
5433759.31	303974.40	213.33	6.47
5433758.31	303972.40	215.54	6.36
5433758.31	303971.40	216.36	6.30
5433757.31	303970.40	217.75	6.19
5433756.31	303969.40	219.15	6.09
5433756.31	303968.40	219.97	6.06
5433755.31	303967.40	221.36	5.97
5433754.31	303966.40	222.75	5.87
5433753.31	303965.40	224.14	5.77
5433752.31	303964.40	225.53	5.67
5433752.31	303963.40	226.36	5.60
5433751.31	303962.40	227.75	5.49
5433750.31	303961.40	229.14	5.40
5433749.31	303959.40	231.35	5.23
5433749.31	303958.40	232.17	5.17
5433748.31	303957.40	233.57	5.07
5433747.31	303956.40	234.96	4.97
5433746.31	303955.40	236.35	4.87
5433745.31	303954.40	237.74	4.77
5433745.31	303953.40	238.56	4.72
5433744.31	303952.40	239.95	4.62
5433743.31	303950.40	242.17	4.49
5433742.31	303949.40	243.56	4.40
5433741.31	303948.40	244.95	4.32
5433741.31	303947.40	245.77	4.27
5433739.31	303945.40	248.56	4.10
5433739.31	303944.40	249.38	4.05
5433738.31	303943.40	250.77	3.97
5433737.31	303942.40	252.16	3.89
5433736.31	303941.40	253.55	3.80
5433735.31	303940.40	254.95	3.72
5433734.31	303939.40	256.34	3.64
5433733.31	303937.40	258.55	3.51
5433732.31	303936.40	259.94	3.43
5433732.31	303935.40	260.76	3.39
5433730.31	303933.40	263.55	3.22
5433729.31	303932.40	264.94	3.13
5433728.31	303931.40	266.33	3.05
5433727.31	303930.40	267.73	2.97
5433726.31	303929.40	269.12	2.89

5433726.31	303928.40	269.94	2.85
5433725.31	303927.40	271.33	2.78
5433724.31	303926.40	272.72	2.73
5433723.31	303925.40	274.12	2.68
5433722.31	303924.40	275.51	2.65

[†]Extracted in PCI Geomatica from a full topographic survey conducted March 6, 2010.

Hawley Beaugrand
Department of Geography, University of Victoria
PO Box 3060 STN CSC
Victoria, BC V8W 3R4
Canada

July 19, 2010

Dear Sibylla Helms,

I am writing in request for permission to reprint your figures in my Master's thesis, *Beach-dune morphodynamics and climate variability impacts on Wickaninnish Beach in Pacific Rim National Park Reserve.*

The University of Victoria requires formal written permission from you, the copyright owner, to reprint the following figures in my thesis:

Please sign and date in the box provided below if you agree to grant reprinting permissions, given the terms provided, and return to me via e-mail at hawley@uvic.ca or send to the address listed above. Your signing of this letter also confirms that you or your company owns the copyright to the above material. Thank you so much.

I authorize you to include the figures listed above in your thesis. I am aware that you are granting an irrevocable non-exclusive license allowing the Library and Archives Canada to reproduce, loan, distribute or sell copies of this thesis by any means and in any form or format to make it available to interested persons.

Signature:
Name: Sibylla Helms
Date: July 3, 2010

Kind regards,
Hawley Beaugrand

Hawley Beaugrand
Department of Geography, University of Victoria
PO Box 3060 STN CSC
Victoria, BC V8W 3R4
Canada

July 19, 2010

Dear Dr. Patrick Hesp,

I am writing in request for permission to reprint your figures in my Master's thesis, *Beach-dune morphodynamics and climate variability impacts on Wickaninnish Beach in Pacific Rim National Park Reserve.*

The University of Victoria requires formal written permission from you, the copyright owner, to reprint the following figures in my thesis:

Hesp, P.A. (2002). Foredunes and blowouts: Initiation, geomorphology and dynamics. *Geomorphology*, 48, 245-268. Figure 3, p. 253, A model of established foredune morphology, dynamics and evolutionary trends on stable, accreting, and eroding coasts.

Please sign and date in the box provided below if you agree to grant reprinting permissions, given the terms provided, and return to me via e-mail at hawley@uvic.ca or send to the address listed above. Your signing of this letter also confirms that you or your company owns the copyright to the above material. Thank you so much.

I authorize you to include the figures listed above in your thesis. I am aware that you are granting an irrevocable non-exclusive license allowing the Library and Archives Canada to reproduce, loan, distribute or sell copies of this thesis by any means and in any form or format to make it available to interested persons.

Signature:
Name: Patrick Hesp
Date: 23/08/10

Kind regards,
Hawley Beaugrand

Hawley Beaugrand
Department of Geography, University of Victoria
PO Box 3060 STN CSC
Victoria, BC V8W 3R4
Canada

July 19, 2010

Dear Derek Heathfield,

I am writing in request for permission to reprint your figures in my Master's thesis, *Beach-dune morphodynamics and climate variability impacts on Wickaninnish Beach in Pacific Rim National Park Reserve.*

The University of Victoria requires formal written permission from you, the copyright owner, to reprint the following figures in my thesis:

Heathfield, D. & Walker, I.J. (in review). *Coastal dune stabilization and large woody debris at Long Beach and Wickaninnish Bay, Pacific Rim National Park, British Columbia.* Manuscript submitted to *The Canadian Geographer* for review.

Figure 3, p. 19, Aerial photograph of southern Combers Beach at Sandhill Creek showing relative shoreline positions for 2007, 1996, and 1973 (yellow, blue, and red, respectively).

Figure 4, p. 20, Aerial photograph of the southern end of Wickaninnish Beach showing beach access trails between (A) and (B), slight shoreline retreat near (B) and notable progradation that has been aided by drift log deposition and stabilization near the outcrop to the south of (C).

Figure 5, p. 21, Aerial photograph of Combers Beach showing relative shoreline positions for 2007, 1996, and 1973 (yellow, blue, and red, respectively).

Figure 7, p. 23, Aerial photograph of the Wickaninnish Beach dune complex showing active sand surface extent for 2007 and 1973 (yellow and red, respectively).

Please sign and date in the box provided below if you agree to grant reprinting permissions, given the terms provided, and return to me via e-mail at hawley@uvic.ca or send to the address listed above. Your signing of this letter also confirms that you or your company owns the copyright to the above material. Thank you so much.

I authorize you to include the figure listed above in your thesis. I am aware that you are granting an irrevocable non-exclusive license allowing the Library and Archives Canada to reproduce, loan, distribute or sell copies of this thesis by any means and in any form or format to make it available to interested persons.

Signature:
Name: Derek Heathfield
Date: 09/10/10

Kind regards,
Hawley Beaugrand

Hawley Beaugrand
Department of Geography, University of Victoria
PO Box 3060 STN CSC
Victoria, BC V8W 3R4
Canada

July 19, 2010

Dear Becs Hoskins,

I am writing in request for permission to reprint your figure in my Master's thesis, *Beach-dune morphodynamics and climate variability impacts on Wickaninnish Beach in Pacific Rim National Park Reserve.*

The University of Victoria requires formal written permission from you, the copyright owner, to reprint the following figure in my thesis:

Cumming, R.M. (2007). *Beach-dune morphodynamics and climatic variability in Gwaii Haanas National Park Reserve and Haida Heritage Site, British Columbia, Canada.* Unpublished master's thesis. University of Victoria, Victoria, Canada. Figure 2.1, p. 15, Basic schematic illustration of quantities used to assess wave runup on beach systems.

Please sign and date in the box provided below if you agree to grant reprinting permissions, given the terms provided, and return to me via e-mail at hawley@uvic.ca or send to the address listed above. Your signing of this letter also confirms that you or your company owns the copyright to the above material. Thank you so much.

I authorize you to include the figure listed above in your thesis. I am aware that you are granting an irrevocable non-exclusive license allowing the Library and Archives Canada to reproduce, loan, distribute or sell copies of this thesis by any means and in any form or format to make it available to interested persons.

Signature:
Name: Rebecca Hoskins (born Rebecca Cumming)
Date: July 20, 2010

Kind regards,
Hawley Beaugrand